ABSTRACT

AMOS, ALISON NICOLE. Adapting Standard Fast-Scan Cyclic Voltammetry Protocols & Sensors for Chronic Biochemical Measurements & *In Vivo* Applications. (Under the direction of Dr. Gregory S. McCarty).

There is a great need in neuroscience to better understand biochemical signaling in the brain. Fluctuation in this signaling can lean to numerous neurological disorders including neurodegenerative disorders, such as Parkinson's disease, and neuropsychiatric disorders, such as addiction. The brain is an extremely complex organ with numerous pathways and signaling molecules that regulate everything from learning to memory, sleep, emotion, risk assessment, reward etc. In damaged signaling pathways, these signaling molecules cannot perform as they would in healthy tissue, producing a wide range of symptoms that reduce the quality of life. This work has identified opportunities to adapt an existing *in vivo* technology to be better-suited for observing biochemical signaling in the brain during more realistic behavioral paradigms and with larger animal models. This ability would enable better long-term study of biochemical signaling during behavioral and pharmacological challenges and the extension of these studies to larger animal models.

Fast-Scan Cyclic Voltammetry (FSCV) at carbon-fiber microelectrodes (CFMs) is a proven *in vivo* technology capable of making electroanalytical measurements of biochemical signaling in the brain of behaving animals. It was initially developed for use in acute, narrowly defined research studies. However, recent advances in science and technology have permitted the development of wireless systems that can make chronic FSCV-based biochemical measurements in large or behaving animal models. Because the technology was created for use in acute experimentation, the measurement protocols were developed without consideration for various engineering parameters, such as power consumption or data transfer

rates, and the sensors were developed without consideration for long-term use. Thus, transitioning FSCV techniques to chronic applications has been limited by both the measurement protocol and the robustness of the sensor.

In an effort to transition the FSCV technology to chronic applications and less rigid behavioral paradigms, this research is focused on 1) adapting FSCV protocols to improve performance in chronic applications while evaluating the effects on the density of collected data and 2) improving the sensor to provide the necessary strength and flexibility for long-term *in vivo* measurements.

Adapting Standard Fast-Scan Cyclic Voltammetry Protocols & Sensors for Chronic Biochemical Measurements & *In Vivo* Applications

by
Alison Nicole Amos

A dissertation submitted to the Graduate Faculty of
North Carolina State University
in partial fulfillment of the
requirements for the degree of
Doctor of Philosophy

Biomedical Engineering

Raleigh, North Carolina

2015

APPROVED BY:

_____	_____
Dr. Gregory S. McCarty Committee Chair	Dr. Glenn M. Walker
_____	_____
Dr. Leslie A. Sombers	Dr. Frances S. Ligler

DEDICATION

For Anjanette, my mother and truest source of inspiration.

BIOGRAPHY

Alison Nicole Amos was born on May 10th, 1987 in Plano, Texas. She grew up with her two brothers in the house her grandfather built, the same house her mother and her siblings grew up in. She spent the years leading up to high school balancing her love for math and science with her love of soccer. After knee surgery to repair a torn ACL her sophomore year in high school, she found engineering.

In August 2005, Alison accepted a place on the soccer team and in the biomedical engineering program at Stevens Institute of Technology in Hoboken, New Jersey. She earned her bachelors of engineering degree there and participated in a cooperative education program that allowed her to work full-time in industry between semesters in the classroom. In her five years at Stevens, she worked for GlaxoSmithKline in their toothpaste production plant and Ethicon, Inc. on two medical device projects for the Johnson & Johnson subsidiary. She decided to continue her education after Stevens and focus on developing research skills in academia rather than industry. Alison moved to Durham, North Carolina, in August 2010 after graduating from Stevens and being admitted to the Joint Program of Biomedical Engineering at North Carolina State University and the University of North Carolina at Chapel Hill. She pursued her doctorate there for five more years under the direction of Dr. Gregory S. McCarty, where she focused on applying practical engineering principles to adapt standard analytical measurement techniques.

TABLE OF CONTENTS

LIST OF TABLES

LIST OF FIGURES

CHAPTER 1

Introduction to Observing Biochemical Measurements with Voltammetric Methods using Biosensors

1.1 BIOCHEMICAL SIGNALING

In the brain, electrically excitable cells process and transmit electrical and chemical signals that regulate voluntary and involuntary movements associated with the nervous system [34]. The nervous system is divided into two parts: the central, including the brain and spinal cord, and the peripheral, which connects the central nervous system to the rest of the body. The defining characteristic of the nervous system is the presence of nerve cells, or neurons. These are highly specialized cells with the ability to precisely transmit information chemically and electrically at very high speeds over very long distances. Neurons communicate with each other via the propagation of electrical signals called action potentials. Input received from surrounding neurons is converted into an action potential by the movement of ions across the cell membrane. Once generated, the action potential is propagated to the terminal region of the neuron where it travels to a connecting neuron by synaptic transmission. At the synapse of a neuron, transmission of the signal can occur electrically or chemically, depending on the type of synapse. Chemical and electrical synaptic transmission is depicted in **Figure 1.1**. In electrically transmitting synapses, two neuronal cell membranes are connected by gap junctions, which allow the direct transfer of ions and small molecules through a channel. As the ions and small molecules move from the

presynaptic cell membrane to the postsynaptic membrane, the charge of the cell is altered relative to its surroundings. This change in cell charge transmits the action potential across the two membranes, where it is picked up by the connecting neuron for further travel. At chemically transmitting synapses, an action potential causes the presynaptic neuron to release chemicals called neurotransmitters into the synaptic space. The electrical signal is converted into the release of neurotransmitters by the activation of voltage-gated ion channels that allow calcium into the cell, activating exocytotic release of the neurotransmitters. Once released, neurotransmitters bind to receptors on the postsynaptic membrane, initiating a response in the connecting neuron. In addition to binding to postsynaptic receptors, neurotransmitters can also be taken back up into the presynaptic cell membrane or diffused in the surrounding extracellular space [34].

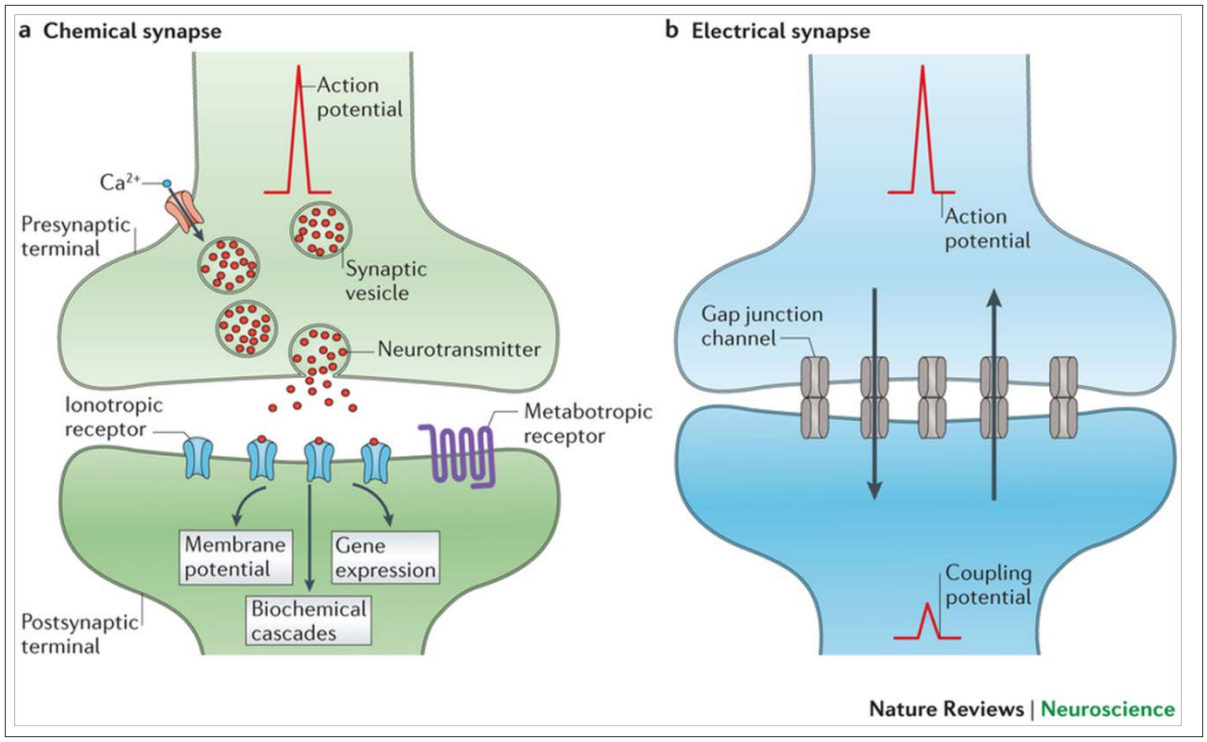

Figure 1.1 – Chemical and electrical synaptic transmission. Reprinted by permission from Macmillan Publishers Ltd: [NATURE REVIEWS NEUROSCIENCE] (A. E. Pereda. Electrical synapses and their functional interactions with chemical synapses. Nat. Rev. Neurosci. 15(4), pp. 250-263. 2014., copyright (2014)).

While there are numerous neurotransmitters that play extensive roles in shaping everyday functions, for the purpose of electroanalytical detection, they can be separated into electrochemically active and non-electrochemically active. Of the electrochemically active neurotransmitters, the research in this dissertation focuses on dopamine (DA), 3, 4-dihydroxyphenylacetic acid (DOPAC), hydrogen peroxide (H_2O_2) and ascorbic acid. DA is a commonly studied neurotransmitter thought to play a major role in reward-motivated behavior [73], [75]. When stimulated, reward pathways increase the levels of DA in the brain. Malfunction in DA pathways have been implicated in disorders such as Parkinson's

disease [33], Alzheimer's disease [78], substance abuse [40], [42] and schizophrenia [22]. DOPAC is generated as a metabolite when DA is catalyzed by monoamine oxidase. H_2O_2 has been studied as a mediator in regulating DA release in the striatum via glutamate [2] and is also thought to contribute to Parkinson's disease [1]. Ascorbic acid is an organic compound with antioxidant properties that is highly concentrated in the central nervous system and thought to play a role in reducing oxidative stress-induced cellular damage [23]. In order to effectively study and understand the role of these small molecules in healthy and diseased states, research is required in the area of developing appropriate detection protocols that are able to function *in-vivo*, in real-time, with the necessary sensitivity and selectivity to capture sub-second neurotransmission events.

1.2 METHODS FOR OBSERVING BIOCHEMICAL SIGNALING

Biochemical measurements are used as an indicator of tissue or organism health in numerous clinical and biomedical research applications [83]. In recent years, research interest has been rapidly expanding in making biochemical measurements in the brain because of its importance in regulating bodily functions. Variations in biochemical signaling can be used to study pharmacological effects in addition to reporting tissue function and health. As such, real-time measurements of biological molecules in functioning tissue provide valuable insights into health and well-being. While signaling mechanisms have been an area of intense research, understanding the successive changes that occur in the brain as a result of fluctuations in this signaling is limited due to lack of appropriate protocols.

Monitoring biochemical signaling, particularly neurotransmitters, in intact brain tissue has been developed using several techniques, including imaging [4], [67], [70], microdialysis [50], [52] and electroanalytical techniques most commonly featuring amperometric [29], [39], [82] or voltammetric [20], [25], [28], [37], [57], [58], [71], [79] – [81] measurements. Imaging techniques such as positron emission tomography (PET) [4], [19], [43], [67], [70], functional magnetic resonance imaging (fMRI) [7], [17], [38], [65] and magnetic resonance spectroscopy (MRS) [11], [12] have all been shown to detect fluctuations in DA levels in various regions of the brain, but are limited in their ability to characterize DA response to stimuli. While these techniques boast advantages including good spatial and temporal resolution with non-invasive measuring, they also lack the ability to quantify concentrations of analytes. Additionally, the expense for these methods and the exposure to associated radiation levels make them poorly-suited to chronically monitor DA and other neurotransmitters.

Though *in vivo* optical methods are currently an area of intense research interest, neuronal signaling has traditionally been monitored using voltammetry and microdialysis. Both microdialysis and voltammetry systems require the implantation of a probe into the tissue to obtain measurements in neurotransmitter fluctuations. In microdialysis, the fluid is removed from the environment and analyzed *ex vivo* using one of several quantitative procedures. In contrast, voltammetry samples the area around the probe without the need for sample collection or removal. This advantage enables voltammetry to be performed with much faster temporal resolution compared to microdialysis and since the probes

(microelectrodes) can be fabricated on the micron scale, voltammetry boasts much better spatial resolution compared to microdialysis. These advantages of voltammetric techniques are expected to be even more advantageous as biomedical scientist move to chronic biochemical monitoring. Chronic monitoring of biochemical signaling *in vivo* requires technologies capable of taking real-time measurements with high sensitivity and selectivity and the necessary temporal resolution to capture second-to-sub-second events.

1.2.1 Microdialysis

Microdialysis is a sampling technique often used in research to determine chemical concentrations in tissue. Microdialysis consists of a probe (typically 0.2-0.5 mm in diameter, 1-2 mm in length) [73] inserted into the region of study that samples an extracellular solution environment through a semi-permeable membrane. The inside of the probe is continually flushed with a "blank" solution, a salt solution without the molecule of interest, allowing small molecules to diffuse across the membrane. The dialysate, the sample solution, in the probe can then be removed and analyzed, most commonly with high-performance liquid chromatography (HPLC). The spectroscopic and chromatographic techniques used to analyze the dialysate can easily distinguish neurotransmitters or other molecules of interest from each other and from possible interferents, giving the technique the necessary selectivity for monitoring neurotransmitters. However, typical microdialysis techniques are limited by their relatively large probe size as well as their sampling rates, with sampling typically occurring on a few minute time scale [6], [49].

Although it demonstrates excellent sensitivity and selectivity to analytes of interest, most adaptations of microdialysis lack the temporal resolution necessary for capturing events that occur on a second to sub-second timescale and are better suited to quantify slowly changing analyte concentration levels. Additionally, the large size of the probes compared to electrochemical sensors causes tissue damage in the measurement area, spatially averages signals, and can inhibit measurement in smaller brain regions [5], [10], [31].

1.2.2 Electrochemical Techniques

Electrochemical techniques involve measuring the potential or current response to an analyte in an electrochemical cell. This class of methods is particularly well-suited for making real-time measurements in functioning tissue because the measurements can be made without removing solution and or without the need for sample purification. These advantages make electrochemical detection methods an ideal candidate for chronic and wireless monitoring of biochemical signaling in behaving animals, and have led to the rapid expansion of its use in neuroscience research. Although the sensors used in conjunction with electrochemical techniques are not as sensitive or selective as can be done with off-line analysis using laboratory analytical methods, their inherent advantage is the ability to collect data with a frequency unmatched by microdialysis or other chemical measurement techniques.

Two widely used electrochemical techniques that have been adapted and developed to monitor rapid fluctuations in the concentration of neurotransmitters are amperometry and

fast-scan cyclic voltammetry [30]. Both these methods are voltammetric in nature, meaning an electrical potential, or voltage, is applied at a level that drives electrolysis of analytes in a solution. Resulting currents from charged particles transferred through the extracellular space are measured via a working electrode. The current response is measured at the surface of the electrode as a function of an applied potential. The potential waveform chosen for application includes the minimum potential required to elicit oxidation or reduction of the species at the electrode surface. The resulting current can then be correlated to the number of molecules being oxidized or reduced and therefore the concentration of the analytes at the sensor surface [73]. Voltammetric techniques are very attractive and have become widely used for biochemical monitoring in the brain because they utilize small electrodes that minimize tissue damage and allow for measurement in very precise regions of the brain with micron spatial resolution.

1.2.3 Amperometry

Amperometry is a voltammetric technique based on the application of a constant electrical potential sufficient enough to elicit electrolysis of an analyte of interest. In amperometry, the sensor is held at a constant potential and resulting currents are recorded from the oxidation or reduction of analyte species in solution. Electroactive species are oxidized and reduced rapidly upon contact with the sensor in amperometry, providing temporal resolution on the microsecond time scale. While it boasts improved temporal resolution compared to both microdialysis and imaging techniques, amperometry has limited

analyte selectivity. The applied potential at the electrode is held constant, rendering the amperometric measurement nonselective, as the oxidation or reduction of any electroactive species present in the solution contributes to the overall current response measured. This convolutes the ability to correlate the current response with one specific analyte, making amperometry problematic in complex environments such as the brain. Chronoamperometry is a similar technique that features a stepped potential held constant for a period of time, then ramped up, and held constant again. Compared to traditional amperometry, the step potential affords some chemical resolution by calculating the ratio of oxidative and reductive currents, but does not compare to the chemical selectivity that can be achieved with fast-scan cyclic voltammetry.

1.2.4 Fast-Scan Cyclic Voltammetry

Fast-scan cyclic voltammetry (FSCV) is another voltammetric measurement technique that allows for monitoring of various signaling molecules in functioning brain tissue. FSCV has been used since the early 1980's for monitoring neurochemicals [30]. Advances have been made in sensor sensitivity and selectivity and in extending the potential waveform, offering the required temporal resolution, sensitivity and analyte selectivity needed to study behaviorally stimulated events on a sub-second time scale. In FSCV, a triangular potential waveform is applied to the working electrode and the resulting current response is recorded. In contrast to amperometric techniques, FSCV provides chemical selectivity due to the applied potential linearly scanned, allowing for flexibility of the

potential window to capture specific analytes and distinguish them from others. **Figure 1.2** schematically depicts the detection of DA, a commonly monitored neurotransmitter, using FSCV coupled with a carbon fiber microelectrode (CFM). Application of the potential waveform for DA (-0.4 V to +1.3 V and back to -0.4 V at 400 V/s) to the electrode generates a large, mostly non-faradic current that is stable over a short period of time. This current is mainly due to the double-layer charging at the electrode-solution interface. Introduction of an electroactive species to the analyte solution generates a small faradic current from the redox reactions of the analyte species that is superimposed on the background current. The large background current masks the considerably smaller faradaic current and can be subtracted out. Background and background-subtracted currents are plotted versus the applied potential as cyclic voltammograms (CV) and provide valuable information about the redox reactions that are occurring at the surface of the CFM.

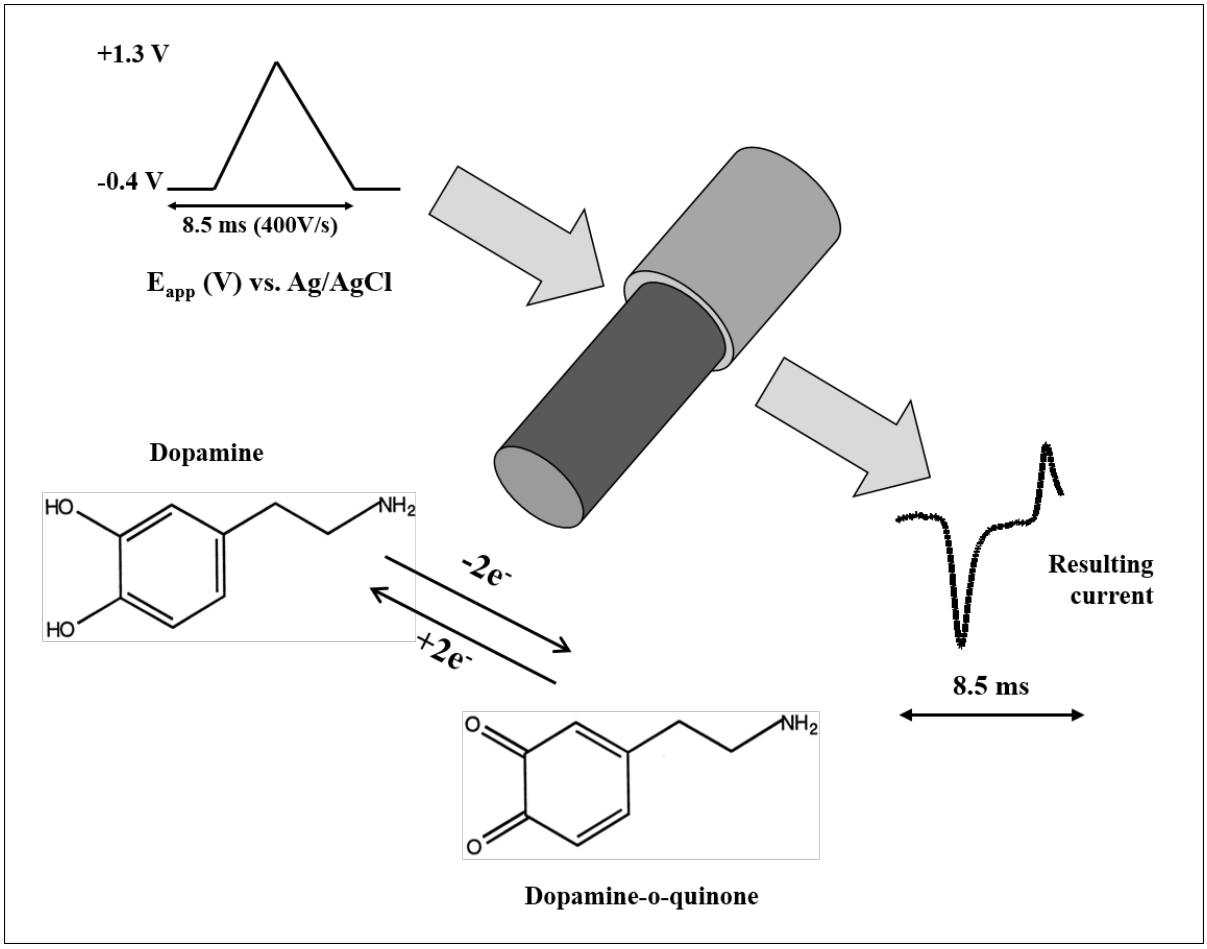

Figure 1.2 – FSCV detection of dopamine.

Typical FSCV current responses are displayed in one of two ways. The first is a background-subtracted CV, where the large non-faradic background current resulting from the application of a rapidly changing potential to the electrode is subtracted from the data, leaving only the small faradic current generated by the oxidation and reduction of the analyte species. The oxidation and reduction peaks in a background-subtracted CV provide a chemical "fingerprint" that is characteristic to individual analytes. Both the identity and

concentration of the electroactive species can be determined from the background-subtracted CV. The second method of displaying FSCV current responses is an electrochemical color plot, shown in **Figure 1.3**, which is comprised of individual background-subtracted CVs taken in series over a period of time. Time is plotted on the x-axis, potential is plotted on the y-axis and the current response is given in false color. Color plots provide detailed information on the measurement performance over time. From the color plot, a vertical line can be extracted at a single time point to produce a background-subtracted CV, while extracting a single horizontal line from the color plot yields a current vs. time trace at a given potential. The current vs. time trace details important information about the dynamic changes in the electroactive species concentration, such as the release (increase in current) and reuptake (decrease in current) of the analyte. Protocols for monitoring DA [3], [14], [20], [26], [36], [57] – [61], [71], [79] – [81], norepinephrine [28], [47], pH [68], [69], oxygen [69], [79], hydrogen peroxide [56], [62], [64] and serotonin [16], [24], [32] in functioning brain tissue have all been reported using this technique.

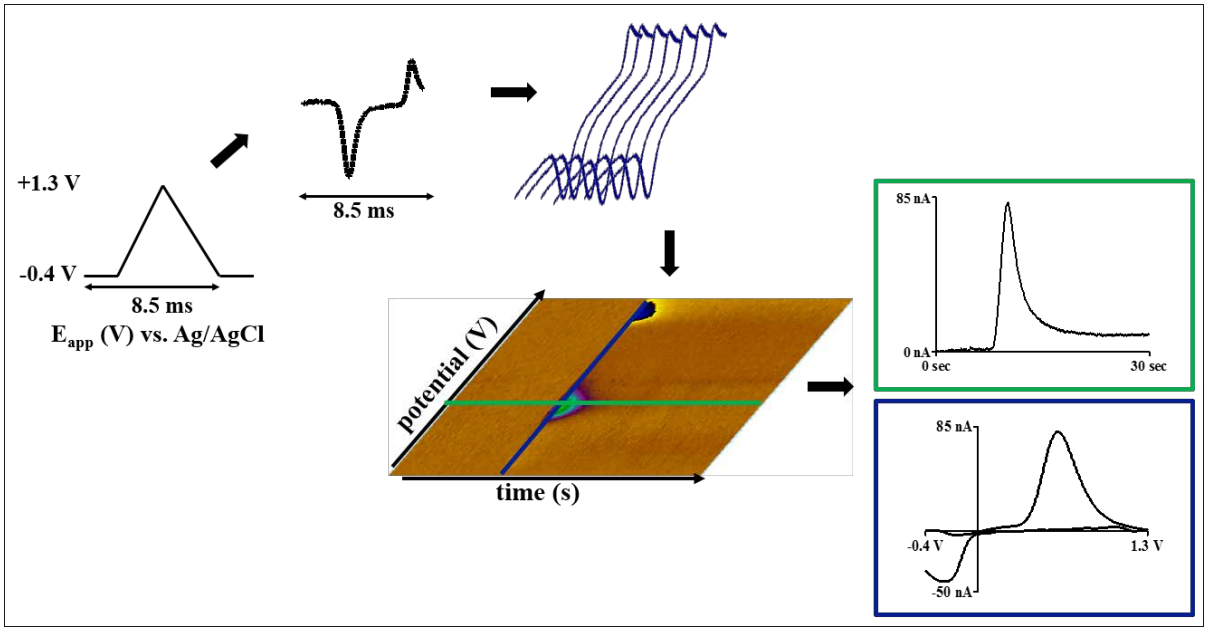

Figure 1.3 – Manipulating FSCV data.

1.2.4.1 Flow Injection Apparatus for *In Vitro* Experiments

In vitro experiments are typically performed in a flow cell that contains an electrochemical cell and a method for flow injection. The working electrode and reference electrodes (typically Ag/AgCl) are placed in an electrochemical cell housed in a Faraday cage. Buffer solution is supplied across the working and reference electrodes via a syringe pump at a constant flow rate. Single injections of analyte can be delivered to the electrodes using an HPLC valve and air actuator controlled by a digital valve interface and recorded using custom hardware and software. **Figure 1.4** illustrates a typical flow injection setup.

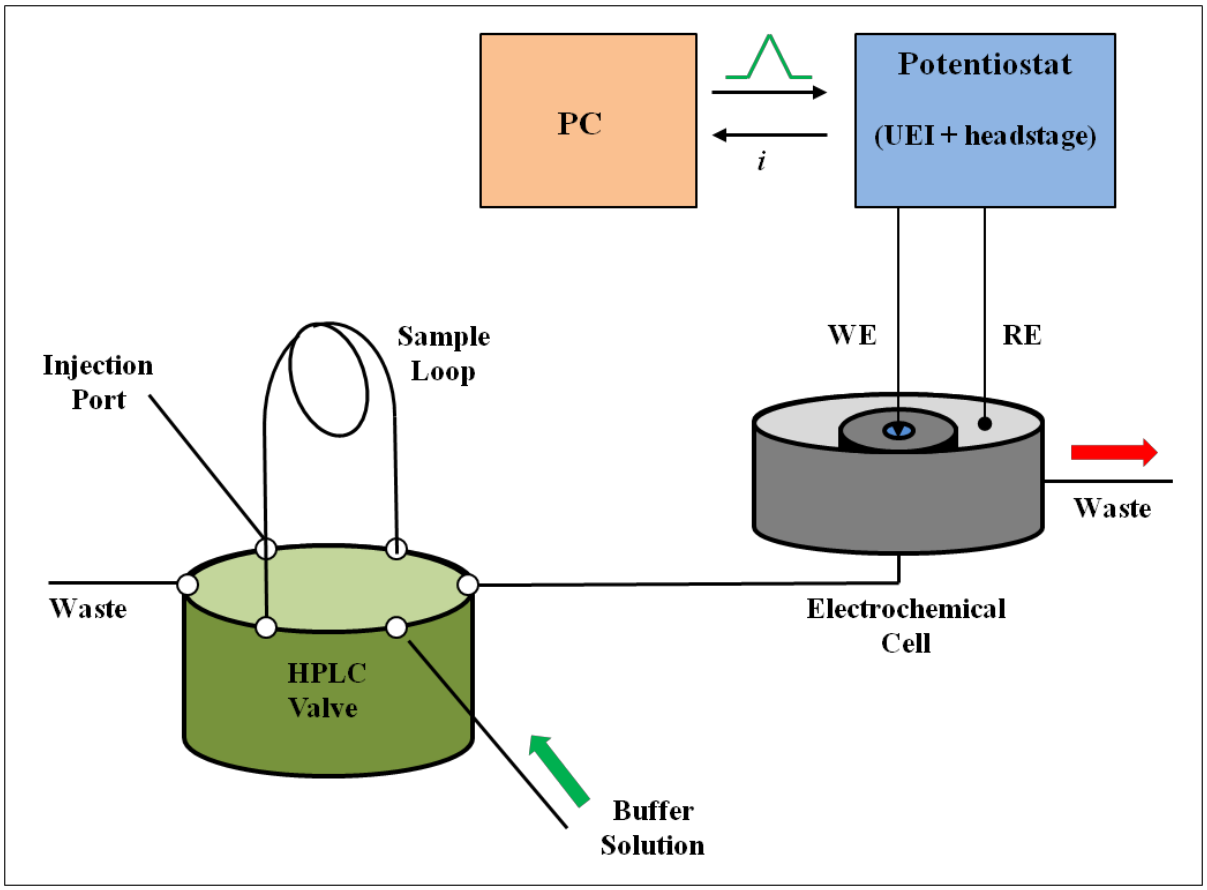

Figure 1.4 – *In vitro* flow injection apparatus.

1.2.4.2 Data Acquisition and Processing

In this research, a standard FSCV waveform for DA is applied to the electrochemical cell within the flow injection apparatus described above using custom built instrumentation (University of North Carolina at Chapel Hill, Department of Chemistry, Electronics Facility). This instrumentation enables FSCV current responses to be recorded, displayed and manipulated. The typical potential waveform for DA ranges from -0.4 V to +1.3 V and back to -0.4 V at a scan rate of 400 V/s and frequency of 10 Hz. The oxidation and reduction

potentials and peak amplitude are easily manipulated with this software and instrumentation. In the case of solutions containing a mixture of analytes, multivariate statistical analysis, such as principal component regression (PCR), can be used to isolate individual analytes from the mixture after data collection. PCR is a commonly used tool to analyze FSCV measurements and requires a training set of the responses for individual molecules and sufficient peak separation between analytes to differentiate the species. PCR is used to isolate specific molecule profiles present in mixed solutions [25], [35], [37], [45], [58], resolving slow changes in baseline DA levels and separating currents from interferents that contribute to the overall current collected on a trace [30].

1.2.4.3 Modifying FSCV Parameters to Reduce Data Generated

Several animal models have been developed in order to better understand how neuronal signaling compares in healthy and diseased states [41], [44], [51], [55], [76]. The incorporation of self-administration of drugs is a leading behavioral paradigm in this area because the animals are allowed to voluntarily seek the drug. The main drawback to current animal models is the tether required to analytically monitor the animal's behavior. Removing the tether from behaving animals will allow for more freedom of motion and an opportunity to evaluate more realistic social and environmental interactions. Additionally, the small movements in the tether often generate a source of noise that can degrade the quality of the measurements. Replacing the traditional hardwired measurement system with wireless communication is a plausible next step to alleviate the limitations found in current behavioral

paradigms. Advances in wireless technology used in medicine (ECG, blood pressure, heart rate) and in communications (Wi-Fi, Bluetooth) make it possible to develop such a system for monitoring biochemical signaling [9]. This long-term goal requires several modifications to the current technology, including reducing the physical size of the system required to support implantable devices and the amount of power the system consumes as a whole. Proof-of-concepts exist for wireless measuring of electrically evoked DA [15], [21], but the majority of the recording systems available consume large amounts of power and are too large to be practical for small-scale and low-power applications.

Research in this work focuses on adapting various FSCV parameters in current protocols to address the mass amounts of data generated that contribute to overall power consumption of the system. One such parameter is sampling rate, or the number of times the electrode samples the environment per second. Conventional protocols utilize a 10 Hz sampling rate, but we show a reduced sampling rate can be utilized without compromising the efficacy of the protocol while reducing the amount of data transferred over time. Additionally, we show the ability to reduce the data density of each sample to further reduce the amount of data generated in each file. The data density refers to the number of data points that comprise each CV, typically 850 or 1000. Each of these parameters have the potential to drastically affect the power required to drive a chronic system where measurements are made over long periods of time and data is wirelessly transferred and received.

1.3 BIOSENSORS

Biochemical sensors are devices that enable biological analytes to be directly measured. Emerging efforts utilizing electroanalytical techniques have led to the development of microelectrodes as biochemical sensors. Microelectrodes have been demonstrated for the detection and characterization of numerous biological species [14], [20], [26], [27], [54], [56] – [58], [71], [79] – [81]. In recent years, there has been considerable interest in the development of microsensors for electroanalytical techniques, particularly microsensors that have versatility across a number of analytes and tissue types without sacrificing accuracy or repeatability. Out of those efforts has come microelectrodes that are quite small, require minimal power and are relatively inexpensive to construct [8], [83]. These microelectrodes are typically carbon-based on a variety of substrates [53], [63], [77], [79], [81], and have been used to make FSCV measurements *in vivo* [74], [83] with excellent sensitivity and selectivity. For this reason, one focus of the research in this dissertation is on improving the state of the art carbon-based electroanalytical microsensors for use in chronic systems with freely moving animals.

1.3.1 Carbon Fiber Microelectrodes

Carbon fiber microelectrodes (CFMs) are the current gold standard sensor used for the electroanalytical measurement of fluctuations in biologically relevant analytes. They have been used to monitor neurotransmitters elicited by electrical stimulation [80], pharmacological agents [72] and behavior [18], [66]. Fabrication of a CFM, shown in **Figure**

1.5, is done by hand. A carbon fiber, typically 7 μm in diameter, is encapsulated in a glass capillary. A micropipette puller is used to draw this assembly to a sharp tip, sealing the carbon fiber in the glass. The carbon fiber extending past the glass seal is manually cut to the desired length and the capillary glass is backfilled with electrolyte or conductive silver paint and fitted with wires for electrical contact.

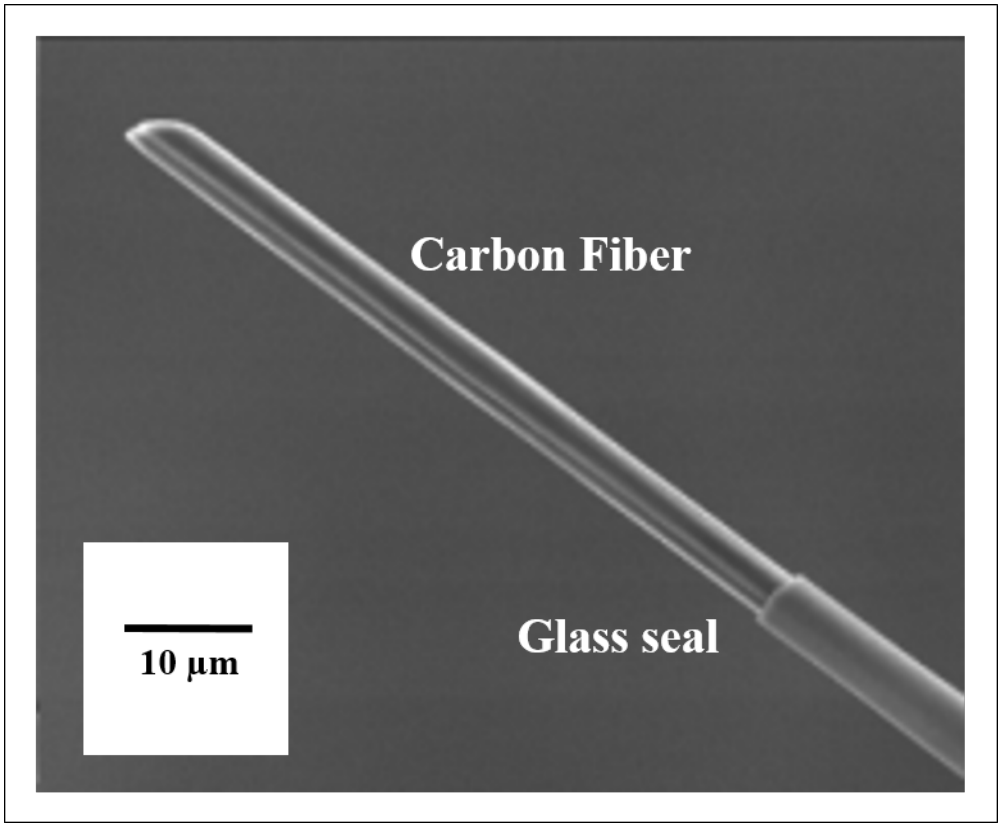

Figure 1.5 – Carbon fiber microelectrode.

CFMs are the most commonly used sensor for *in vivo* electroanalytical applications due to their straightforward fabrication, low cost and ability to demonstrate consistency and accuracy in measuring a variety of analytes. Unfortunately, their design is not well-suited for chronic *in vivo* measurements in behaving animals. Specifically, the flimsy nature of the carbon fiber combined with the fragility of the glass seal is not ideal for long term, sustainable microelectrodes. This limitation hampers the types of measurements that can be done with electroanalytical techniques in behaving animals as the fracture of the electrode poses a risk to the animal in addition to compromising data acquisition. Due to these limitations, efforts are being made to improve upon the weaknesses of CFMs [20], [26], [27], [46], [81] and develop sensors that have greater stability over a longer period of time. Part of the research in this work will discuss the drawbacks of CFMs and present an alternatively fabricated microelectrode that is better suited for chronic measurements and for use in freely moving animals.

1.3.2 Chronic Microsensors

Chronic measurements with the current sensor technology are possible, but it is difficult and cumbersome. These measurements feature a sensor that still utilizes a carbon fiber, but removes the fragile glass insulation and replaces it with a more flexible fused silica [13]. This sensor can successfully measure DA fluctuations over a period of months after implantation. However, one of the main limitations of the CFM remain in the chronic microsensor in that it still uses a carbon fiber which is flimsy and often will break off the end

of the sensor during implantation. Part of the work presented here discusses the potential of a more rigid sensor as an alternative replacement to the recently emerged chronic sensor, where not only is the flimsy carbon replaced with a stronger substrate, but the glass insulation is replaced with fused silica.

1.4 OVERVIEW OF DISSERTATION

This dissertation consists of five additional chapters that expand on the topics presented in this introduction, focusing on the adaptation of standard FSCV protocols and sensors for long-term biochemical measurements and *in vivo* applications. **Chapters 2**, **3** and **4** address modifications to the current FSCV measurement protocol used for monitoring biochemical signaling. **Chapter 2** discusses the reduction of an FSCV parameter, sampling rate, in an effort to reduce the large amounts of data that are collected in typical experiments. **Chapter 3** expands on the reduction of data generation in FSCV experimentation by exploring the effects of reducing of a second FSCV parameter, data density, or number of data points per CV. It also discusses the implications of reducing both the sampling rate and data density in the same protocol. **Chapter 4** shows *in vivo* findings from the use of protocols combining a reduced sampling rate and reduced data density. **Chapter 5** presents an alternative sensor to be used with FSCV that improves on the weaknesses of the current sensor as they relate to chronic experiments in freely moving or behaving animals. **Chapter 6** details an ongoing study for evaluating use of the alternative carbonized tungsten

microsensors for use in freely moving animals. **Chapter 7** offers a summary of all the findings included in this work and recommendations for future work in this area.

1.5 REFERENCES

[1] V. Anantharam, E. Lehrmann, A. Kanthasamy, Y. Yang, P. Banerjee, K. G. Becker, W. J. Freed and A. G. Kanthasamy. Microarray analysis of oxidative stress regulated genes in mesencephalic dopaminergic neuronal cells: Relevance to oxidative damage in Parkinson's disease. Neurochem. Int. 50(6), pp. 834-847. 2007.

[2] L. Bao, M. V. Avshalumov, J. C. Patel, C. R. Lee, E. W. Miller, C. J. Chang and M. E. Rice. Mitochondria are the source of hydrogen peroxide for dynamic brain-cell signaling. J. Neurosci. 29(28), pp. 9002-9010. 2009.

[3] B. D. Bath, D. J. Michael, B. J. Trafton, J. D. Joseph, P. L. Runnels and R. M. Wightman. Subsecond adsorption and desorption of dopamine at carbon-fiber microelectrodes. Anal. Chem. 72(24), pp. 5994-6002. 2000.

[4] I. Boileau, D. Payer, B. Chugani, D. S. Lobo, S. Houle, A. A. Wilson, J. Warsh, S. J. Kish and M. Zack. *In vivo* evidence for greater amphetamine-induced dopamine release in pathological gambling: A positron emission tomography study with [C]-(+)-PHNO. Mol. Psychiatry 2013.

[5] L. M. Borland, G. Shi, H. Yang and A. C. Michael. Voltammetric study of extracellular dopamine near microdialysis probes acutely implanted in the striatum of the anesthetized rat. J. Neurosci. Methods 146(2), pp. 149-158. 2005.

[6] M. T. Bowser and R. T. Kennedy. *In vivo* monitoring of amine neurotransmitters using microdialysis with on-line capillary electrophoresis. Electrophoresis 22(17), pp. 3668-3676. 2001.

[7] H. C. Breiter, R. L. Gollub, R. M. Weisskoff, D. N. Kennedy, N. Makris, J. D. Berke, J. M. Goodman, H. L. Kantor, D. R. Gastfriend, J. P. Riorden, R. T. Mathew, B. R. Rosen and S. E. Hyman. Acute effects of cocaine on human brain activity and emotion. Neuron 19(3), pp. 591-611. 1997.

[8] J. D. Bronzino and R. C. Dorf. The Biomedical Engineering Handbook (2nd ed.) 2000.

[9] B. Bucur. Technological barriers in the use of electrochemical microsensors and microbiosensors for *in vivo* analysis of neurological relevant substances. Curr. Neuropharmacol. 10(3), pp. 197-211. 2012.

[10] P. M. Bungay, P. Newton-Vinson, W. Isele, P. A. Garris and J. B. Justice. Microdialysis of dopamine interpreted with quantitative model incorporating probe implantation trauma. J. Neurochem.86(4), pp. 932-946. 2003.

[11] L. Chang, C. C. Cloak and T. Ernst. Magnetic resonance spectroscopy studies of GABA in neuropsychiatric disorders. J. Clin. Psychiatry 64 Suppl 3pp. 7-14. 2003.

[12] L. Chang, T. Ernst, R. E. Poland and D. J. Jenden. *In vivo* proton magnetic resonance spectroscopy of the normal aging human brain. Life Sci. 58(22), pp. 2049-2056. 1996.

[13] J. J. Clark, S. G. Sandberg, M. J. Wanat, J. O. Gan, E. A. Horne, A. S. Hart, C. A. Akers, J. G. Parker, I. Willuhn, V. Martinez, S. B. Evans, N. Stella and P. E. Phillips. Chronic microsensors for longitudinal, subsecond dopamine detection in behaving animals. Nat. Methods 7(2), pp. 126-129. 2010.

[14] J. C. Conti, E. Strope, R. N. Adams and C. A. Marsden. Voltammetry in brain-tissue - chronic recording of stimulated dopamine and 5-hydroxytryptamine release. Life Sci. 23(27-2), pp. 2705-2715. 1978.

[15] F. Crespi. Wireless *in vivo* voltammetric measurements of neurotransmitters in freely behaving rats. Biosens. Bioelectron. 25(11), pp. 2425-2430. 2010.

[16] E. C. Dankoski and R. M. Wightman. Monitoring serotonin signaling on a subsecond time scale. Front. Integr.Neurosci.7pp. 44. 2013.

[17] J. Daumann, B. Fimm, K. Willmes, A. Thron and E. Gouzoulis-Mayfrank. Cerebral activation in abstinent ecstasy (MDMA) users during a working memory task: A functional magnetic resonance imaging (fMRI) study. Brain Res. Cogn. Brain Res. 16(3), pp. 479-487. 2003.

[18] J. J. Day, M. F. Roitman, R. M. Wightman and R. M. Carelli. Associative learning mediates dynamic shifts in dopamine signaling in the nucleus accumbens. Nat. Neurosci. 10(8), pp. 1020-1028. 2007.

[19] W. C. Drevets, C. Gautier, J. C. Price, D. J. Kupfer, P. E. Kinahan, A. A. Grace, J. L. Price and C. A. Mathis. Amphetamine-induced dopamine release in human ventral striatum correlates with euphoria. Biol. Psychiatry 49(2), pp. 81-96. 2001.

[20] A. G. Ewing and R. M. Wightman. Monitoring the stimulated release of dopamine with *in vivo* voltammetry .2.clearance of released dopamine from extracellular fluid. J. Neurochem. 43(2), pp. 570-577. 1984.

[21] P. A. Garris, R. Ensman, J. Poehlman, A. Alexander, P. E. Langley, S. G. Sandberg, P. G. Greco, R. M. Wightman and G. V. Rebec. Wireless transmission of fast-scan cyclic voltammetry at a carbon-fiber microelectrode: Proof of principle. J. Neurosci. Methods 140(1-2), pp. 103-115. 2004.

[22] A. A. Grace. Phasic versus tonic dopamine release and the modulation of dopamine system responsivity: A hypothesis for the etiology of schizophrenia. Neuroscience 41(1), pp. 1-24. 1991.

[23] F. E. Harrison, G. L. Bowman and M. C. Polidori. Ascorbic acid and the brain: Rationale for the use against cognitive decline. Nutrients 6(4), pp. 1752-1781. 2014.

[24] P. Hashemi, E. C. Dankoski, R. Lama, K. M. Wood, P. Takmakov and R. M. Wightman. Brain dopamine and serotonin differ in regulation and its consequences. Proc. Natl. Acad. Sci. U. S. A. 109(29), pp. 11510-11515. 2012.

[25] M. L. Heien, M. A. Johnson and R. M. Wightman. Resolving neurotransmitters detected by fast-scan cyclic voltammetry. Anal. Chem. 76(19), pp. 5697-5704. 2004.

[26] M. L. A. V. Heien, P. E. M. Phillips, G. D. Stuber, A. T. Seipel and R. M. Wightman. Overoxidation of carbon-fiber microelectrodes enhances dopamine adsorption and increases sensitivity. Analyst 128(12), pp. 1413-1419. 2003.

[27] A. Hermans and R. M. Wightman. Conical tungsten tips as substrates for the preparation of ultramicroelectrodes. Langmuir 22(25), pp. 10348-10353. 2006.

[28] N. R. Herr, J. Park, Z. A. McElligott, A. M. Belle, R. M. Carelli and R. M. Wightman. *In vivo* voltammetry monitoring of electrically evoked extracellular norepinephrine in subregions of the bed nucleus of the striaterminalis. J. Neurophysiol. 107(6), pp. 1731-1737. 2012.

[29] A. F. Hoffman, C. R. Lupica and G. A. Gerhardt. Dopamine transporter activity in the substantianigra and striatum assessed by high-speed chronoamperometric recordings in brain slices. J. Pharmacol. Exp. Ther. 287(2), pp. 487-496. 1998.

[30] K. Iniewski. Integrated microsystems. 2012.

[31] A. Jaquins-Gerstl and A. C. Michael. Comparison of the brain penetration injury associated with microdialysis and voltammetry. J. Neurosci. Methods 183(2), pp. 127-135. 2009.

[32] C. E. John and S. R. Jones. "Fast scan cyclic voltammetry of dopamine and serotonin in mouse brain slices," in Electrochemical Methods for Neuroscience, A. C. Michael and L. M. Borland, Eds. 2007.

[33] P. Jokinen, M. Karrasch, A. Bruck, J. Johansson, J. Bergman and J. O. Rinne. Cognitive slowing in Parkinson's disease is related to frontostriatal dopaminergic dysfunction. J. Neurol. Sci. 329(1-2), pp. 23-28. 2013.

[34] E. R. Kandel. Principles of Neural Science (5th ed.) 2013.

[35] R. B. Keithley, M. L. Heien and R. M. Wightman. Multivariate concentration determination using principal component regression with residual analysis. Trends Analyt Chem. 28(9), pp. 1127-1136. 2009.

[36] R. B. Keithley, P. Takmakov, E. S. Bucher, A. M. Belle, C. A. Owesson-White, J. Park and R. M. Wightman. Higher sensitivity dopamine measurements with faster-scan cyclic voltammetry. Anal. Chem. 83(9), pp. 3563-3571. 2011.

[37] R. B. Keithley and R. M. Wightman. Assessing principal component regression prediction of neurochemicals detected with fast-scan cyclic voltammetry. ACS Chem. Neurosci. 2(9), pp. 514-525. 2011.

[38] D. Y. Kimberg, G. K. Aguirre, J. Lease and M. D'Esposito. Cortical effects of bromocriptine, a D-2 dopamine receptor agonist, in human subjects, revealed by fMRI. Hum. Brain Mapp. 12(4), pp. 246-257. 2001.

[39] E. A. Kiyatkin. Cocaine enhances the changes in extracellular dopamine in nucleus accumbens associated with reinforcing stimuli: A high-speed chronoamperometric study in freely moving rats. Eur. J. Neurosci. 5(3), pp. 284-291. 1993.

[40] G. F. Koob and F. E. Bloom. Cellular and molecular mechanisms of drug dependence. Science 242(4879), pp. 715-723. 1988.

[41] G. F. Koob and M. Le Moal. Addiction and the brain antireward system. Annu. Rev. Psychol. 59, pp. 29-53. 2008.

[42] R. Kuczenski, D. S. Segal and P. K. Todd. Behavioral sensitization and extracellular dopamine responses to amphetamine after various treatments. Psychopharmacology (Berl) 134(3), pp. 221-229. 1997.

[43] C. Martin-Soelch, A. F. Chevalley, G. Kunig, J. Missimer, S. Magyar, A. Mino, W. Schultz and K. L. Leenders. Changes in reward-induced brain activation in opiate addicts. Eur. J. Neurosci. 14(8), pp. 1360-1368. 2001.

[44] D. L. McKinzie, Z. A. Rodd-Henricks, C. T. Dagon, J. M. Murphy and W. J. McBride. Cocaine is self-administered into the shell region of the nucleus accumbens in wistar rats. Ann. N. Y. Acad. Sci. 877, pp. 788-791. 1999.

[45] D. J. Michael, J. D. Joseph, M. R. Kilpatrick, E. R. Travis and R. M. Wightman. Improving data acquisition for fast-scan cyclic voltammetry. Anal. Chem. 71(18), pp. 3941-3947. 1999.

[46] K. C. Morton, C. A. Morris, M. A. Derylo, R. Thakar and L. A. Baker. Carbon electrode fabrication from pyrolyzed Parylene-C. Anal. Chem. 83(13), pp. 5447-5452. 2011.

[47] J. Park, P. Takmakov and R. M. Wightman. *In vivo* comparison of norepinephrine and dopamine release in rat brain by simultaneous measurements with fast-scan cyclic voltammetry. J. Neurochem. 119(5), pp. 932-944. 2011.

[48] A. E. Pereda. Electrical synapses and their functional interactions with chemical synapses. Nat. Rev. Neurosci. 15(4), pp. 250-263. 2014.

[49] M. Perry, Q. Li and R. T. Kennedy. Review of recent advances in analytical techniques for the determination of neurotransmitters. Anal. Chim. Acta 653(1), pp. 1-22. 2009.

[50] H. O. Pettit and J. B. Justice Jr. Dopamine in the nucleus accumbens during cocaine self-administration as studied by *in vivo* microdialysis. Pharmacol. Biochem. Behav. 34(4), pp. 899-904. 1989.

[51] P. E. Phillips, G. D. Stuber, M. L. Heien, R. M. Wightman and R. M. Carelli. Subsecond dopamine release promotes cocaine seeking. Nature 422(6932), pp. 614-618. 2003.

[52] S. Rahman, J. Zhang, E. A. Engleman and W. A. Corrigall. Neuroadaptive changes in the mesoaccumbens dopamine system after chronic nicotine self-administration: A microdialysis study. Neuroscience 129(2), pp. 415-424. 2004.

[53] S. Ranganathan, R. McCreery, S. M. Majji and M. Madou. Photoresist-derived carbon for microelectromechanical systems and electrochemical applications. J. Electrochem. Soc. 147(1), pp. 277-282. 2000.

[54] S. Ranganathan and R. L. McCreery. Electroanalytical performance of carbon films with near-atomic flatness. Anal. Chem. 73(5), pp. 893-900. 2001.

[55] D. C. Roberts and G. F. Koob. Disruption of cocaine self-administration following 6-hydroxydopamine lesions of the ventral tegmental area in rats. Pharmacol. Biochem. Behav. 17(5), pp. 901-904. 1982.

[56] J. G. Roberts, K. L. Hamilton and L. A. Sombers. Comparison of electrode materials for the detection of rapid hydrogen peroxide fluctuations using background-subtracted fast scan cyclic voltammetry. Analyst 136(17), pp. 3550-3556. 2011.

[57] J. G. Roberts, L. Z. Lugo-Morales, P. L. Loziuk and L. A. Sombers. Real-time chemical measurements of dopamine release in the brain. Methods Mol. Biol. 964, pp. 275-294. 2013.

[58] J. G. Roberts, B. P. Moody, G. S. McCarty and L. A. Sombers. Specific oxygen-containing functional groups on the carbon surface underlie an enhanced sensitivity to dopamine at electrochemically pretreated carbon fiber microelectrodes. Langmuir 26(11), pp. 9116-9122. 2010.

[59] D. L. Robinson, B. J. Venton, M. L. Heien and R. M. Wightman. Detecting subsecond dopamine release with fast-scan cyclic voltammetry *in vivo*. Clin. Chem. 49(10), pp. 1763-1773. 2003.

[60] D. L. Robinson and R. M. Wightman. "Rapid dopamine release in freely moving rats," in Electrochemical Methods for Neuroscience, A. C. Michael and L. M. Borland, Eds. 2007.

[61] M. Roham, D. P. Covey, D. P. Daberkow, E. S. Ramsson, C. D. Howard, P. A. Garris and P. Mohseni. A miniaturized device for wireless FSCV monitoring of dopamine in an ambulatory subject. Conf. Proc. IEEE Eng. Med. Biol. Soc., pp. 5322-5325. 2010.

[62] A. L. Sanford, S. W. Morton, K. L. Whitehouse, H. M. Oara, L. Z. Lugo-Morales, J. G. Roberts and L. A. Sombers. Voltammetric detection of hydrogen peroxide at carbon fiber microelectrodes. Anal. Chem. 82(12), pp. 5205-5210. 2010.

[63] A. C. Schmidt, X. Wang, Y. Zhu and L. A. Sombers. Carbon nanotube yarn electrodes for enhanced detection of neurotransmitter dynamics in live brain tissue. ACS Nano 2013.

[64] M. Spanos, J. Gras-Najjar, J. M. Letchworth, A. L. Sanford, J. V. Toups and L. A. Sombers. Quantitation of hydrogen peroxide fluctuations and their modulation of dopamine dynamics in the rat dorsal striatum using fast-scan cyclic voltammetry. ACS Chem. Neurosci. 4(5), pp. 782-789. 2013.

[65] E. A. Stein. fMRI: A new tool for the *in vivo* localization of drug actions in the brain. J. Anal. Toxicol. 25(5), pp. 419-424. 2001.

[66] G. D. Stuber, R. M. Wightman and R. M. Carelli. Extinction of cocaine self-administration reveals functionally and temporally distinct dopaminergic signals in the nucleus accumbens. Neuron 46(4), pp. 661-669. 2005.

[67] H. Takahashi. PET neuroimaging of extrastriatal dopamine receptors and prefrontal cortex functions. J. Physiol. Paris 107(6), pp. 503-509. 2013.

[68] P. Takmakov, M. K. Zachek, R. B. Keithley, E. S. Bucher, G. S. McCarty and R. M. Wightman. Characterization of local pH changes in brain using fast-scan cyclic voltammetry with carbon microelectrodes. Anal. Chem. 82(23), pp. 9892-9900. 2010.

[69] B. J. Venton, D. J. Michael and R. M. Wightman. Correlation of local changes in extracellular oxygen and pH that accompany dopaminergic terminal activity in the rat caudate-putamen. J. Neurochem. 84(2), pp. 373-381. 2003.

[70] N. D. Volkow, J. S. Fowler and G. J. Wang. The addicted human brain viewed in the light of imaging studies: Brain circuits and treatment strategies. Neuropharmacology 47 Suppl 1, pp. 3-13. 2004.

[71] R. M. Wightman, M. L. Heien, K. M. Wassum, L. A. Sombers, B. J. Aragona, A. S. Khan, J. L. Ariansen, J. F. Cheer, P. E. Phillips and R. M. Carelli. Dopamine release is heterogeneous within microenvironments of the rat nucleus accumbens. Eur. J. Neurosci. 26(7), pp. 2046-2054. 2007.

[72] J. E. Williams, W. Wieczorek, P. Willner and Z. L. Kruk. Parametric analysis of the effects of cocaine and cocaine pretreatment on dopamine release in the nucleus accumbens measured by fast cyclic voltammetry. Brain Res. 678(1-2), pp. 225-232. 1995.

[73] I. Willuhn, M. J. Wanat, J. J. Clark and P. E. Phillips. Dopamine signaling in the nucleus accumbens of animals self-administering drugs of abuse. Curr. Top. Behav. Neurosci. 3, pp. 29-71. 2010.

[74] G. S. Wilson and M. A. Johnson. *In-vivo* electrochemistry: What can we learn about living systems? Chem. Rev. 108(7), pp. 2462-2481. 2008.

[75] R. A. Wise. Roles for nigrostriatal--not just mesocorticolimbic--dopamine in reward and addiction. Trends Neurosci. 32(10), pp. 517-524. 2009.

[76] W. L. Woolverton, L. I. Goldberg and J. Z. Ginos. Intravenous self-administration of dopamine receptor agonists by rhesus monkeys. J. Pharmacol. Exp. Ther. 230(3), pp. 678-683. 1984.

[77] N. Xiao and B. J. Venton. Rapid, sensitive detection of neurotransmitters at microelectrodes modified with self-assembled SWCNT forests. Anal. Chem. 84(18), pp. 7816-7822. 2012.

[78] Y. Xu, J. Yan, P. Zhou, J. Li, H. Gao, Y. Xia and Q. Wang. Neurotransmitter receptors and cognitive dysfunction in Alzheimer's disease and Parkinson's disease. Prog. Neurobiol. 97(1), pp. 1-13. 2012.

[79] M. K. Zachek, P. Takmakov, B. Moody, R. M. Wightman and G. S. McCarty. Simultaneous decoupled detection of dopamine and oxygen using pyrolyzed carbon microarrays and fast-scan cyclic voltammetry. Anal. Chem. 81(15), pp. 6258-6265. 2009.

[80] M. K. Zachek, P. Takmakov, J. Park, R. M. Wightman and G. S. McCarty. Simultaneous monitoring of dopamine concentration at spatially different brain locations *in vivo*. Biosens. Bioelectron. 25(5), pp. 1179-1185. 2010.

[81] M. K. Zachek, J. Park, P. Takmakov, R. M. Wightman and G. S. McCarty. Microfabricated FSCV-compatible microelectrode array for real-time monitoring of heterogeneous dopamine release. Analyst 135(7), pp. 1556-1563. 2010.

[82] N. R. Zahniser, S. D. Dickinson and G. A. Gerhardt. High-speed chronoamperometric electrochemical measurements of dopamine clearance. Methods Enzymol. 296, pp. 708-719. 1998.

[83] X. Zhang, H. Ju, J. Wang and I. ebrary. Electrochemical sensors, biosensors and their biomedical applications. pp. 593. 2008.

CHAPTER 2

Reducing the Sampling Rate of Biochemical Measurements using Fast-Scan Cyclic Voltammetry for *In Vivo* Applications

2.1 INTRODUCTION

Biochemical signaling can be used as a reporter for tissue health and function, or to study pharmacological effects. As such, real-time biochemical measurements in functioning tissue can provide valuable insight into health and well-being, and has been an area of intense research. Electroanalytical measurements can be made *in situ* and without sample purification, making these techniques particularly well suited for real-time biochemical measurements in functioning tissue. In addition, electroanalytical sensors can be produced that are quite small, require minimal power, and are relatively inexpensive to construct [3], [29]. These advantages make electrochemical detection methods ideal for chronic and wireless monitoring of biochemical signaling in behaving animals or medical patients.

The inherent advantages of electroanalytical biochemical measurements have led to the rapid expansion of their use in neuroscience research. In this field, electrochemical techniques have been adapted and continually developed to monitor rapid fluctuations in the concentration of neurotransmitters and neuromodulators in live brain tissue. For example,

monoamines are a group of electroactive neurotransmitters involved in numerous brain functions, including voluntary movement, attention, learning, and reward [24]. The concentration of these important signaling molecules can be monitored in functioning brain tissue using electroanalytical protocols based on fast-scan cyclic voltammetry (FSCV) at carbon-fiber microelectrodes (CFMs). FSCV protocols for monitoring dopamine (DA) [5], [8] - [11], [13] - [16], [25] - [28], norepinephrine [7], [10], pH [21], [23], oxygen [23], [27], hydrogen peroxide [12], [18], [20] and serotonin [4], [5], [8] in brain tissue have been reported. In FSCV, a potential waveform is applied to the working electrode and the resulting current response is recorded. These currents are plotted versus the applied voltage as a cyclic voltammogram (CV), providing information about the redox reactions occurring at the sensor surface. The identity and concentration of the species undergoing redox reactions can be determined from peak location and magnitude, respectively [1]. For biochemical measurements, CVs are recorded at regular intervals to provide temporal information about the fluctuations in the concentrations of electroactive species. Unfortunately, the existing FSCV protocols were developed with no regard for data transfer rates or power consumption. These engineering parameters are becoming more important as there is a critical need to move to longer term experiments and to wireless systems to allow behaving animals more freedom of motion.

DA is the most commonly monitored neurotransmitter using FSCV due to its importance in guiding behaviors and its relatively high signaling concentrations *in vivo* [15]. The protocol for DA detection applies a triangular potential waveform to the sensor that

starts at -0.4 V, ramps up to +1.3 V and back down to -0.4 V at a scan rate of 400 V/s. Each scan, or CV, takes 8.5 ms to complete. For *in vivo* DA measurements, the waveform is typically applied to the sensor to sample the environment at the electrode surface every 100 ms, resulting in a 10 Hz sampling rate with 10 CVs collected per second. Typical acute experiments, both *in vitro* and *in vivo*, last several hours. Chronic experiments can last days or weeks, generating a tremendous amount of data.

In this work, the sampling rate was reduced from the standard 10 Hz to 1 Hz, and this protocol was evaluated for efficacy in monitoring DA in living brain tissue. *In vitro* studies showed that sensor responsivity and sensitivity for DA was maintained at the reduced sampling rate. Despite the reduced temporal resolution, *in vivo* experiments demonstrated that the proposed FSCV protocol was capable of monitoring dynamic fluctuations in DA concentration *in vivo*. The decreased sampling rate will reduce the overall volume of data collected and the amount of power needed to operate the electrochemical system. Power consumption was not measured in this study because the electrochemical measurements are made using a traditional bench-top potentiostat and would not accurately reflect power savings in a compact wireless low-power potentiostat. However, reducing the power and amount of data generated will assist in the miniaturization of FSCV systems, while preserving the applicability of this powerful approach for *in vivo* measurements.

2.2 METHODS

2.2.1 Materials and Chemicals

Unless noted, all chemicals were purchased from Sigma Aldrich and used as received. Phosphate buffered saline (PBS) (0.01 M Na_2HPO_4, 0.138 M NaCl, 0.0027 M KCl) was used in all flow injection experiments. Stock solutions of analyte were prepared in 0.1 N $HClO_4$, and dilutions were prepared in PBS on the day of use.

2.2.2 Microelectrode Fabrication

Single carbon fibers (Cytec Industries, Inc., Woodland Park, NJ) of 7 µm diameter were sealed in glass capillaries (A-M Systems, Sequim, WA) using a micropipette puller (Narishige International USA, Inc., East Meadow, NY). The carbon fiber extending beyond the glass insulation was cut to a length of 100 µm. The open end of the glass capillary was backfilled with electrolyte (4 M CH_3CO_2K, 150 mM KCl) and fitted with stainless steel wire for electrical contact. A Ag/AgCl reference electrode was utilized to complete the two electrode electrochemical cell (World Precision Instruments, Sarasota, FL).

2.2.3 *In Vitro* Methods

For *in vitro* experiments, both working and reference electrodes were positioned in a custom electrochemical cell housed in a Faraday cage. A continuous flow of PBS was supplied at 1 mL/min across the working and reference electrodes. Single injections of analyte were supplied to the electrodes using an HPLC valve and air actuator controlled by a

digital valve interface (Valco Instruments Co., Inc., Houston, TX). CVs were acquired using a triangular waveform ranging from -0.4 V to +1.3 V and back to -0.4 V at 400 V/s. The FSCV waveform was applied to the electrochemical cell within the flow injection apparatus using custom built instrumentation (University of North Carolina at Chapel Hill, Department of Chemistry, Electronics Facility).

2.2.4 *In Vivo* Methods

For *in vivo* experiments, male Sprague-Dawley rats (~300 g) were deeply anesthetized with sodium urethane (1.5 g/kg i.p.) and placed in a stereotaxic frame (Kopf Instrumentation, Tujunga, CA). The skull was exposed to reveal reference points (bregma and lamda) that aided leveling and electrode placement. A CFM was positioned in the caudate-putamen (CPu) (+1.2 mm AP, +1.5 mm ML, -4.5 mm DV) and a bipolar stimulating electrode was placed in the medial forebrain bundle (MFB) (-4.6 mm AP, +1.3 mm ML, -8.8 mm DV). A Ag/AgCl reference electrode was positioned in the contralateral hemisphere, relative to the CFM. The electrochemical waveform was applied to the CFM at 1 Hz to monitor electrically evoked DA fluctuations. The stimulating electrode was used to drive electrically evoked release of DA in the CPu (60 Hz, 24 pulses, 150 µA). The animal's body temperature was maintained at 37 °C by a heating pad. Animal care and use was in accordance with North Carolina State University Institutional Animal Care and Use Committee (IACUC) guidelines.

2.3 RESULTS AND DISCUSSION

2.3.1 Electrochemical Performance of CFMs at Reduced Sampling Rates

FSCV has become a common method for monitoring electroactive neurotransmitters, such as DA, in functioning tissue [15], [16], and is commonly paired with a CFM as the sensor. The typical DA protocol employed is referred herein as the "standard protocol." The standard protocol involves applying the potential waveform at a sampling rate of 10 Hz, generating 10 CVs each second. In this work, the sampling rate was reduced to 1 Hz with the goal of reducing the volume of data acquired and transferred. **Figure 2.1** outlines the work presented in this article. A potential waveform was applied from -0.4 V to +1.3 V and scanned back to -0.4 V at 400 V/s. This waveform had an 8.5 ms duration and was applied at either 10 Hz or 1 Hz to a cylindrical CFM, **Figure 2.1 (a)**. A scanning electron micrograph image of a typical glass-insulated cylindrical CFM is shown in **Figure 2.1 (b)**. The application of the potential waveform results in large non-faradaic background currents that are largely capacitive in nature and stable over short periods of time (10s of seconds). **Figure 2.1 (c)** plots representative background voltammograms collected using both the 1 Hz waveform (solid line) and the 10 Hz waveform (dashed line). The addition of an electroactive species, such as DA, induces the generation of faradaic current that is superimposed on this stable background. The background current is then subtracted from the fluctuating signal, resulting in a background-subtracted CV. The characteristics of this voltammogram serve to quantitatively identify the redox-active molecule detected. Peak intensity correlates with analyte concentration, and peak location is used in analyte identification. **Figure 2.1 (d)**

shows representative background-subtracted CVs for a 1 µM change in DA concentration collected using the 1 Hz (solid line) and 10 Hz (dashed line) sampling rates.

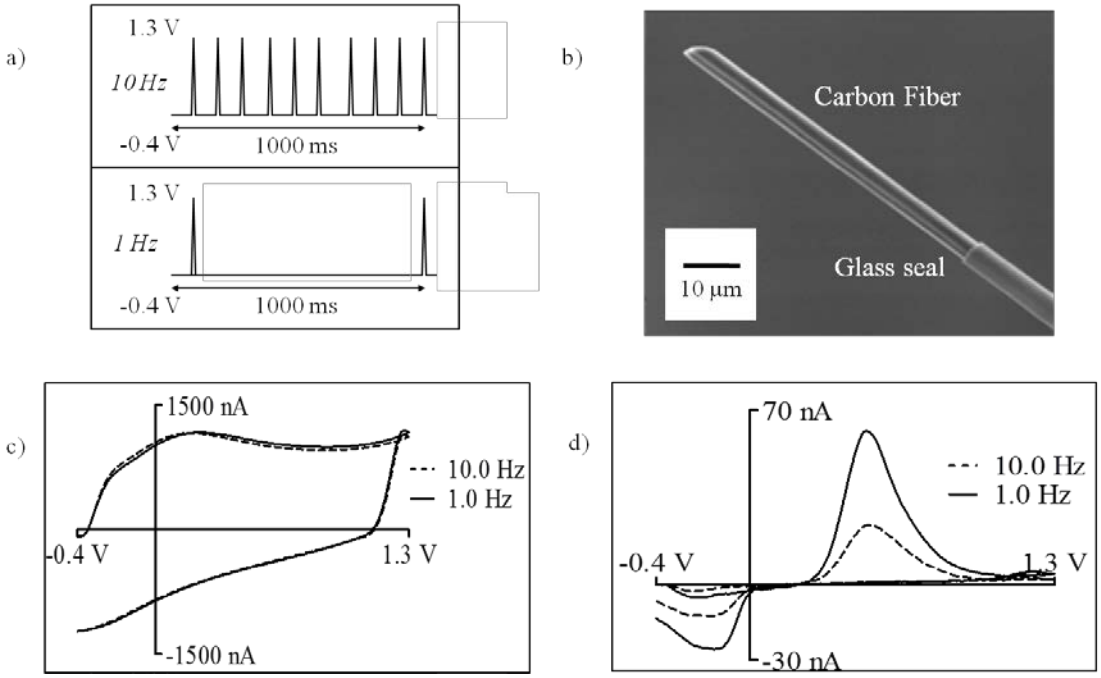

Figure 2.1 – Overview of fast-scan cyclic voltammetry. (a) Fast-scan cyclic voltammetry is applied to CFMs at the standard 10 Hz and reduced 1 Hz sampling rates for the characterization of monoamines. (b) Scanning electron micrograph of a typical CFM. (c) Representative background CVs collected using 10 Hz and 1 Hz sampling rates. (d) Background-subtracted CVs for 1 µM DA collected using the standard and reduced sampling rates.

To evaluate the effect of sampling rate on the responsivity of the sensing protocol for DA, four sampling rates (0.5, 1, 5, and 10 Hz) were tested. Physiological changes in concentrations of monoamines in the body occur on the second-to-sub-second time scale [15]. Sampling rates were selected to encompass the expected requirements to monitor

physiological monoamine signaling. In the flow injection apparatus, a CFM was immersed in a flowing solution that was rapidly changed from PBS to a solution of 1 μM DA in PBS. **Figure 2.2** shows representative background-subtracted CVs for a 1 μM change in DA using the four chosen sampling rates, including the standard 10 Hz rate. All three sampling rates tested against the standard rate of 10 Hz elicited an increased current response to DA. This increase can be explained by the increased time available for DA to adsorb to the surface of the CFM between sampling points. This adsorption is dependent on electrode charge and surface chemistry [2], [6], [14]. Sampling rates of 0.5, 1, 5, and 10 Hz result in 1991.5, 991.5, 191.5, and 91.5 ms available for adsorption to the carbon surface, respectively. However, a diminished current response was observed using a sampling rate of 0.5 Hz when compared to the 1 Hz sampling rate. The carbon surface has been shown to "renew" itself in a self-cleaning process when the electrode experiences sufficiently anodic potentials (~1.3V) [22]. We speculate that the sensor is susceptible to more fouling at the 0.5 Hz sampling rate, because it experiences less time at higher potentials. Examining peak anodic current in the CV, it was determined that the 1 Hz sampling rate had an average responsivity for DA of 105 ± 5 nA/μM, compared to 62 ± 12 nA/μM at 0.5 Hz, 56 ± 11 nA/μM at 5 Hz, and 27 ± 5 nA/μM at the standard 10 Hz sampling rate (n = 5 electrodes, values are given as the average ± the standard deviation).

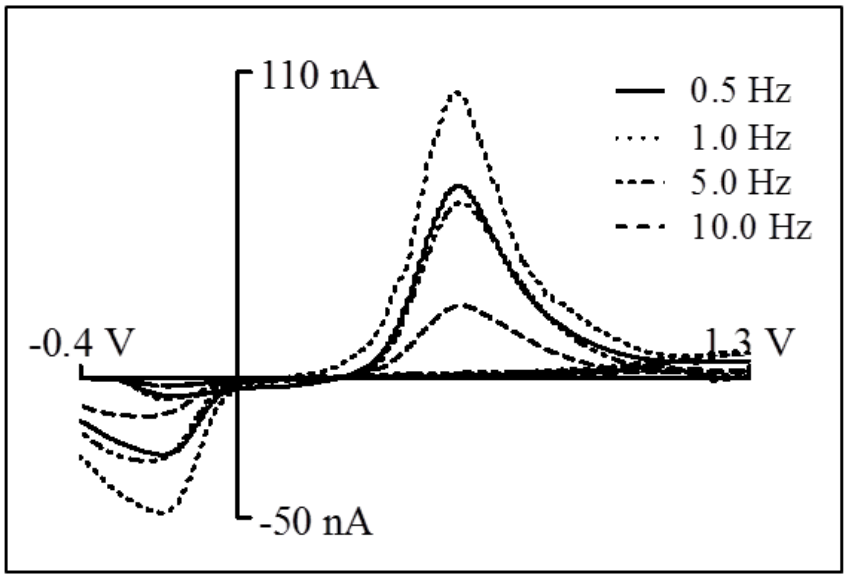

Figure 2.2 –Characterization of various sampling rates. Average background-subtracted CVs for 1 µM dopamine collected at 4 different sampling rates. These were investigated to determine the lowest rate that could be used without compromising the responsivity of the sensor.

Additionally, the limit of detection (LOD) for DA was calculated as 3 times the root mean squared (RMS) noise for each of the sampling rates investigated. All sampling rates exhibited a LOD of 3 - 5 nM. While some variation in the detection limit was observed, the small differences were not statistically significant (n = 5 electrodes, p = 0.26, 2-tailed, paired Student's t-test). The 1 Hz sampling rate was chosen for further *in vitro* and *in vivo* study, given that the responsivity was increased and the LOD was unaffected.

2.3.2 Selectivity of CFMs at Reduced Sampling Rate

After verifying that the 1 Hz sampling rate maintained the necessary responsivity and LOD for *in vitro* studies, the reduced sampling rate was tested for chemical selectivity.

Several biologically relevant analytes (hydrogen peroxide (H2O2), pH, adenosine, ascorbic acid, and 3,4-dihydroxyphenylacetic acid (DOPAC)) were evaluated to verify that they could be effectively distinguished from DA and determine any correlation between their electrochemical properties and those of DA. **Figure 2.3** shows the background-subtracted CVs for these analytes collected at the reduced sampling rate (1 Hz), as compared to the standard sampling rate (10 Hz).

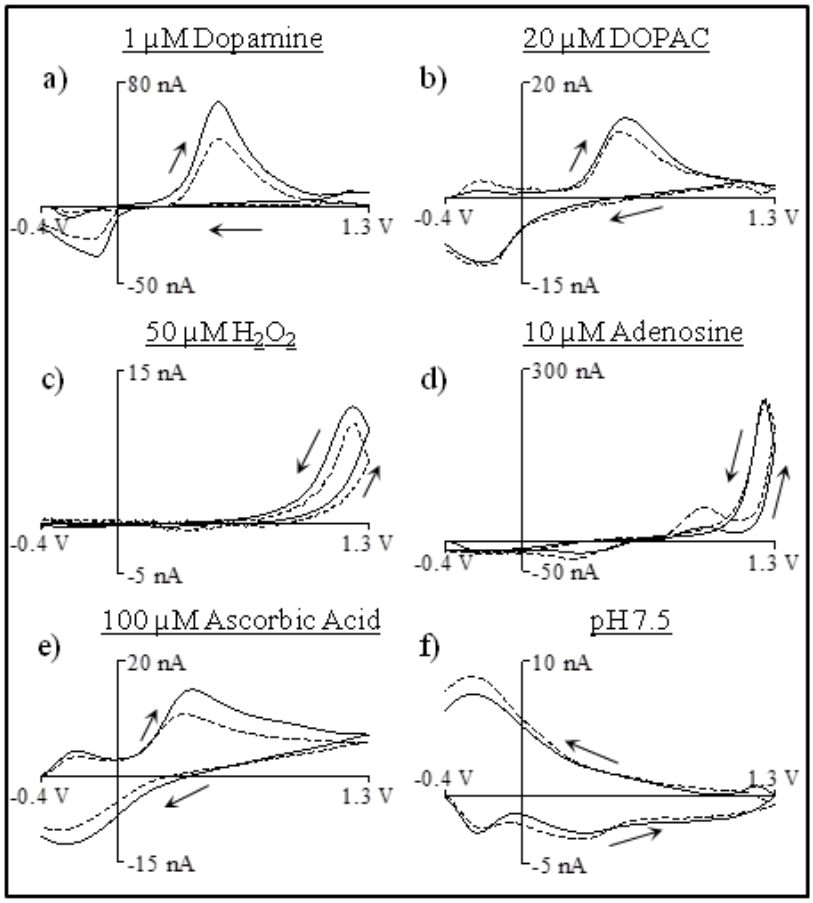

Figure 2.3 – Selectivity of reduced sampling rate. Representative background-subtracted CVs for several biologically relevant analytes collected at a CFM using a sampling rate of 1 Hz (solid line) and 10 Hz (dashed line). Arrows indicate direction of the scan.

Table 2.1 lists the correlation factors calculated for a comparison of the voltammogram for each analyte to that of DA, using both sampling rates (n = 5 electrodes, values are given as the average ± the standard deviation). A correlation factor of 1 represents an exact match, and lower correlation factors indicate voltammetric discrimination between species. DOPAC and ascorbic acid have CVs that are somewhat similar to the voltammogram for DA; thus the correlation factors are much higher than those generated when comparing the voltammograms for adenosine and hydrogen peroxide to that of DA. These molecules exhibit significantly different redox chemistry. Importantly, the correlation factors were consistent for both sampling rates across all analytes tested, and were similar to those previously reported [6], [19]. From these findings, it was concluded that the reduced sampling rate did not compromise the chemical selectivity of the voltammetric approach to molecular monitoring.

Table 2.1 – Correlation factors quantifying voltammetric discrimination between species.

	DOPAC	Ascorbic Acid	Adenosine	H_2O_2	pH
1 Hz	0.85 ± 0.03	0.64 ± 0.02	0.020 ± 0.005	0.0 ± 0.0	0.44 ± 0.03
10 Hz	0.89 ± 0.03	0.71 ± 0.03	0.010 ± 0.005	0.0 ± 0.0	0.41 ± 0.03

2.3.3 Stability

Typical *in vivo* experiments can span several hours, so a reliable *in vivo* measurement protocol requires stable analyte detection for at least this time frame. The stability of the reduced sampling rate was tested *in vitro* against the standard sampling rate over the course

of six hours, using an *in vitro* flow injection apparatus. PBS was continuously supplied and several short injections of DA were presented to the sensor every fifteen minutes. Representative data from three time points comparing 10 Hz and 1 Hz sampling rates are shown in **Figures 2.4 (a)** and **2.4 (b)**, respectively. There was no significant change in sensor performance observed over this time period. **Figure 2.4 (c)** shows the current response of the sensor over a six hour time period when scanning at 1 Hz. These data verify the stability of the sensor at the reduced scanning rate, further demonstrating the utility of this protocol. Small variations in current response are typical in long-term experiments, and can be attributed to changes in the surface chemistry of the sensor. However, a paired t-test between time 0 and time 6 hours showed that the difference in current response over this time period was not significant (n = 6 electrodes, p = 0.51, 2-tailed, paired Student's t-test).

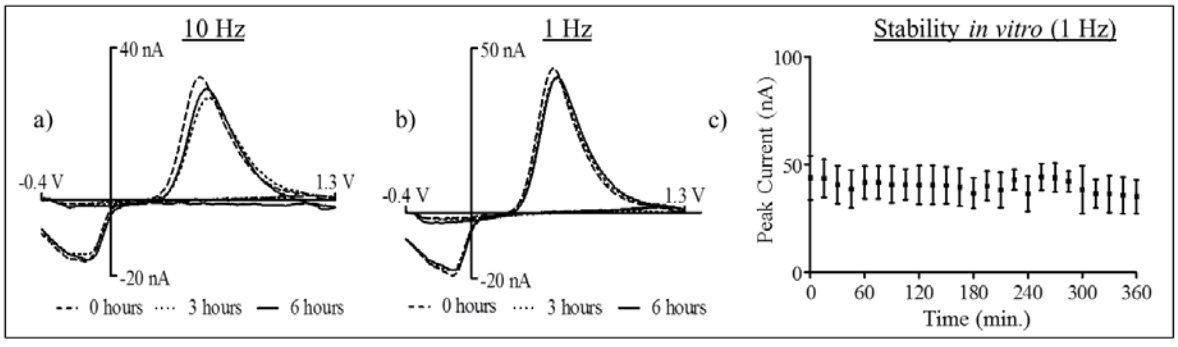

Figure 2.4 – Stability of reduced sampling rate *in vitro*. Representative background-subtracted CVs of 1 µM dopamine characterizing 0, 3 and 6 hours of electrochemically cycling at a sampling rate of 10 Hz (a), and 1 Hz (b). (c) *In vitro* peak current response of CFM (n = 6 electrodes, 15 min interval) to 1 µM dopamine when sampling at 1 Hz over six hour experiment (p = 0.51, Student's t-test).

2.3.4 *In Vivo* Experiments

Since the *in vitro* results suggested that the reduced sampling rate protocol had the required criteria, it was necessary to verify *in vivo* performance. A CFM electrode was implanted in the CPu of an anesthetized rat and electrically elicited DA release was monitored over a period of eight hours using a 1 Hz sampling rate. **Figure 2.5 (a)** overlays representative CVs for the detection of DA using 1 Hz collected at the beginning and end of the experiment, demonstrating minimal decrease in current. These current responses were converted to concentration using a typical post-calibration procedure [13]. **Figure 2.5 (b)** plots the fluctuations in DA concentration detected over 8 hours for both the 1 Hz and 10 Hz rates. Both rates exhibit minimal decrease in current response over the time period. The difference in detected concentration between the two rates is not a reflection of the sampling rate but of the use of separate animals for each rate tested. These data verify the performance of the reduced sampling rate for *in vivo* measurements of DA.

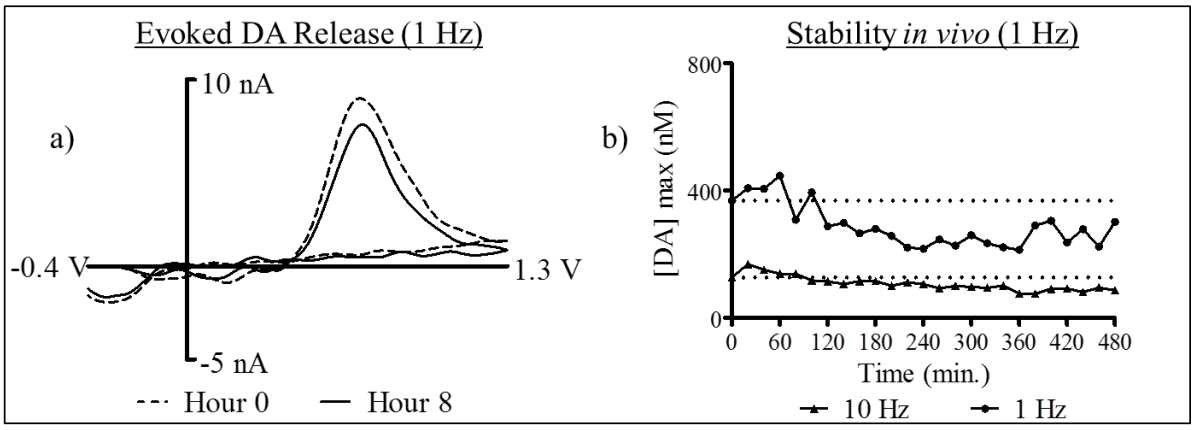

Figure 2.5 – *In vivo* characterization of reduced sampling rate. (a) Background-subtracted CVs for evoked dopamine release in the CPu, taken at 0 and 8 hours using a sampling rate of 1 Hz. (b) A line graph plotting the amplitude of electrically evoked DA release over time for the 1 Hz and 10 Hz sampling rates. Concentration changes were measured every fifteen minutes. The dotted line represents the amplitude of the first data point.

2.4 CONCLUSIONS

The results demonstrate that *in vitro* and *in vivo* DA fluctuations can be monitored using a reduced sampling rate, with minimal impact on measurement performance. The quantity of data collected and transferred per second is reduced by an order of magnitude compared to the standard protocol by using this reduced sampling rate. We expect that this reduction will facilitate chronic and wireless biochemical measurement systems without compromising the quantitative and qualitative performance of this approach to *in vivo* molecular monitoring. This work lays a foundation for future studies of power consumption during experimentation, including the development and integration of hardware to monitor real-time power usage. By duty cycling the sensor during the measurements, it is expected

that the power consumption can be reduced by an order of magnitude compared to the standard protocol.

2.5 REFERENCES

[1] A. J. Bard and L. R. Faulkner. *Electrochemical Methods: Fundamentals and Applications,* 2nd ed. New York, John Wiley & Sons. 2001.

[2] B. D. Bath, D. J. Michael, B. J. Trafton, J. D. Joseph, P. L. Runnels and R. M. Wightman. Subsecond adsorption and desorption of dopamine at carbon-fiber microelectrodes. *Anal. Chem.72(24),* pp. 5994-6002. 2000.

[3] J. D. Bronzino and R. C. Dorf. *The Biomedical Engineering Handbook*, 2nd ed. Boca Raton, CRC Press. 1999.

[4] E. C. Dankoski and R. M. Wightman. Monitoring serotonin signaling on a subsecond time scale. *Front. Integr. Neurosci.7* pp. 44. 2013.

[5] P. Hashemi, E. C. Dankoski, R. Lama, K. M. Wood, P. Takmakov and R. M. Wightman. Brain dopamine and serotonin differ in regulation and its consequences. *Proc. Natl. Acad. Sci. U. S. A.109(29),* pp. 11510-11515. 2012.

[6] M. L. Heien, P. E. Phillips, G. D. Stuber, A. T. Seipel and R. M. Wightman. Overoxidation of carbon-fiber microelectrodes enhances dopamine adsorption and increases sensitivity. *Analyst128(12),* pp. 1413-1419. 2003.

[7] N. R. Herr, J. Park, Z. A. McElligott, A. M. Belle, R. M. Carelli and R. M. Wightman. *In vivo* voltammetry monitoring of electrically evoked extracellular norepinephrine in subregions of the bed nucleus of the striaterminalis. *J. Neurophysiol.107(6),* pp. 1731-1737. 2012.

[8] C. E. John and S. R. Jones. "Fast scan cyclic voltammetry of dopamine and serotonin in mouse brain slices," in *Electrochemical Methods for Neuroscience,* A. C. Michael and L. M. Borland, Eds. 2007.

[9] R. B. Keithley, P. Takmakov, E. S. Bucher, A. M. Belle, C. A. Owesson-White, J. Park and R. M. Wightman. Higher sensitivity dopamine measurements with faster-scan cyclic voltammetry. *Anal. Chem.83(9),* pp. 3563-3571. 2011.

[10] J. Park, P. Takmakov and R. M. Wightman. *In vivo* comparison of norepinephrine and dopamine release in rat brain by simultaneous measurements with fast-scan cyclic voltammetry. *J. Neurochem.119(5),* pp. 932-944. 2011.

[11] J. Park, R. A. Wheeler, K. Fontillas, R. B. Keithley, R. M. Carelli and R. M. Wightman. Catecholamines in the bed nucleus of the striaterminalis reciprocally respond to reward and aversion. *Biol. Psychiatry71(4),* pp. 327-334. 2012.

[12] J. G. Roberts, K. L. Hamilton and L. A. Sombers. Comparison of electrode materials for the detection of rapid hydrogen peroxide fluctuations using background-subtracted fast scan cyclic voltammetry. *Analyst136(17),* pp. 3550-3556. 2011.

[13] J. G. Roberts, L. Z. Lugo-Morales, P. L. Loziuk and L. A. Sombers. Real-time chemical measurements of dopamine release in the brain. *Methods Mol. Biol.964* pp. 275-294. 2013.

[14]J. G. Roberts, B. P. Moody, G. S. McCarty and L. A. Sombers. Specific oxygen-containing functional groups on the carbon surface underlie an enhanced sensitivity to dopamine at electrochemically pretreated carbon fiber microelectrodes. *Langmuir26(11),* pp. 9116-9122. 2010.

[15] D. L. Robinson, B. J. Venton, M. L. Heien and R. M. Wightman. Detecting subsecond dopamine release with fast-scan cyclic voltammetry *in vivo*. *Clin. Chem.49(10),* pp. 1763-1773. 2003.

[16] D. L. Robinson and R. M. Wightman. "Rapid dopamine release in freely moving rats," in *Electrochemical Methods for Neuroscience,* A. C. Michael and L. M. Borland, Eds. 2007.

[17] M. Roham, D. P. Covey, D. P. Daberkow, E. S. Ramsson, C. D. Howard, P. A. Garris and P. Mohseni. A miniaturized device for wireless FSCV monitoring of dopamine in an ambulatory subject. *Conf. Proc. IEEE Eng. Med. Biol. Soc.2010* pp. 5322-5325. 2010.

[18] A. L. Sanford, S. W. Morton, K. L. Whitehouse, H. M. Oara, L. Z. Lugo-Morales, J. G. Roberts and L. A. Sombers. Voltammetric detection of hydrogen peroxide at carbon fiber microelectrodes. *Anal. Chem.82(12),* pp. 5205-5210. 2010.

[19] A. C. Schmidt, X. Wang, Y. Zhu and L. A. Sombers. Carbon nanotube yarn electrodes for enhanced detection of neurotransmitter dynamics in live brain tissue. *ACS Nano7(9),* pp. 7864-7873. 2013.

[20] M. Spanos, J. Gras-Najjar, J. M. Letchworth, A. L. Sanford, J. V. Toups and L. A. Sombers. Quantitation of hydrogen peroxide fluctuations and their modulation of dopamine dynamics in the rat dorsal striatum using fast-scan cyclic voltammetry. *ACS Chem. Neurosci.4(5),* pp. 782-789. 2013.

[21] P. Takmakov, M. K. Zachek, R. B. Keithley, E. S. Bucher, G. S. McCarty and R. M. Wightman. Characterization of local pH changes in brain using fast-scan cyclic voltammetry with carbon microelectrodes. *Anal. Chem.82(23),* pp. 9892-9900. 2010.

[22] P. Takmakov, M. K. Zachek, R. B. Keithley, P. L. Walsh, C. Donley, G. S. McCarty and R. M. Wightman. Carbon microelectrodes with a renewable surface. *Anal. Chem.82(5),* pp. 2020-2028. 2010.

[23]B. J. Venton, D. J. Michael and R. M. Wightman. Correlation of local changes in extracellular oxygen and pH that accompany dopaminergic terminal activity in the rat caudate-putamen. *J. Neurochem. 84(2),* pp. 373-381. 2003.

[24] R. A. Webster. *Neurotransmitters, Drugs, and Brain Function,* 1st ed. Chichester, John Wiley & Sons. 2001.

[25] R. M. Wightman, M. L. Heien, K. M. Wassum, L. A. Sombers, B. J. Aragona, A. S. Khan, J. L. Ariansen, J. F. Cheer, P. E. Phillips and R. M. Carelli. Dopamine release is heterogeneous within microenvironments of the rat nucleus accumbens. *Eur. J. Neurosci.26(7),* pp. 2046-2054. 2007.

[26] M. K. Zachek, J. Park, P. Takmakov, R. M. Wightman and G. S. McCarty. Microfabricated FSCV-compatible microelectrode array for real-time monitoring of heterogeneous dopamine release. *Analyst 135(7),* pp. 1556-1563. 2010.

[27] M. K. Zachek, P. Takmakov, B. Moody, R. M. Wightman and G. S. McCarty. Simultaneous decoupled detection of dopamine and oxygen using pyrolyzed carbon microarrays and fast-scan cyclic voltammetry. *Anal. Chem. 81(15),* pp. 6258-6265. 2009.

[28] M. K. Zachek, P. Takmakov, J. Park, R. M. Wightman and G. S. McCarty. Simultaneous monitoring of dopamine concentration at spatially different brain locations *in vivo*. *Biosens. Bioelectron. 25(5),* pp. 1179-1185. 2010.

[29] X. Zhang, H. Ju, J. Wang. *Electrochemical Sensors, Biosensors and their Biomedical Applications,* 1st ed. San Diego, Elsevier Inc. 2008.

CHAPTER 3

Evaluation of a Reduced Data Density in Fast-Scan Cyclic Voltammetry Measurements of Biochemical Signaling

This work was completed in collaboration with: Lingjiao Qi, James G. Roberts, Leslie A. Sombers and Gregory S. McCarty, and is in preparation for submission to *Analytical Chemistry*.

3.1 INTRODUCTION

Biochemical measurements are important measurements for detailing tissue function and health and have significance in the investigation of various neurodegenerative disorders. Monitoring real-time biochemical measurements in living tissue has been extensively studied in recent years in numerous biomedical research applications. Electroanalytical detection techniques are very compatible with these types of measurements as they utilize small, inexpensive sensors and provide fast temporal resolution [3], [25], [33]. These benefits make electroanalytical detection an excellent choice for chronic monitoring of biochemical signaling and for use in behaving animals.

Electroanalytical techniques have quickly become commonplace in neuroscience research for observing fluctuations in the concentrations of various electroactive neurotransmitters and other molecules present in functioning tissue. These electroactive molecules impact various brain functions, including reward, voluntary movement and learning [26], [29]. Electroanalytical monitoring of these neurotransmitters can be done using

an existing *in vivo* measurement technology, FSCV, with a carbon-fiber microelectrode (CFM) as the sensor. With FSCV, the change in concentration of many electroactive molecules can be recorded and displayed. FSCV protocols for measuring DA [5], [9], [11], [14], [15], [17] – [20], [27], [30] – [32], hydrogen peroxide [16], [21], [23], oxygen [25], [31], norepinephrine [8], [14], serotonin [4], [5] and pH [24], [25] have all be reported. In FSCV, a potential waveform is applied to a working electrode, generating a current response. The recorded currents are typically displayed versus the applied potential as a cyclic voltammogram (CV). CVs offer valuable insight into the redox reactions that occur at the surface of the electrode by creating a chemical fingerprint of the molecule. This fingerprint contains both the identity and concentration of the species derived from the peak location and magnitude, respectively [2]. FSCV has been utilized *in vivo* for many years. As this technology moves toward longer-term experiments and use in freely moving animals, there is a need to improve the engineering performance of FSCV. Existing FSCV protocols were developed initially for use in narrowly defined, acute experimentation, thus little consideration was placed on data transfer requirements. In a typical experiment the electrochemical information is oversampled leading to large volumes of data. Limitations in data transfer hinders the ability to move towards a system that takes measurements over a longer period of time as well as the application of a wireless system that would provide animals greater freedom of motion.

One of the commonly monitored molecules using FSCV is dopamine (DA), due to its behavioral importance and high concentrations *in vivo* [19]. We have previously reported a

protocol for monitoring DA using FSCV [1]. A triangular potential waveform between -0.4 V and +1.3 V is applied to the sensor and each potential scan, or CV, takes 8.5 ms to complete. Typical *in vivo* measurements sample at a rate of 10 Hz, resulting in 10 CVs collected per second. Monitoring the biological function of DA and other molecules can involve experiments that last several hours, days or weeks, collecting immense amounts of data. We have previously described a protocol that reduces the sampling rate to 1 Hz compared to a standard 10 Hz rate for moderating the amount of data generated without compromising the applicability of FSCV for *in vivo* biochemical measurements [1]. In this work, the experimental FSCV parameters that contribute to the amount of data collected are evaluated to understand their impact on the performance of the FSCV measurement. Here, the data density, or number of data points per CV, is reduced below the standard 850 pts/CV. Additionally, protocols featuring combinations of reduced sampling rate and reduced data density were evaluated for efficacy of observing DA in living tissue. Decreasing the sampling rate and data density drastically reduces the overall volume of data collected, enabling much longer experimental files to be collected without generating massive data files. The reduction of experimental data density will play a role in the creation of practical chronic wireless measurement systems where power consumption and data transfer rates become critical system parameters.

3.2 METHODS

3.2.1 Materials and Chemicals

Unless noted, all chemicals were purchased from Sigma Aldrich and used as received. Phosphate buffered saline (PBS) (10 mM Na_2HPO_4, 138 mM NaCl, 2.7 mM KCl) and Tris buffer (15 mM Tris, 3.25 mM KCl, 1.2 mM $CaCl_2$, 1.2 mM $MgCl_2$, 2 mM Na_2SO_4, 1.25 mM NaH_2PO_4, 145 mM NaCl) were used in flow injection experiments. Stock solutions of analyte were prepared in 0.1 N $HClO_4$, and dilutions were prepared in either PBS or Tris buffer on the day of use.

3.2.2 Microelectrode Fabrication

Single carbon fibers (Cytec Industries, Inc., Woodland Park, NJ) of 7 µm in diameter were sealed in glass capillaries (A-M Systems, Sequim, WA) using a micropipette puller (Narishige International USA, Inc., East Meadow, NY). The carbon fiber extending beyond the glass seal was cut to a length of 100 µm. The open end of the glass capillary was backfilled with electrolyte (4 M KCH_3CO_2, 150 mM KCl) and fitted with stainless steel wire for electrical contact. Silver/silver chloride (Ag/AgCl) (World Precision Instruments, Sarasota, FL) was used as a reference electrode.

3.2.3 *In Vitro* Methods

For *in vitro* experiments, both working and reference electrodes were positioned in a custom electrochemical cell housed in a Faraday cage. A continuous flow of buffer was

supplied at 1 mL/min across the working and reference electrodes. Single injections of analyte were supplied to the electrodes using an HPLC valve and air actuator controlled by a digital valve interface (Valco Instruments Co., Inc., Houston, TX). CVs were acquired using a triangular waveform ranging from -0.4 V to +1.3 V and back to -0.4 V at 400 V/s. The FSCV waveform was applied to the electrochemical cell within the flow injection apparatus using a custom built instrument (University of North Carolina at Chapel Hill, Department of Chemistry, Electronics Facility).

3.2.4 *Ex Vivo* Methods

For *ex vivo* methods, male Sprague-Dawley rats (300 - 500 g, Charles River Laboratories, Raleigh, NC) were anesthetized with urethane (4 g/kg i.p.) before decapitation to rapidly remove the brain. Coronal slices (400 µm thick) containing the striatum were prepared using a vibratome (World Precision Instruments, Sarasota, FL). Slices were incubated in aCSF buffer (1.24 mM NaCl, 3.7 mM KCl, 2.6 mM $NaHCO_3$, 2.4 mM $CaCl_2$, 1.3 mM $MgCl_2$, 1.3 mM NaH_2PO_4, 10 mM Glucose) with 20 mM HEPES, at pH 7.4, continually saturated with 95 % O_2, 5 % CO_2, and allowed to equilibrate in buffer for 45 minutes. Slices were then placed in a heated recording chamber (Warner Instruments, Hamden, CT) and superfused with aCSF at 34 °C to perform electrochemical measurements. DA was detected in the caudate putamen (CPu) (1.2 mm anterior to bregma) using a standard CFM. Neurotransmitter release was electrically evoked using a biphasic constant current pulse (400 µA, 2 ms each pulse, 5 pulses, 60 Hz) delivered by a bipolar stimulating electrode

(FHC Inc., Bowdoin, ME). The working electrode and stimulating electrode placements were made with the aid of a microscope (Nikon Instruments, Inc., Melville, NY), and the electrodes were positioned ~50 μm below the surface of the slice. The tip of the CFM was located 1 mm away from the stimulating electrode. All procedures were performed in accordance with the North Carolina State University Institutional Animal Care and Use Committee (IACUC).

3.3 RESULTS AND DISCUSSION

3.3.1 Electrochemical Performance of Microelectrodes at Reduced Sampling Rates and Data Densities

FSCV is a common technique used to observe neurotransmitters in functioning tissue [19], [22], [28]. DA is a commonly monitored neurotransmitter detected with a widely-used FSCV protocol and a CFM sensor [19]. This standard protocol utilizes a potential waveform applied at a sampling rate of 10 Hz, collecting 10 CVs per second with 850 data points collected per CV. The goal of this work is to understand the implications of the number of data points collected per second on the performance of the FSCV technique for monitoring common biological analytes. Reducing the amount of data acquired and transferred has the potential of increasing the applicability of FSCV in chronic measurements. **Figure 3.1** outlines the application of FSCV using various sampling rates and data densities. A potential waveform is applied from -0.4 V to +1.3 V and back to -0.4 V to a standard CFM at 20 Hz, 10 Hz, 3 Hz or 1 Hz, **Figure 3.1 (a)**. This application results in 20, 10, 3, or 1 CV collected

every second. Additionally, each CV collected is comprised of 850, 250 or 100 data points, **Figure 3.1 (b)**. **Figure 3.1 (c)** plots the large, acutely stable background current generated by the application of the potential waveform to the CFM and the resulting background-subtracted CV after an electroactive species, such as DA, is introduced. Introduction of this species causes current fluctuations that are superimposed on the background. Once the background is subtracted out, the background-subtracted CV gives a characteristic fingerprint of the oxidation and reduction of the molecule. **Figures 3.1 (d, e)** show representative background-subtracted CVs for a 1µM change in DA concentration at varying sampling rates (20, 10, 3, 1 Hz) and data densities (850, 250, 100 pts/CV), respectively. We have previously reported how varying the sampling rate affects the responsivity of the sensor to DA [1]. In this work, we are investigating the impact of reducing the data density as well as the simultaneous reduction of sampling rate and data density on the electrochemical performance.

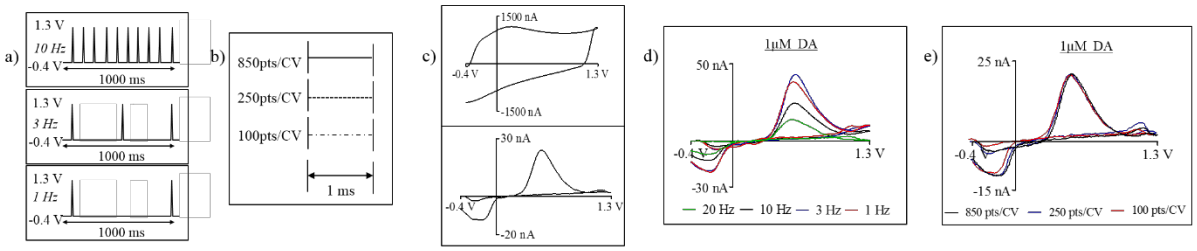

Figure 3.1 – Fast-scan cyclic voltammetry applied at varying sampling rates and data densities for the characterization of dopamine. FSCV can be applied at varying sampling rates (a) and with varying data densities (b) to a CFM for the characterization of monoamines. (c) Representative background CV (top) and background-subtracted CV for 1 μM DA (bottom). (d) Representative background-subtracted CVs for 1 μM DA at 20 Hz, 10 Hz, 3 Hz, and 1 Hz sampling rates and with (e) data densities of 850 pts/CV, 250 pts/CV, and 100 pts/CV.

3.3.2 Selectivity of Microelectrodes at Reduced Data Densities

In order to determine the effect of a reduced data density on the electrochemical performance of the protocol, several reduced data densities were evaluated against the standard 850 pts/CV for responsivity to 1μM DA. In these initial experiments, DA responsivity was evaluated versus points per CV. The collection of CVs with less than 100 data points caused significant reductions in the responsivity, **Figure 3.2 (a)**. Values are plotted as average ± standard deviation (n = 5). For this reason, 100 data points per CV is the fewest number presented in the remainder of this work.

Responsivity to DA and several other biologically-relevant analytes (3, 4-dihydroxyphenylacetic acid (DOPAC), hydrogen peroxide (H2O2), ascorbic acid and pH was evaluated at the standard and reduced data densities. **Figures 3.2 (b - f)** show the

background-subtracted CVs for various analytes run with a 10 Hz sampling rate at the standard and reduced data densities.

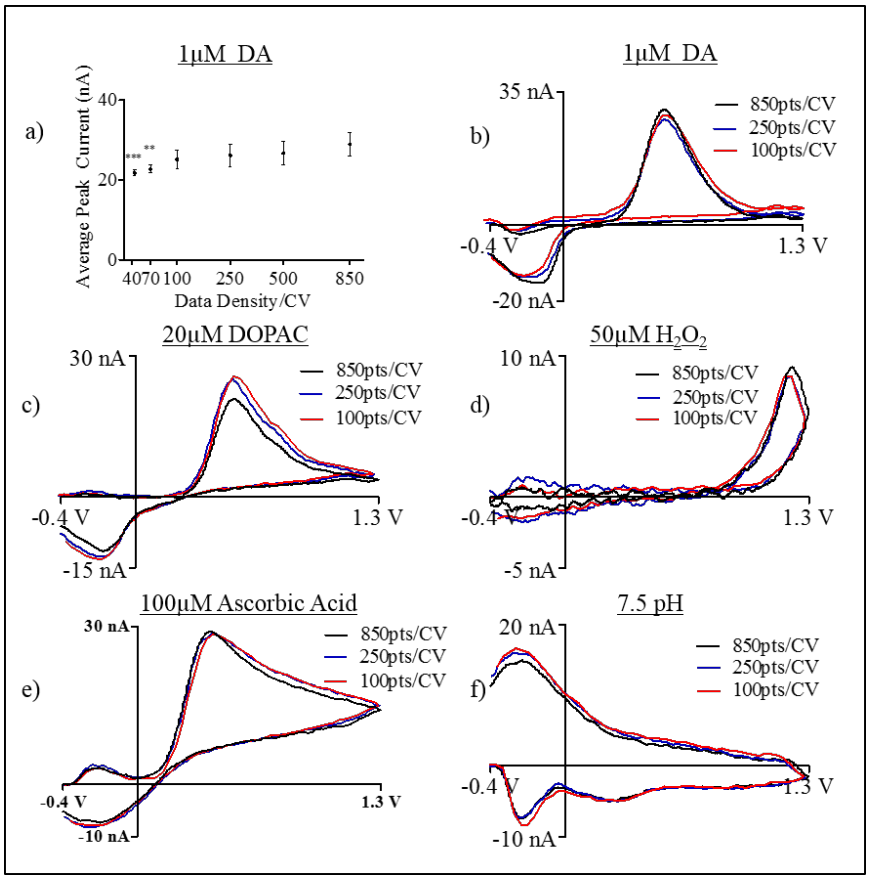

Figure 3.2 – Reducing data density does not compromise selectivity. (a) Average current response to 1 µM DA for various data densities (n = 5). Data densities of 40 and 70 pts/CV show statistical difference compared to standard density of 850 pts/CV ($p < 0.001$ and $p < 0.01$, respectively, ANCOVA). (b - f) Representative background-subtracted CVs for several biologically relevant analytes collected at a CFM using a sampling rate of 10 Hz with either 850pts/CV, 250 pts/CV, or 100 pts/CV. Arrows indicate direction of the scan. CVs shown for (b) 1 µM dopamine, (c) 20 µM 3,4-dihydroxyphenylacetic acid, (d) 50 µM hydrogen peroxide, (e) 100 µM ascorbic acid, (f) pH 7.5 in PBS solution.

Figure 3.3 gives results of a common statistical technique, principal component regression (PCR), for four additional analytes tested. PCR is a common technique that uses known concentrations of analyte species and tests them against collected CV responses [6], [10], [12], [13]. Varying concentrations of each analyte were injected in separate solutions and CVs were recorded. PCR was then used to evaluate the species present and its concentration. Each graph depicts the known concentration of analyte versus the predicted concentration of analyte determined by PCR for each data density tested. The slopes of the regressions lines for each data density tested are given by the average ± standard deviation and unity slope is given by the diagonal line. No statistical significant differences were found between any of the data densities tested and unity slope (n = 4, ANCOVA). PCR accurately predicted concentrations for each analyte species at the standard 850 pts/CV and both reduced data densities tested. These data show that a reduction in data density of 250 pts/CV and 100 pts/CV compared to the standard 850 pts/CV does not compromise chemical selectivity.

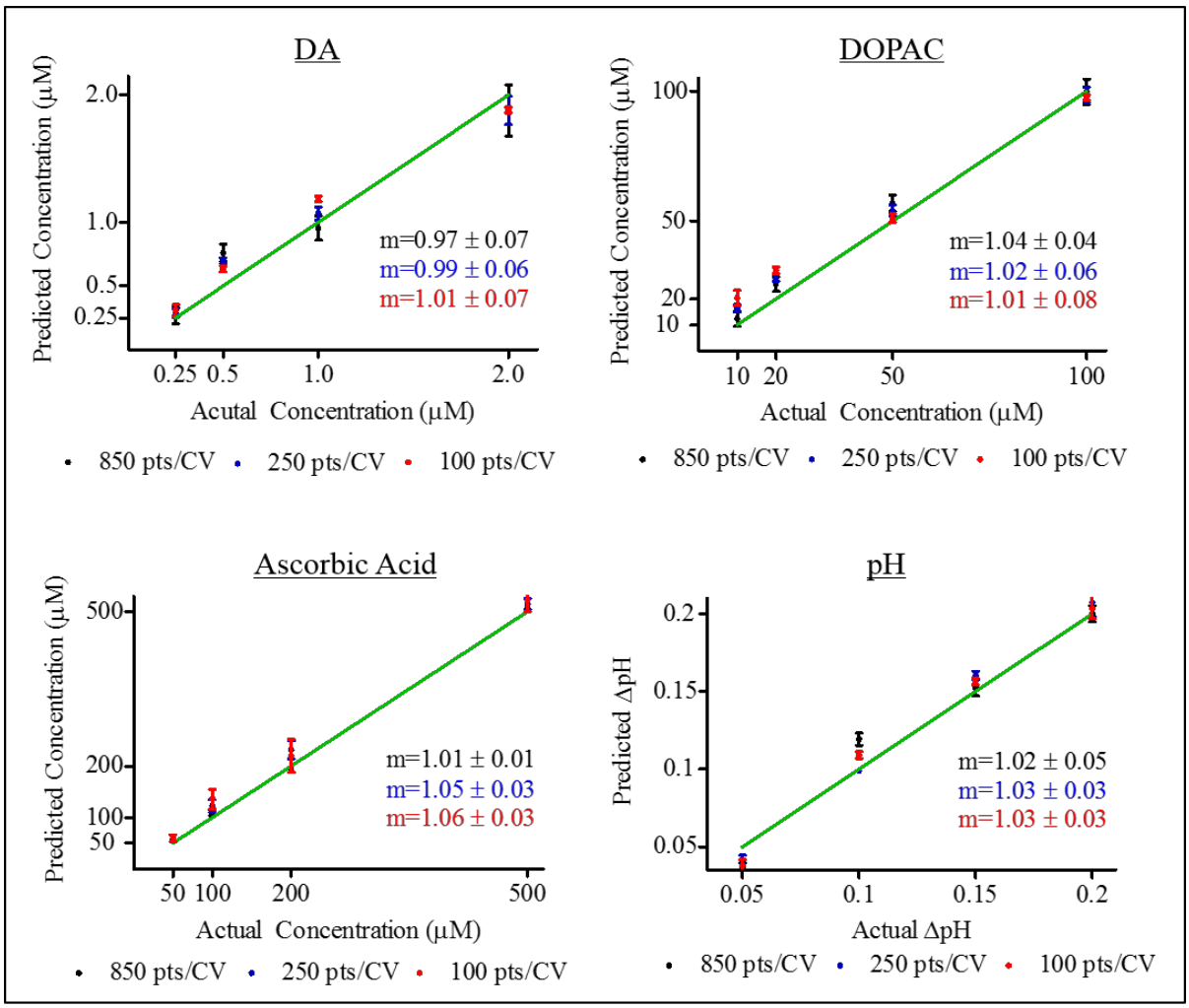

Figure 3.3 – Verifying chemical selectivity with statistics. Known concentrations of analytes compared to concentrations evaluated by PCR for the collected 850 pts/CV, 250 pts/CV and 100 pts/CV. The slopes of the regression lines were determined to be 0.97 ± 0.07 for dopamine at 850 pts/CV (r^2 = 0.97), 0.99 ± 0.06 (r^2 = 0.99) at 250 pts/CV and 1.01 ± 0.07 (r^2 = 0.98) at 100 pts/CV; 1.04 ± 0.04 (r^2 = 0.99) for DOPAC at 850 pts/CV, 1.02 ± 0.06 (r^2 = 0.99) at 250 pts/CV and 1.01 ± 0.08 (r^2 = 0.99) at 100 pts/CV; 1.01 ± 0.01 (r^2 = 0.99) for ascorbic acid at 850 pts/CV, 1.05 ± 0.03 (r^2 = 0.99) at 250 pts/CV and 1.06 ± 0.03 (r^2 = 0.99) at 100 pts/CV; 1.02 ± 0.05 (r^2 = 0.96) for a change in pH at 850 pts/CV, 1.03 ± 0.03 (r^2 = 0.99) at 250 pts/CV and 1.03 ± 0.03 (r^2 = 0.98) at 100 pts/CV. Error bars represent standard deviation (n = 4). The diagonal lines represent unity slope.

3.3.3 Sensitivity of Microelectrodes to Dopamine using Reduced Parameters

After verifying the reduced data densities maintained the necessary responsivity and selectivity of the standard protocol, the sensitivity of experimental protocols with varying data density and protocols with varying sampling rate was determined for DA, **Figure 3.4**. Four concentrations of DA were tested for responsivity with each experimental protocol. **Figure 3.4 (a)** gives the average peak current for each concentration of DA at each data density (n = 4). Sensitivity of each data density is given by the slopes of the regression lines (values shown as average ± standard deviation). Sensitivity to DA at 10 Hz for the standard data density of 850 pts/CV was determined to be 31 ± 4 nA/µM, for 250 pts/CV the sensitivity was 30 ± 1 nA/µM, and 32 ± 1 nA/µM for 100 pts/CV. Sensitivity to DA for the reduced 250 pts/CV and 100 pts/CV are not statistically significant compared to the standard 850 pts/CV ($p = 0.82$, $p = 0.90$, respectively, ANCOVA). The sensitivity to DA was then evaluated for varying sampling rates, 20, 3 and 1 CV per second, and compared to the standard 10 CVs per second, **Figure 3.4 (b)**. All sampling rates were run at the standard 850 pts/CV. Similar to the testing for data densities, four concentrations of DA were tested for responsivity using each sampling rate, with sensitivities given by the slopes of the regression lines (n=4, values shown as average ± standard deviation). Sensitivity to DA for a 20 Hz sampling rate was determined to be 23 ± 1 nA/µM, 31 ± 4 nA/µM for 10 Hz, 48 ± 2 nA/µM for 3 Hz, and 44 ± 2 nA/µM for 1 Hz. Sensitivity to DA for 1 Hz and 3 Hz were both statistically significant compared to 10 Hz ($p = 0.042$, $p = 0.016$, respectively, ANCOVA).

No significance was found in the sensitivities between 20 Hz and 10 Hz. We have previously reported a significant increase in sensitivity between 10 Hz and 1 Hz in PBS buffer [1].

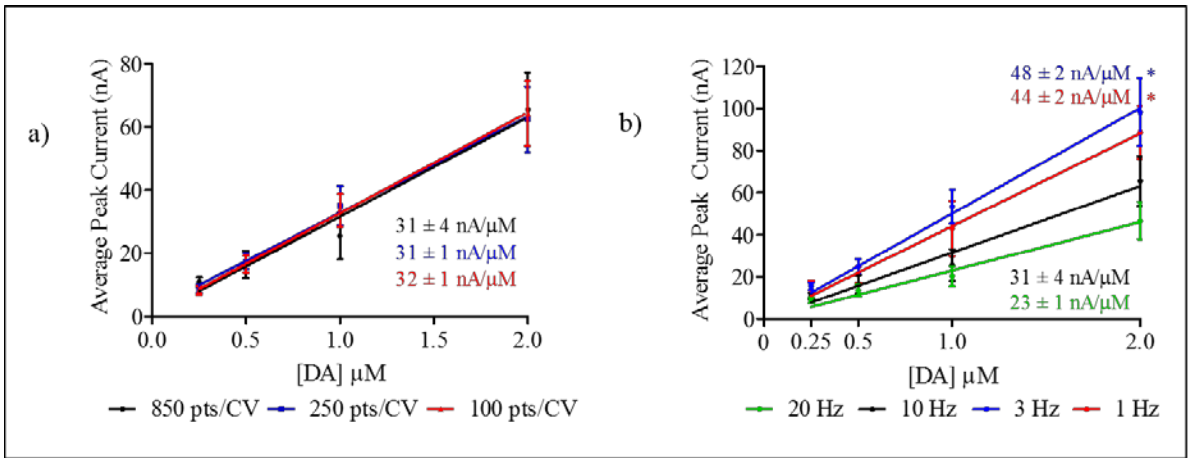

Figure 3.4 – Evaluating dopamine sensitivity with data density and sampling rates. (a) Sensitivity to DA for various data densities collected at 10 Hz in PBS buffer, given by the slopes of the regression lines. Error bars represent standard deviation (n=4). Sensitivity to DA for data density of 850 pts/CV was determined to be 31 ± 4 nA/µM, 30 ± 1 nA/µM for 250 pts/CV, and 32 ± 1 nA/µM for 100 pts/CV. Sensitivity to DA for the reduced 250 pts/CV and 100 pts/CV are not statistically significant compared to 850 pts/CV ($p = 0.82$, $p = 0.90$, respectively, ANCOVA). (b) Sensitivity to DA for various sampling rates using the standard 850 pts/CV protocol, given by the slopes of the regression lines. Error bars represent standard deviation (n=4). Sensitivity to DA for a 20 Hz sampling rate was determined to be 23 ± 1 nA/µM, 31 ± 4 nA/µM for 10 Hz, 48 ± 2 nA/µM for 3 Hz, and 44 ± 2 nA/µM for 1 Hz. Sensitivity to DA for 1 Hz and 3 Hz are both statistically significant compared to 10 Hz ($p = 0.042$, $p = 0.016$, respectively, ANCOVA). No significance was found when comparing the sensitivities of 20 Hz and 10 Hz sampling rates.

3.3.4 Evaluation of Simultaneous Parameter Reduction *In Vitro*

The transition of FSCV protocols to more chronic, long-term experiments in tissue will require the conservation of data collection and transfer as a key aspect of optimization.

With this in mind, the combination of a reduced data density and sampling rate protocol was evaluated for efficacy based on the findings of reducing each parameter separately. To assess the validity of a simultaneously reduced parameter protocol, responsivity and sensitivity to DA was determined for three combined parameter protocols. The first protocol features the standard 10 Hz sampling rate and the standard 850 pts/CV data density. Two reduced parameter protocols were tested against the standard protocol. The first features a 3 Hz sampling rate combined with a data density of 250 pts/CV and the second combines a 1 Hz sampling rate with a 100 pts/CV data density. **Figure 3.5** depicts the results of the electrochemical characterization of DA using these three protocols. **Figure 3.5 (a)** shows the average responsivity to 1 µM DA collected with 10 Hz, 850 pts/CV and compares it to the reduced 3 Hz, 250 pts/CV and 1 Hz, 100 pts/CV protocols. Error bars represent the standard deviation at the peak current for each protocol (n = 7). **Figure 3.5 (b)** further characterizes the three protocols with the sensitivities to DA for each (n = 7). Sensitivity to DA was determined to be 26 ± 1 nA/µM for the 10 Hz, 850 pts/CV protocol, 49 ± 4 nA/µM for the 3 Hz, 250 pts/CV protocol and 46 ± 2 nA/µM for the 1 Hz, 100 pts/CV protocol. The sensitivities (inset) for both the 3 Hz, 250 pts/CV and 1 Hz, 100 pts/CV protocols differ statistically from the sensitivity of the 10 Hz, 850 pts/CV protocol ($p = 0.003$ and $p = 0.005$, respectively, ANCOVA).

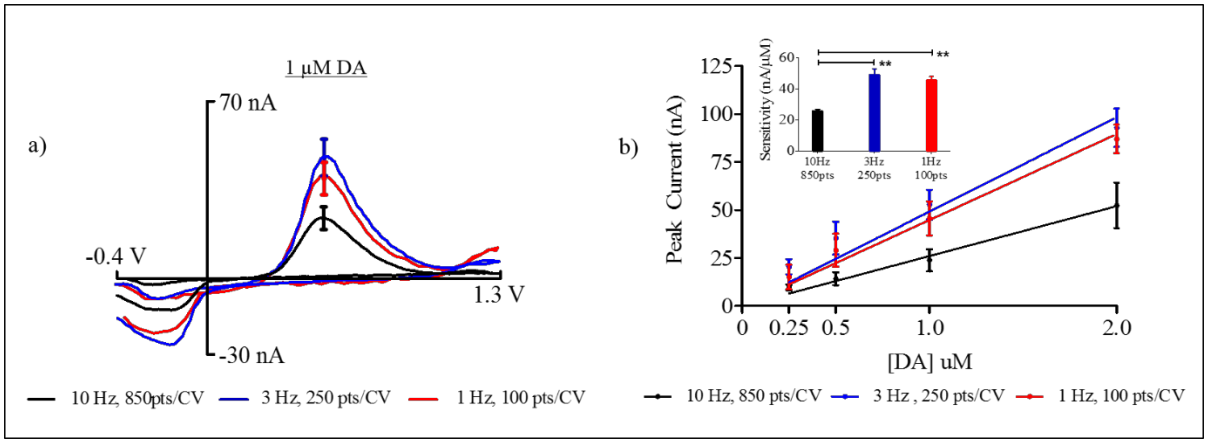

Figure 3.5 – Electrochemical characterization of dopamine with reduced sampling rate and reduced data density. (a) Average background-subtracted CVs of peak current for 1 µM DA collected using the standard 10 Hz, 850 pts/CV protocol compared to the reduced 3 Hz, 250 pts/CV and 1 Hz, 100 pts/CV protocols (n = 7). Error bars represent standard deviation at peak current for each protocol. (b) Sensitivity to DA for the standard 10 Hz, 850 pts/CV protocol and the reduced 3 Hz, 250 pts/CV and 1 Hz, 100 pts/CV protocols. Error bars represent standard deviation (n = 7). Sensitivity to DA in PBS buffer, given by the slopes of the regression lines, was determined to be 26 ± 1 nA/µM for the 10 Hz, 850 pts/CV protocol, 49 ± 4 nA/µM for the 3 Hz, 250 pts/CV protocol and 46 ± 2 nA/µM for the 1 Hz, 100 pts/CV protocol (inset). The sensitivities for both the 3 Hz, 250 pts/CV and 1 Hz, 100 pts/CV protocols differ from the sensitivity of the 10 Hz, 850 pts/CV protocol ($p = 0.003$ and $p = 0.005$, ANCOVA).

While reduction in each of the FSCV parameters separately impacts the overall file size collected in an experiment, reducing both the sampling rate and data density in the same protocol has potential to drastically reduce the overall size of each data file collected in a single experiment. For long-term *in vivo* experiments, data acquisition transfer and storage are important factors in experimentation. **Table 3.1** quantifies the file sizes in a typical 30 second experimental file for the standard 10 Hz, 850 pts/CV protocol and several reduced protocols based on reducing the sampling rate and data density. Percent reduction in file size

for each reduced protocol is given compared to the standard protocol. A typical 30 second file run with the standard protocol collects a file size of 4078 KB using the current FSCV software. Collecting the same 30 second file using a reduced protocol featuring a 3 Hz sampling rate and data density of 250 pts/CV results in an 89 % reduction in file size. Using a 1 Hz, 100 pts/CV protocol further reduces the file size, giving an overall 96 % reduction compared to the standard protocol. We show that the reduction of sampling rate and data density, both separately and in combination with each other, do not compromise responsivity, sensitivity or selectivity of the sensor. However, the reduction of both these parameters has the ability to greatly minimize the data transfer requirements of these conventional experiments. This minimization can have a great impact on the current limitations of long-term experimentation using FSCV.

Table 3.1 – Quantifying a reduced data density.

sampling rate (Hz)	# data pts/CV	# data points in 30 second file	30 second file size (KB)	% reduction in file size from standard protocol
10	***850***	***255000***	***4078***	***0 %***
	250	75000	1210	70 %
	100	30300	498	88 %
3	850	76500	1471	64 %
	250	22500	443	89 %
	100	9090	187	95 %
1	850	25500	1195	71 %
	250	7500	362	91 %
	100	3030	155	96 %

3.3.5 *Ex Vivo* Performance of Simultaneous Parameter Reduction

After *in vitro* response of the reduced protocols was studied, the reduced parameter protocols were tested in coronal slices of rat brain to observe their response in live tissue. A CFM was placed in the striatum of an excised rat brain slice and electrically elicited DA was recorded using external electrical stimulation. A stainless steel stimulating electrode provided 5 pulses of 400 μA amplitude to the striatum at 60 Hz. The CFM recorded the elicited DA at the standard 10 Hz, 850 pts/CV protocol, as well as the two reduced protocols, 3 Hz, 250 pts/CV and 1 Hz, 100 pts/CV. **Figure 3.6** reports the stimulated DA results. In **Figure 3.6 (a)**, we report an electrochemical color plot of the response for each of the three protocols. Each color plot is taken over 5 seconds and provides detailed information on the performance of the protocol. Time is plotted on the x-axis, applied potential on the y-axis, and elicited current is shown in false color. The color plot for the 10 Hz, 850 pts/CV protocol is comprised of 50 individual CVs, with 15 CVs making up the color plot for 3 Hz, 250 pts/CV protocol and 5 CVs in the 1 Hz, 100 pts/CV color plot. Electrical stimulation is given by the white arrow for each protocol. **Figure 3.6 (b)** plots the resulting background-subtracted CVs for each protocol, displaying the concentration of DA each protocol collected. Post calibration of the electrodes in 1 X Tris buffer was used to convert raw current collected after stimulation into concentration. Sensitivities to DA in Tris buffer, **Figure 3.6 (c)** were used to calibrate tissue measurements instead of PBS as it more closely mimics a live tissue environment [7].

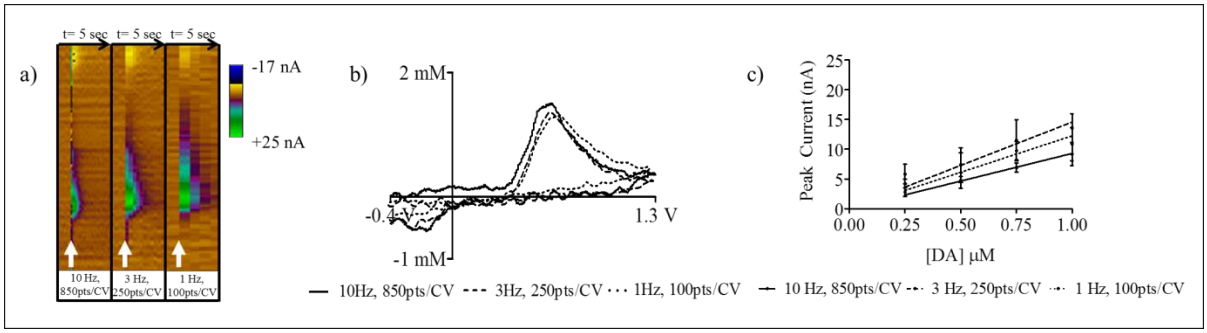

Figure 3.6 – Reduced data density and sampling rate in tissue. *Ex vivo* response to electrically stimulated DA in striatal slices of rat brain using the standard 10 Hz, 850 pts/CV protocol and the reduced 3 Hz, 250pts/CV and 1 Hz, 100 pts/CV protocols. (a) Representative color plot response to stimulated DA release for each protocol. Stimulation of DA release is indicated by the white arrows. (b) Representative background-subtracted CVs of electrically elicited DA for all three protocols, stimulated with 5 pulses, 400 µA, at 60 Hz. (c) Post-calibration of the electrodes in 1 X Tris buffer used to convert current elicited from stimulation into concentration. Sensitivity to DA in Tris buffer, given by the slopes of the regression lines, was determined to be 9 ± 0 nA/µM for the 10 Hz, 850 pts/CV protocol, 15 ± 1 nA/µM for the 3 Hz, 250 pts/CV protocol and 12 ± 1 nA/µM for the 1 Hz, 100 pts/CV protocol. No significance was found between the three protocols in Tris buffer (n = 5, ANCOVA).

3.4 CONCLUSIONS

These studies examined the performance of data collection parameters on the performance of FSCV measurements of DA. Emphasis was placed on understanding changes in performance for experimental protocols to monitor DA and other analyte fluctuations that have reduced data densities compared to conventional experiments. Results are also presented for *in vitro* and *ex vivo* protocols that combine reduced sampling rates and data density for monitoring DA without significantly impacting measurement performance. The overall data collected and transferred from the reduced data density protocols is reduced by 89 % and 96 % compared to the standard protocol. These results will help to guide future

longer-term *in vivo* electrochemical experiments without the need for modifying existing software or hardware.

3.5 REFERENCES

[1] A. N. Amos, J. G. Roberts, L. Qi, L.A. Sombers, &G. S. McCarty. Reducing the sampling rate of biochemical measurements using fast-scan cyclic voltammetry for *in vivo* applications. *IEEE Sensors14,* 2975-2980 (2014).

[2] A. J. Bard and L. R. Faulkner. *Electrochemical Methods: Fundamentals and Applications,* 2nd ed. New York, John Wiley & Sons. 2001.

[3] J. D. Bronzino and R. C. Dorf. *The Biomedical Engineering Handbook* (2nd ed.) 2000.

[4] E. C. Dankoski and R. M. Wightman. Monitoring serotonin signaling on a subsecond time scale. *Front. Integr. Neurosci. 7*pp. 44. 2013.

[5] P. Hashemi, E. C. Dankoski, R. Lama, K. M. Wood, P. Takmakov and R. M. Wightman. Brain dopamine and serotonin differ in regulation and its consequences. *Proc. Natl. Acad. Sci. U. S. A. 109(29),* pp. 11510-11515. 2012.

[6] M. L. Heien, M. A. Johnson and R. M. Wightman. Resolving neurotransmitters detected by fast-scan cyclic voltammetry. *Anal. Chem. 76(19),* pp. 5697-5704. 2004.

[7] M. L. A. V. Heien, P. E. M. Phillips, G. D. Stuber, A. T. Seipel and R. M. Wightman. Overoxidation of carbon-fiber microelectrodes enhances dopamine adsorption and increases sensitivity. *Analyst 128(12),* pp. 1413-1419. 2003.

[8] N. R. Herr, J. Park, Z. A. McElligott, A. M. Belle, R. M. Carelli and R. M. Wightman. *In vivo* voltammetry monitoring of electrically evoked extracellular norepinephrine in subregions of the bed nucleus of the striaterminalis. *J. Neurophysiol. 107(6),* pp. 1731-1737. 2012.

[9] C. E. John and S. R. Jones. "Fast scan cyclic voltammetry of dopamine and serotonin in mouse brain slices," in *Electrochemical Methods for Neuroscience,* A. C. Michael and L. M. Borland, Eds. 2007,

[10] R. B. Keithley, M. L. Heien and R. M. Wightman. Multivariate concentration determination using principal component regression with residual analysis. *Trends Analyt Chem. 28(9),* pp. 1127-1136. 2009.

[11] R. B. Keithley, P. Takmakov, E. S. Bucher, A. M. Belle, C. A. Owesson-White, J. Park and R. M. Wightman. Higher sensitivity dopamine measurements with faster-scan cyclic voltammetry. *Anal.Chem.83(9),* pp. 3563-3571. 2011.

[12] R. B. Keithley and R. M. Wightman. Assessing principal component regression prediction of neurochemicals detected with fast-scan cyclic voltammetry. *ACS Chem. Neurosci. 2(9),* pp. 514-525. 2011.

[13] D. J. Michael, J. D. Joseph, M. R. Kilpatrick, E. R. Travis and R. M. Wightman. Improving data acquisition for fast-scan cyclic voltammetry. *Anal. Chem. 71(18),* pp. 3941-3947. 1999.

[14] J. Park, P. Takmakov and R. M. Wightman. *In vivo* comparison of norepinephrine and dopamine release in rat brain by simultaneous measurements with fast-scan cyclic voltammetry. *J. Neurochem.119(5),* pp. 932-944. 2011.

[15] J. Park, R. A. Wheeler, K. Fontillas, R. B. Keithley, R. M. Carelli and R. M. Wightman. Catecholamines in the bed nucleus of the striaterminalis reciprocally respond to reward and aversion. *Biol. Psychiatry71(4),* pp. 327-334. 2012.

[16] J. G. Roberts, K. L. Hamilton and L. A. Sombers. Comparison of electrode materials for the detection of rapid hydrogen peroxide fluctuations using background-subtracted fast scan cyclic voltammetry. *Analyst 136(17),* pp. 3550-3556. 2011.

[17] J. G. Roberts, L. Z. Lugo-Morales, P. L. Loziuk and L. A. Sombers. Real-time chemical measurements of dopamine release in the brain. *Methods Mol. Biol. 964*pp. 275-294. 2013.

[18] J. G. Roberts, B. P. Moody, G. S. McCarty and L. A. Sombers. Specific oxygen-containing functional groups on the carbon surface underlie an enhanced sensitivity to dopamine at electrochemically pretreated carbon fiber microelectrodes. *Langmuir 26(11),* pp. 9116-9122. 2010.

[19] D. L. Robinson, B. J. Venton, M. L. Heien and R. M. Wightman. Detecting subsecond dopamine release with fast-scan cyclic voltammetry *in vivo*. *Clin. Chem. 49(10),* pp. 1763-1773. 2003.

[20] D. L. Robinson and R. M. Wightman. "Rapid dopamine release in freely moving rats," in *Electrochemical Methods for Neuroscience,* A. C. Michael and L. M. Borland, Eds. 2007.

[21] A. L. Sanford, S. W. Morton, K. L. Whitehouse, H. M. Oara, L. Z. Lugo-Morales, J. G. Roberts and L. A. Sombers. Voltammetric detection of hydrogen peroxide at carbon fiber microelectrodes. *Anal.Chem.82(12),* pp. 5205-5210. 2010.

[22] A. C. Schmidt, X. Wang, Y. Zhu and L. A. Sombers. Carbon nanotube yarn electrodes for enhanced detection of neurotransmitter dynamics in live brain tissue. *ACS Nano* 2013.

[23] M. Spanos, J. Gras-Najjar, J. M. Letchworth, A. L. Sanford, J. V. Toups and L. A. Sombers. Quantitation of hydrogen peroxide fluctuations and their modulation of dopamine dynamics in the rat dorsal striatum using fast-scan cyclic voltammetry. *ACS Chem. Neurosci. 4(5),* pp. 782-789. 2013.

[24] P. Takmakov, M. K. Zachek, R. B. Keithley, E. S. Bucher, G. S. McCarty and R. M. Wightman. Characterization of local pH changes in brain using fast-scan cyclic voltammetry with carbon microelectrodes. *Anal. Chem. 82(23),* pp. 9892-9900. 2010.

[25] B. J. Venton, D. J. Michael and R. M. Wightman. Correlation of local changes in extracellular oxygen and pH that accompany dopaminergic terminal activity in the rat caudate-putamen. *J. Neurochem.84(2),* pp. 373-381. 2003.

[26] R. A. Webster. *Neurotransmitters, Drugs, and Brain Function* 2001.

[27] R. M. Wightman, M. L. Heien, K. M. Wassum, L. A. Sombers, B. J. Aragona, A. S. Khan, J. L. Ariansen, J. F. Cheer, P. E. Phillips and R. M. Carelli. Dopamine release is heterogeneous within microenvironments of the rat nucleus accumbens. *Eur. J. Neurosci. 26(7),* pp. 2046-2054. 2007.

[28] G. S. Wilson and M. A. Johnson. *In-viv*o electrochemistry: What can we learn about living systems? *Chem. Rev. 108(7),* pp. 2462-2481. 2008.

[29] R. A. Wise. Roles for nigrostriatal--not just mesocorticolimbic--dopamine in reward and addiction. *Trends Neurosci. 32(10),* pp. 517-524. 2009.

[30] M. K. Zachek, J. Park, P. Takmakov, R. M. Wightman and G. S. McCarty. Microfabricated FSCV-compatible microelectrode array for real-time monitoring of heterogeneous dopamine release. *Analyst 135(7),*pp. 1556-1563. 2010.

[31] M. K. Zachek, P. Takmakov, B. Moody, R. M. Wightman and G. S. McCarty. Simultaneous decoupled detection of dopamine and oxygen using pyrolyzed carbon microarrays and fast-scan cyclic voltammetry. *Anal. Chem. 81(15),* pp. 6258-6265. 2009.

[32] M. K. Zachek, P. Takmakov, J. Park, R. M. Wightman and G. S. McCarty. Simultaneous monitoring of dopamine concentration at spatially different brain locations *in vivo*. *Biosens. Bioelectron. 25(5),* pp. 1179-1185. 2010.

[33] X. Zhang, H. Ju, J. Wang and I. ebrary. Electrochemical sensors, biosensors and their biomedical applications. pp. 593. 2008.

CHAPTER 4

Reducing Data Density for Fast-Scan Cyclic Voltammetry Measurements in Freely Moving Rats

This work was part of a collaborative effort with: Lingjiao Qi, Kristen Blanton, Christie Lee, Gregory S. McCarty and Leslie A. Sombers, and is in preparation for submission to *ACS Neuroscience*. Only a portion of the chapter constitutes the author's personal dissertation research; however, all results are shown to allow for a complete interpretation of the findings.

4.1 INTRODUCTION

Neurotransmitters in the brain play significant roles in various behaviors in normal and pathological disease states. Thus, understanding the rapid dynamics of neurotransmitters *in vivo* is critical for advancing research in biology, psychology and neuropharmacology. A commonly used *in vivo* chemical sampling technique is microdialysis, which is a diffusion-based sampling method that is well suited to examine steady-state or slowly changing levels of analytes in the extracellular fluid [1] – [3], yet lacks the temporal resolution to detect chemical fluctuations that occur on the second or sub-second time scale [1]. In contrast, electrochemical techniques are especially useful for monitoring rapid chemical changes resulting from discrete neurochemical events *in vivo*. Among them, fast scan cyclic voltammetry (FSCV) is a proven technology for monitoring rapid chemical changes in the brain and associating these changes with behavior [4]. Coupled with carbon-fiber microelectrodes, background-subtracted FSCV provides fast, sensitive and selective

determination for analytes of interest within a small spatial location. Typically with FSCV, a triangular potential waveform is applied to the electrode at a scan rate of 400 V/s at a frequency of 10 Hz, generating a cyclic voltammogram that allows distinction among different electroactive molecules. Over the past 30 years, FSCV has been extensively developed and widely used in monitoring rapid dynamics of dopamine (DA), glutamate, adenosine, norepinephrine, oxygen, pH, hydrogen peroxide and serotonin in live animals [5] – [9].

Recent advances have further enabled FSCV to be capable of making long-term electrochemical measurements in the same animal over a period of days to months. This allows tracking of longitudinal changes in neurotransmitter dynamics over the course of disease progression in animal models or throughout various learning paradigms [10], [11]. Additionally, FSCV has been successfully extended to make wireless *in vivo* measurements that eliminate the cable between the animal and equipment, permitting the animal more unrestricted motion and reducing susceptibility to ambient electrical noise [12] – [16]. However, the amount of data generated and transferred in a typical FSCV system has imposed significant difficulties for the continued development and application of long-term data measurements and wireless data transmission [16]. Existing FSCV protocols to measure neurotransmitter signaling in the brain were created without consideration for data generation or data transfer rates. Traditionally, FSCV collects 10 cyclic voltammograms per second with 1000 data points per cyclic voltammogram. Therefore, in a single 30 second file, there are

300,000 data points collected. Ultimately, in chronic experiments over several days to months, there is a tremendous amount of data generated.

In an effort to create protocols that will reduce the data generated and transferred in FSCV for real-time longitudinal wireless measurements, we evaluated the *in vivo* performance of FSCV at reduced sampling rates with reduced data points collected per cyclic voltammogram. Recently, we have demonstrated that FSCV applied at a lower sampling rate (1 Hz), which compared with the existing protocol reduced the quantity of data generated by an order of magnitude, did not affect the capability of rapid measurements of electrically-evoked DA in an anesthetized rat [17]. In the current work, we have furthered our investigation to include the reduction of data points per cyclic voltammogram with reduced sampling rates, and evaluated the performance of this application in monitoring electrically-evoked and spontaneous sub-second DA fluctuations in freely moving rats. Furthermore, we directly compared the *in vivo* performances of reduced data points with the standard protocol in assessing the effects of cocaine on electrically evoked DA kinetics and naturally occurring DA events in behaving animals. Our work demonstrates that FSCV applied at 1 Hz with 100 data points collected per cyclic voltammetry is still capable of detecting sub-second DA dynamics in freely moving animals and monitoring the real-time effects of pharmacological drugs. Utilizing the 1 Hz sampling rate at 100 data points reduces the quantity of data generated by two orders of magnitude compared to the traditional protocol. It is expected to increase data transfer rate and might also have an impact on reducing power consumption.

Importantly, this work serves to aid the development of wireless FSCV for chronic measurements and will benefit a wide variety of biological studies in the near future.

4.2 MATERIALS AND METHODS

4.2.1 Chemicals

All chemicals were purchased from Sigma-Aldrich (St. Louis, MO) and used as received, unless otherwise noted. Solutions were prepared using doubly distilled deionized water (Milli-Q Millipore, Billerica, MA). *In vitro* characterization of electrode response to DA was conducted in Tris buffer (15 mM Trisma HCl, 3.25 mM KCl, 1.2 mM $CaCl_2$, 1.2 mM $MgCl_2$, 2.0 mM Na_2SO_4, 1.25 mM NaH_2PO_4, and 145 nM NaCl) at pH 7.4.

4.2.2 Carbon Fiber Microelectrode Fabrication

Carbon-fiber microelectrodes were fabricated as described previously in literature (18). Briefly, a single T-650 carbon fiber (7 µm diameter) (Cytec Industries, West Patterson, NJ) was aspirated into a glass capillary tube (0.60 mm external diameter and 0.40 mm internal diameter, A-M Systems, Carlsburg, WA) and heat pulled with a micropipette puller (Narishige, Tokyo, Japan) to taper the glass to form two sealed microelectrodes. The exposed carbon-fiber beyond the glass seal was cut to approximately 100 µm under an optical microscope. A stainless steel lead wire with conductive silver paint (GC Electronics, Rockford, IL) was inserted into the capillary for electrical contact. The reference electrodes were chloridized silver wires. All potentials reported are versus Ag/AgCl.

4.2.3 Data Acquisition

A triangular cyclic waveform ramped from -0.4 V to +1.3 V with a resting potential of -0.4 V versus Ag/AgCl was applied to the electrodes at a scan rate of 400 V/ s for all experiments. The FSCV waveform was applied at various frequencies (20, 10, 5, 1 Hz) and data was collected at various data points (1000, 500, 100 per cyclic voltammogram) in randomized order. Commercially available TH-1 software (ESA, Chelmsford, MA), written in LabVIEW (National Instruments, Austin, TX), was used with a DAC/ADC card (NI 6251) for waveform generation and data collection. A second card (NI 6711) was used for synchronization of waveform acquisition, flow injection, data collection and stimulation delivery. Signal processing (background subtraction, signal averaging and digital filtering) was software-controlled.

4.2.4 *In Vitro* Experiments

A syringe pump (New Era Pump System, Wantagh, NY) was used to supply a continuous buffer flow of 1 mL/min across the working and reference electrodes, which were positioned in a custom electrochemical cell. A 6-port HPLC injection valve (Valco Instruments Co., Inc., Houston, TX), mounted on a two-position air actuator and controlled by a digital pneumatic solenoid valve kit, was used to introduce analyte from an injection loop (0.5 mL) to the electrode surface.

4.2.5 Animals and Surgery

Adult male Sprague-Dawley rats weighing between 250-300 g were purchased from Charles River Laboratories (Wilmington, MA). Animals were individually housed on a 12:12 hr light : dark cycle with access to food and water. The surgical procedure was performed as described previously [18]. Briefly, rats were anesthetized with isoflurane (Vetqeuip; Pleasanton, CA), which was induced at 4% and maintained at 1.5-2.0 % during surgery. Rats were positioned into a stereotaxic frame (Kopf Instrumentation; Tujunga, CA). A heating pad (Harvard Apparatus, Holliston, MA) was used to maintain body temperature at 37 °C. Holes for electrodes were drilled in the skull according to coordinates from the brain atlas of Paxinos and Watson [19]. The Ag/AgCl reference electrode was placed in the forebrain, and a guide cannula (BASi instruments, West Lafayette, IN) was placed above the contralateral nucleus accumbens (NAc) (1.7 mm anterior, 0.8 mm lateral, 2.5 mm ventral relative to bregma). The bipolar stimulating electrode (Plastics One, Roanoke, VA) was implanted unilaterally into the ventral tegmental area (VTA) (5.9 mm posterior, 1.0 mm lateral, 8.9 mm ventral relative to bregma). The components were permanently affixed with dental cement. The animals were allowed to recover for at least 2 days before experiments. All experimental procedures were approved by the Institutional Animal Care and Use Committees at North Carolina State University.

4.2.6 *In Vivo* Experiments

On the experimental day, a detachable micromanipulator containing a fresh carbon-fiber microelectrode was inserted into the guide cannula and the electrode was lowered into the NAc. The electrodes were connected to a head-mounted amplifier attached to a commutator (Crist Instrument Company). After electrodes were electrochemically stable, a time course of evoked and non-evoked signals was collected with electrical stimulation applied every 5 min. For varying sampling rate experiments, the waveform was applied at 20, 10, 5 or 1 Hz in randomized order. Data was collected at 1000 data points per cyclic voltammogram for each of the sampling rates. For varying data points experiments, the waveform was applied to the electrode at 1 Hz and data was collected at either 1000, 500 or 100 data points per cyclic voltammogram in randomized order. The electrode position was optimized by monitoring naturally occurring and electrically-evoked (biphasic, 2 ms/phase, 24 pulses, 150 μA) DA release. Data was collected for at least 30 min for each protocol. A subgroup of rats received intraperitoneal cocaine (Sigma-Aldrich, St. Louis, MO, 10 mg/kg) administration. Data was collected for at least 30 min before and after cocaine administration. DA signals were characterized with Mini Analysis software (Synaptosoft, Fort Lee, NJ).

4.2.7 Statistics

All data are presented as the mean ± standard error of the mean (SEM), unless otherwise noted. Statistical and graphical analysis was carried out using GraphPad Prism 5

(GraphPad Software, Inc., La Jolla, CA). Student's t-test was used to compare two groups. One-way analysis of variance (ANOVA) with Tukey's post hoc tests was used to determine statistical differences between three or more groups. Significance was designated at $p < 0.05$.

4.3 RESULTS AND DISCUSSION

4.3.1 *In Vitro* Electrochemical Performance of Carbon Fiber Microelectrode at Various Sampling Rates

FSCV has been a powerful technique for monitoring neurotransmitters in real time when coupled with carbon-fiber microelectrodes. Typically, a triangular potential waveform was applied from -0.4 V to +1.3 V with a holding potential at -0.4 V. The waveform is usually applied at a sampling rate of 10 Hz, which generates 10 cyclic voltammograms per second, with each cyclic voltammogram containing 1000 data points. In an effort to reduce the volume of data generated and transferred, we first investigated the electrochemical performance of FSCV *in vitro* for detecting DA signals at various sampling rates. To evaluate the effect of sampling rates on the responsivity of FSCV to DA, four sampling rates (20, 10, 5 and 1 Hz) were tested. **Figure 4.1 (a)** schematically presents the various applied sampling rates with FSCV. The potential waveform was applied from -0.4 V to +1.3 V and scanned back to -0.4 V at 400 V/s. Each waveform has an 8.5 ms duration. The intervals between each waveform for 20, 10, 5 and 1 Hz are 50 ms, 100 ms, 200 ms and 1000 ms, respectively. **Figure 4.1 (b)** shows the *in vitro* sensitivity of FSCV applied at different sampling rates to DA in Tris buffer. Sensitivity to DA was determined to be 11.44 ± 2.08 nA/

µM when sampled at 20 Hz, 12.76 ± 0.46 nA/µM at 10 Hz, 13.21 ± 0.36 nA/µM at 5 Hz, and 14.82 ± 1.94 nA/ µM at 1 Hz. Surprisingly, the sensitivity to DA for all tested sampling rates are not statistically significant from each other. These results differ from those reported previously [17] in which the sensitivity to DA was reported to be significantly different at two separate sampling rates in PBS buffer. PBS is a buffer solution with chemical components different from Tris. Tris buffer has been traditionally used for *in vivo* calibration of carbon-fiber microelectrodes, as it more closely mimics a live tissue environment. The same response to DA at various sampling rates indicates that adsorption of DA to the carbon-fiber microelectrode has been saturated at the interval of 20 Hz sampling rate.

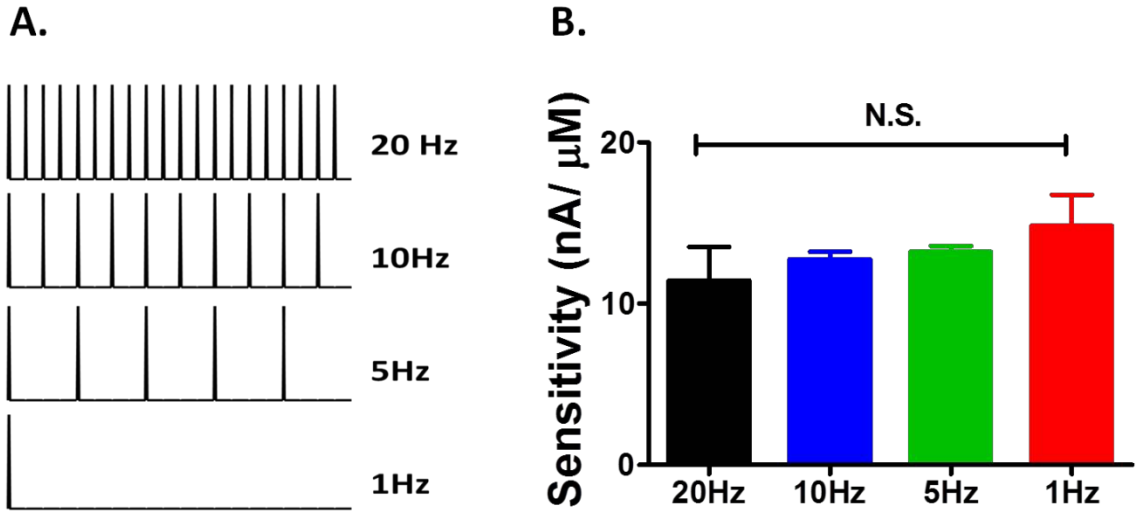

Figure 4.1 – Sensitivity to dopamine at various sampling rates using FSCV. (a) Schematic showing FSCV applied at various sampling rates (20, 10, 5 and 1Hz). (b) Characterizing sensitivity to DA with various sampling rates. Data is presented as averages ± SEM. (n = 7 for each group, one-way ANOVA, $p > 0.05$)

4.3.2 Characterizing Dopamine Signals in Freely Moving Animals with Various Sampling Rates

After verifying that varying sampling rates from 1 to 20 Hz did not affect the response to DA *in vitro*, the electrochemical performance of these sampling rates were tested *in vivo* in freely moving animals. To examine how the sampling rate of FSCV affects measurements of DA dynamics *in vivo*, both electrically-evoked and spontaneous DA events in the same location were compared when the waveform was applied at either 20, 10, 5 or 1 Hz. **Figure 4.2** shows the electrically elicited DA signals monitored at different sampling rates. Representative color plots, each containing 150 background-subtracted voltammograms, are shown in **Figure 4.2 (a).** These plots provide a two-dimensional representation of all changes in current collected across the entire potential window, enabling discrimination of specific electroactive species as they fluctuate over time [20]. The data collected at 1 Hz appears more pixelated than other sampling rates due to the lower collection speed. A DA cyclic voltammogram is shown at the lower panel of **Figure 4.2 (a)**. A current versus time trace was extracted at the oxidation potential of DA, and was converted to concentration with applying the calibration factors from **Figure 4.1 (b)**. In this representative example, electrical stimulation elicited the release of 507, 443, 313, and 419 nM DA when recorded at a sampling rate of 20 Hz, 10 Hz, 5 Hz, and 1 Hz respectively. **Figure 4.2 (b)** summarizes the entire data set (n = 5 animals) by plotting the concentrations of electrically-evoked DA release measured at individual sampling rates. There is no significant difference in detected DA signal across all applied sampling rates.

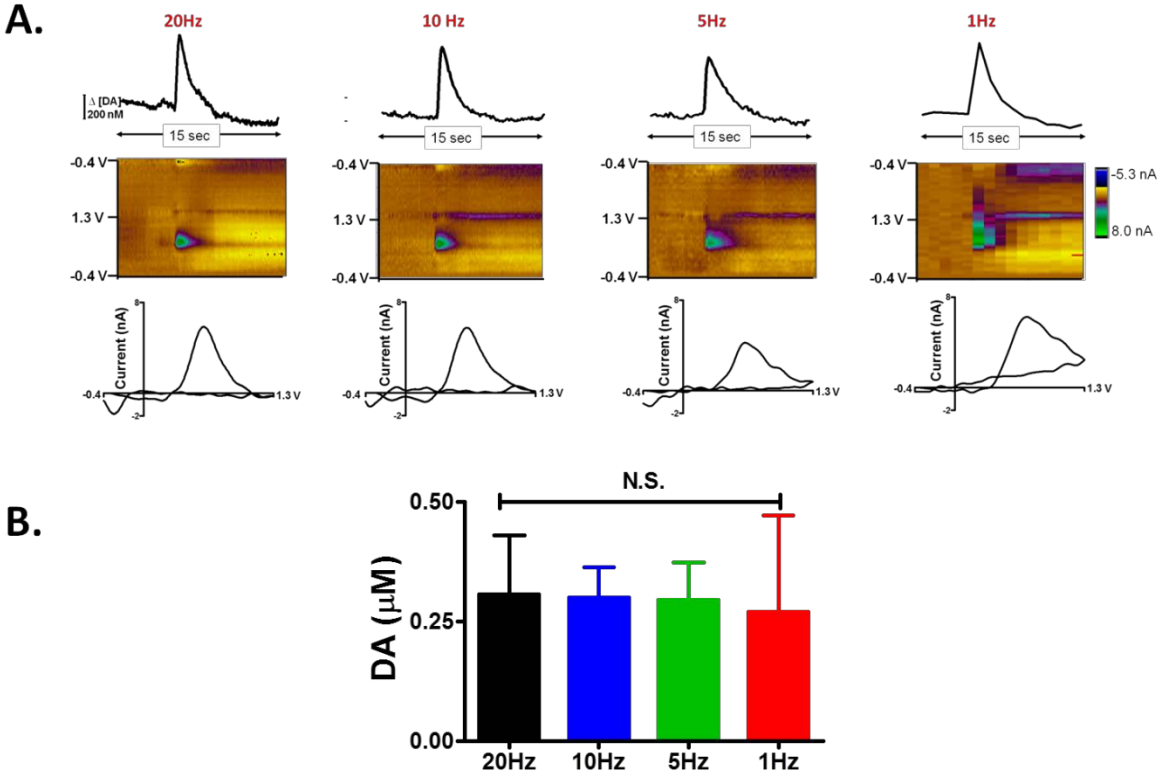

Figure 4.2 – Electrically evoked dopamine signal at various sampling rates. (a) Representative data collected at various sampling rates. Top: concentration vs. time traces for DA. Middle: color plots depicting all changes in current (false color) collected over a 15 s window (x-axis) across all potential (y-axis). Electrical stimulation of the VTA is at 5 s. Bottom: cyclic voltammograms for DA extracted from the data. (b) Across the entire data set, there is no significant difference in electrically-evoked DA release at varying sampling rates ($n = 5$, $p > 0.05$, one-way ANOVA).

Dopaminergic neurons can spontaneously fire at a phasic pattern, which reveals naturally occurring, subsecond DA concentration fluctuations in the NAc [21], [22]. These DA transients have been shown to provide a critical modulatory influence in drug and reward seeking, prediction error and reinforcement. FSCV coupled with carbon-fiber microelectrodes has been widely used to characterize and study naturally occurring DA

dynamics in awake animals. Under basal conditions, these transients are reported to occur at > 1 min^{-1} in the NAc with a mean maximal concentration of ~40 nM and durations of ~1 s [22], when collected at the sampling rate of 10 Hz [3]. Here, we characterized naturally occurring DA dynamics at various sampling rates. Representative color plots with corresponding DA concentration traces and CVs are shown in **Figure 4.3 (a)**. In this representative example, there are ~10 DA transients with an amplitude of ~ 40 nM at a duration of 0.2 s for 20 Hz, ~ 5 DA transients with an amplitude of 35 nM at a duration of 0.8 s for 10 Hz, ~ 3 DA transients with an amplitude of 48 nM at a duration of 1.4 s for 5 Hz, and ~2 DA transients with an amplitude of 50 nM at a duration of 2 s for 1 Hz. **Figure 4.3 (b)** characterizes the naturally occurring DA events for the entire data set (n = 11 animals) collected at various sampling rates. There was no significant difference found for the magnitude of the DA transients detected at various sampling rates. However, compared to 20 Hz, 1 Hz monitored a significantly wider duration and lower frequency for spontaneous DA events (n = 11, * $p < 0.05$, ** $p < 0.001$). This might be because faster acquisition led to diminished time delays of the recordings that tracked faster measurements. Despite this, FSCV collection at 10 Hz and 1 Hz provide identical results when studying the characteristics of naturally occurring DA events. Thus, the sampling rate of 1 Hz is not only capable of detecting naturally occurring sub-second DA signals *in vivo*, but also can provide comparable information of sub-second DA dynamics as sampling rate of 10 Hz.

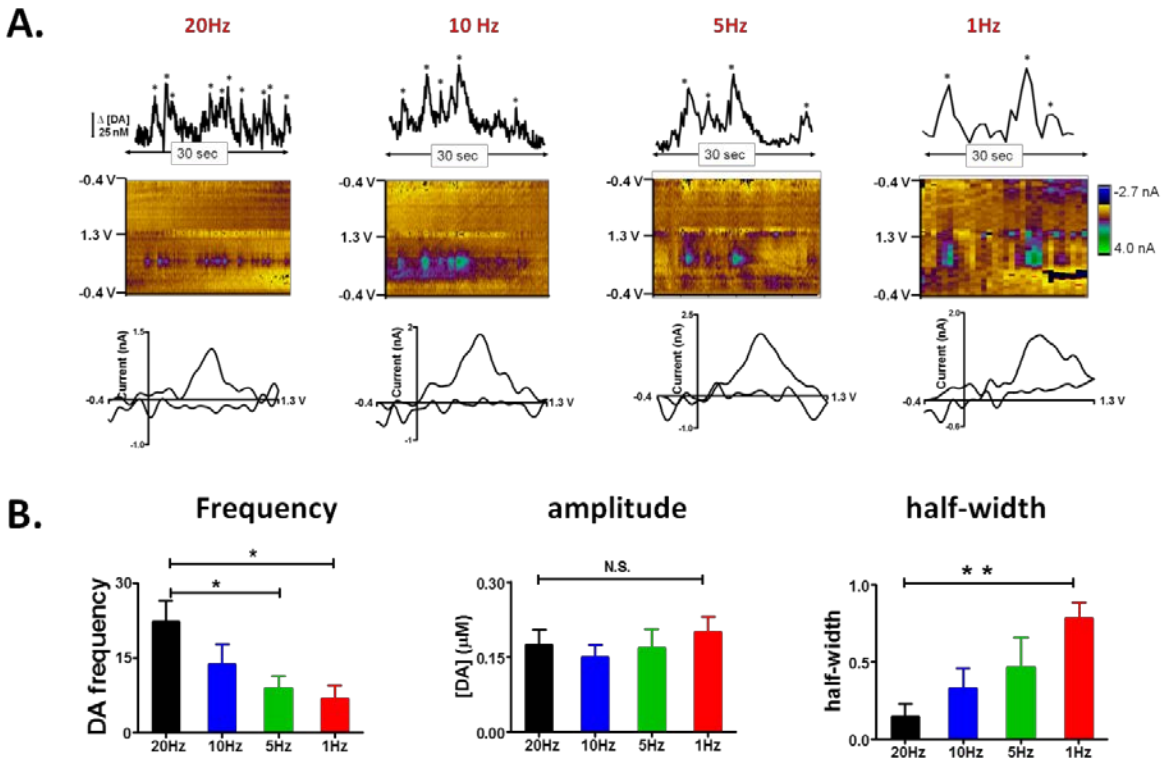

Figure 4.3 – Characterization of dopamine transients at varying sampling rates. (a) Representative data collected at varying sampling rates. (b) Across all animals, 20 Hz detected higher frequency of DA transients than other sampling rates while 1 Hz detected wider duration of DA transients than other sampling rates. 1 Hz shows comparable information of DA characteristics at 10Hz. (n = 11, one-way ANOVA, * $p < 0.05$, ** $p < 0.01$).

4.3.3 Dopamine Signal at Reduced Data Points *In Vitro*

The amount of data transferred, collected and stored is a critical factor for wireless long-term biological measurements. In order to reduce the data generated in FSCV, we further evaluated the performance of reduced data points collected in a typical experimental file. In this work, 1000, 500 and 100 data points per cyclic voltammogram were chosen to

test for their electrochemical performance. **Figure 4.4 (a)** outlines the cyclic voltammogram collected at 1000, 500 and 100 data points. **Figure 4.4 (b)** presents the effect of reduced data points on the sensitivity to DA *in vitro*. All data were collected at 1 Hz, as this sampling rat was demonstrated to maintain comparable sensitivity to DA. Reducing the data points from 1000 to 100 has no significant effect on the sensitivity to DA (n = 7, one-way ANOVA, $p > 0.05$). Data collected at 100 data points maintain similar sensitivity to DA as data collected at 1000 data points.

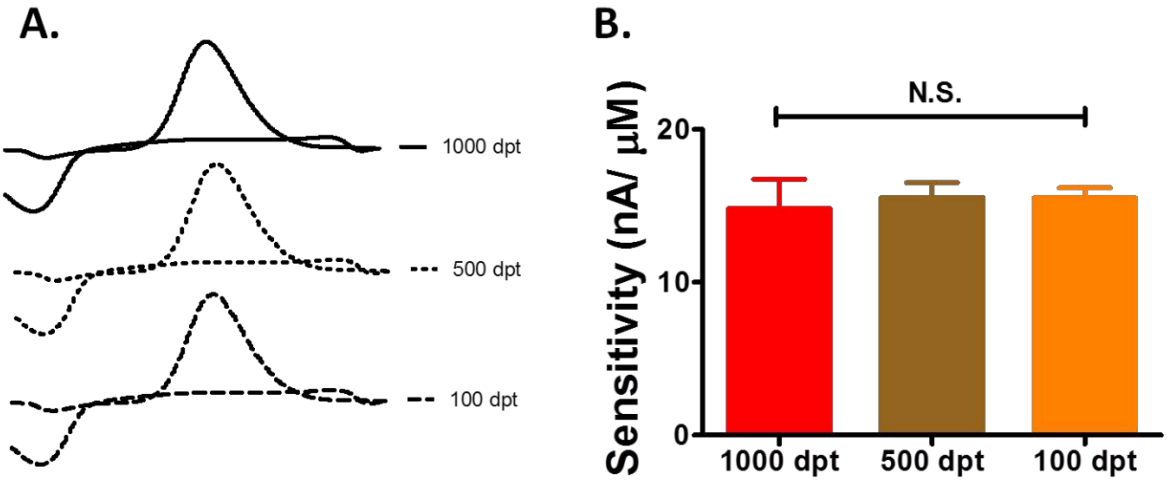

Figure 4.4 – Electrochemical performance of reduced data points. (a). Schematics showing DA cyclic voltammograms made of varying data points (dpt). (b). Sensitivity to DA *in vitro* collected at 1 Hz with different data points. (n = 7, one way ANOVA, $p > 0.05$).

4.3.4 Characterizing Dopamine Signals Collected at Reduced Data Points in Freely Moving Rats

Since the *in vitro* results suggested that the reduced data points protocol had the required criteria for DA detection, it was necessary to verify its *in vivo* performance. FSCV applied at 1Hz was utilized to monitor sub-second DA signals in the NAc of behaving rats. Data was collected with either 1000, 500 or 100 data points per cyclic voltammogram. Electrically-evoked DA release is shown in **Figure 4.5**. Representative color plots with corresponding DA concentration traces and cyclic voltammograms are shown in **Figure 4.5 (a).** In this example, the maximum concentration of elicited DA was determined to be 201 nM at 1000 data points, 225 nM at 500 data points, and 190 nM at 100 data points. When data from all animals was grouped, **Figure 4.5 (b)** demonstrates that there is no significant difference for stimulated DA release when detected with decreased data points ($n = 8$, one-way ANOVA, $p > 0.05$).

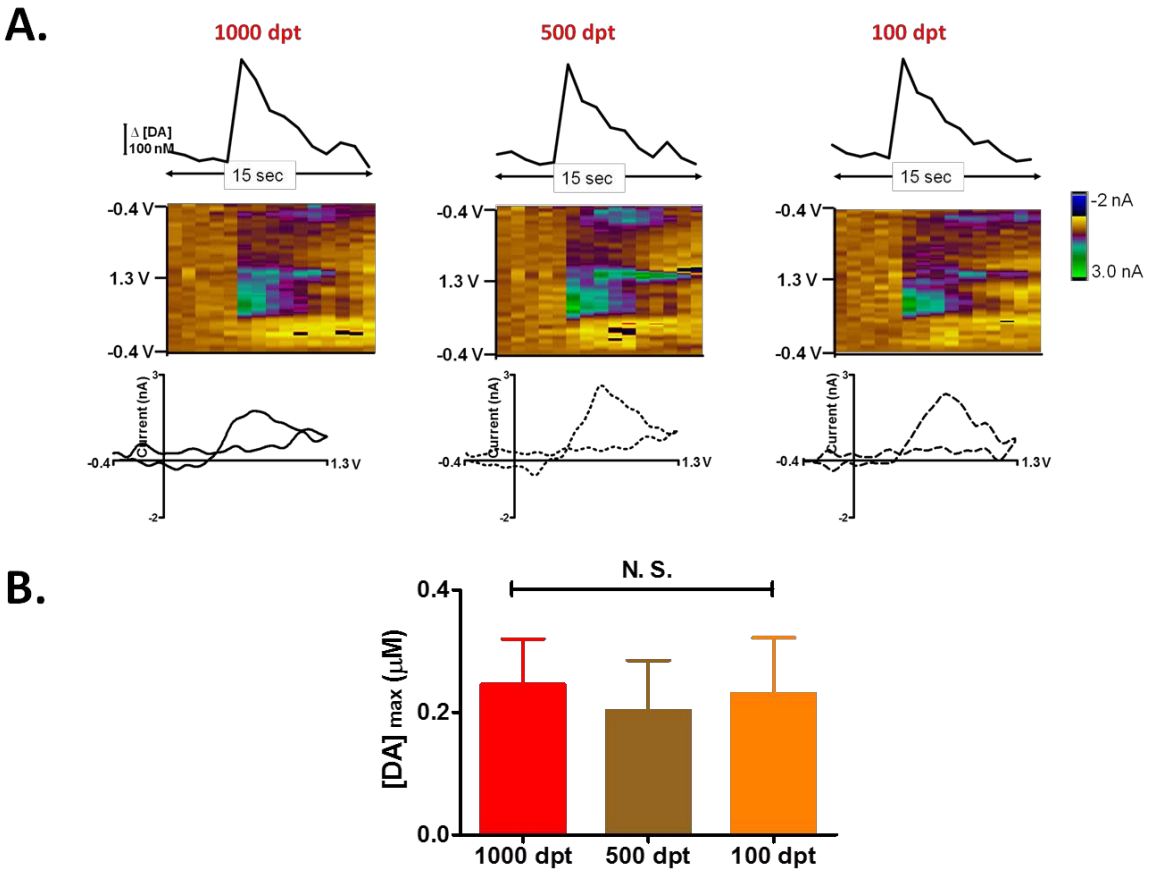

Figure 4.5 – Electrically evoked dopamine signal at reduced data densities.(a) Representative data collected at 1000, 500 and 100 data points per cyclic voltammogram. (b) Across all animals, there is no significant effect on DA signals collected at reduced data points (n = 8, one-way ANOVA, $p > 0.05$).

Naturally occurring DA events were also characterized with reduced data points. Representative color plots with corresponding DA concentration traces and cyclic voltammograms are shown in **Figure 4.6 (a)**. In the 30 s interval shown below, 3 DA transients were found with a mean concentration of 20 ± 6 nM with a duration of ~1.2 s for 1000 data points, 1 DA transient with an amplitude of 19 nM at a duration of ~1.4 s for 500

data points, 3 DA transients with an amplitude of 18 ± 5 nM at a duration of 1.1 s for 100 data points. **Figure 4.6 (b)** summarizes the characteristics of those spontaneous DA events collected with various data points, which clearly shows that reducing the data points per cyclic voltammogram has no negative impact on the detection of DA transients.

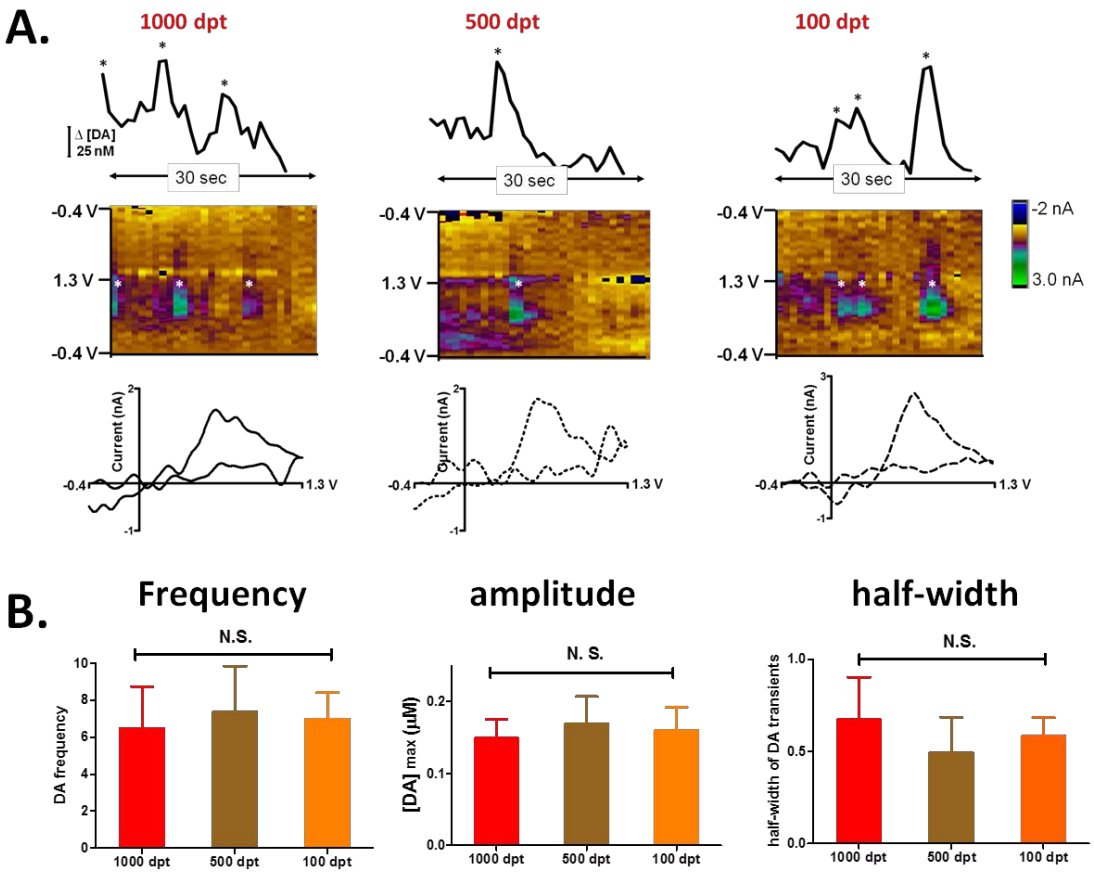

Figure 4.6 – Characterization of dopamine transients at reduced data points. (a) Representative data collected with reduced data points. (b) Across all animals, there is no significance among various data points for detecting DA transients (n =7, one-way ANOVA, $p > 0.05$).

4.3.5 Effects of Cocaine on Dopamine in Freely Moving Rats

DA signals can be pharmacologically manipulated by administration of drugs of abuse, which directly or indirectly target DA transmission [23]. Cocaine, which is a classic DA uptake inhibitor, has been reported to significantly increase both the electrically evoked DA release and naturally occurring DA fluctuations *in vivo* [23] – [25]. In order to further verify the capability of reduced data point protocols, the effects of cocaine on electrically-evoked DA release and spontaneous occurring DA transients were studied in freely behaving rats. Since the reduced sampling rate of 1 Hz shows no significant difference to the standard frequency (10 Hz) with the same number of data points collected per cyclic voltammogram, and varying the number of data points at the same applied sampling rates shows no significant difference from each other, the *in vivo* performance of the traditional protocol (10 Hz with 1000 data points), a reduced sampling rate of 1 Hz with 1000 data points, and a combination of reduced sampling rate of 1 Hz with reduced data density of 100 data points were examined. The effects of cocaine on electrically-evoked DA release are shown in **Figure 4.7**. The primary pharmacological effect of cocaine on dopamine-containing neurons is inhibition of uptake [26]. In this study, uptake inhibition is observed by the increased amplitude of DA release and decreased rate of DA uptake following its stimulated release. Representative color plots with corresponding DA concentrations traces are shown in **Figure 4.7 (a)**. In this specific example, electrically-evoked DA release was increased from 250 nM to 780 nM at sampling rate of 10 Hz with 1000 data points, from 190 nM to 652 nM at sampling rate of 1 Hz with 1000 data points, and from 320 nM to 810 nM at sampling rate of

1 Hz with 100 data points. Additionally, the effects of cocaine on the kinetics of DA uptake were also evaluated. In this representative example, the DA uptake rate was increased to 150 % at a sampling rate of 10 Hz with 1000 data points, 175 % at a sampling rate of 1 Hz with 1000 data points and 174 % at a sampling rate of 1 Hz with 100 data points. In the entire data set, all three protocols measured a significant increase of the amplitude and DA uptake rate upon cocaine administration (**Figures 4.7 (b)** and **4.7 (c)**). The amplitude of evoked DA release was increased to 150 % at 10 Hz at 1000 data points, 175 % at 1 Hz at 1000 data points, and 162 % at 1 Hz at 100 data points. The DA uptake rate was measured to be increased to 147 % at 10 Hz at 1000 data points, 154 % at 1 Hz at 1000, and 190 % at 1 Hz at 100 data points ($n = 6\text{-}7$, student t-test, $*p < 0.05$, $** p < 0.01$, ***, $p < 0.001$). The increased DA uptake rate shows prolonged DA clearance, consistent with previous results [27], [28]. Uptake inhibition increases the lifetime of DA in the extracellular space, allowing diffusion over greater distances and the opportunity to interact with remote receptors, leading to a rise in DA concentration. **Figure 4.7 (d)** demonstrates that there is no significant difference among these three protocols when measuring the effects of cocaine on electrically evoked DA release. ($n = 9$, one way ANOVA, $p > 0.05$).

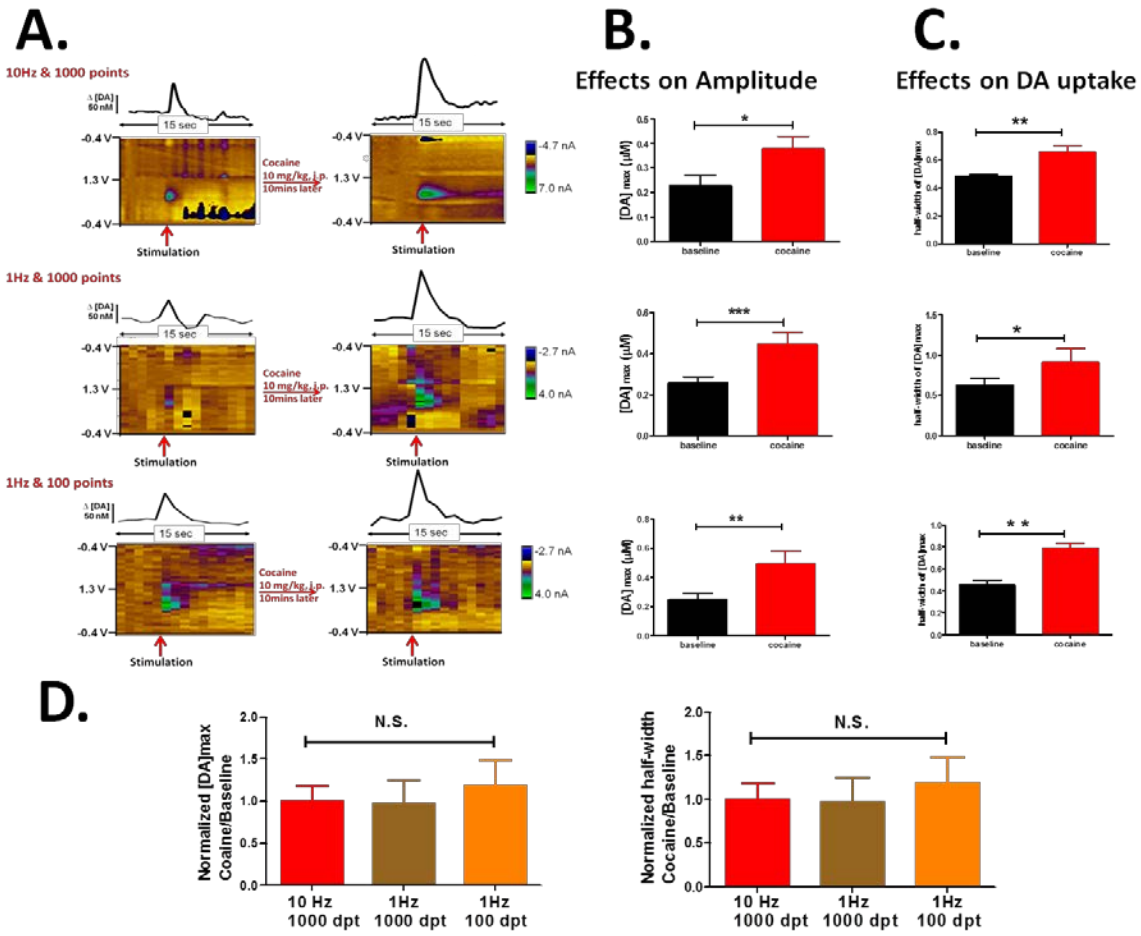

Figure 4.7 – Effects of cocaine on electrically induced dopamine release. (a) Representative data collected with varying data points in an intact animal before cocaine administration (left column), and 10 min after administration of cocaine (right column). (b) Cocaine significantly increased the amplitude of electrically-evoked DA measured with varying data points. (c) Cocaine significantly increases the uptake rate of DA (n = 6-7 for each group, student t-test, * $p < 0.05$ **$p < 0.01$, *** $p < 0.001$). (d) There is no significant difference among the effects of cocaine measured at different data points per cyclic voltammogram (n = 6-7, one-way ANOVA, $p > 0.05$).

Figure 4.8 presents the effects of cocaine on spontaneous DA transients monitored with three different protocols with FSCV. As reported previously, large DA transients occur in the NAc after cocaine [23], [24], [29], largely due to the inhibition of DA uptake. The color representation of the background-subtracted cyclic voltammograms shows several transient events at the potential at which DA is oxidized (**Figure 4.8 (a)**). Across all animals, **Figure 4.8 (b)** determines that the amplitude of DA transients was increased from 22 nM to 45 nM at 10 Hz at 1000 data points, from 30 nM to 53 nM at 1 Hz at 1000 data points, and from 30 nM to 54 nM at 1 Hz at 100 data points. The frequency of spontaneous DA dynamics was increased to 210 % at 10 Hz at 1000 data points, 170 % at 1 Hz at 1000 data points, and 190 % at 1 Hz at 100 data points ($n = 7$ to 11, student t-test, $*p < 0.05$, $** p < 0.01$, ***, $p < 0.001$). A comparison of these three different methods for monitoring the effects of cocaine on DA transients is shown in **Figure 4.8 (d)**, which demonstrates that there is no significant difference among these three protocols when measuring the effects of cocaine on spontaneous DA events. ($n = 7$ - 11, one way ANOVA, $p > 0.05$). Our results showed that applying a voltammetric waveform at 1 Hz with data collected at 100 data points adequately monitored the effects of pharmacological agents, and offered accurate information compared to the traditional protocol with 10 Hz at 1000 data points.

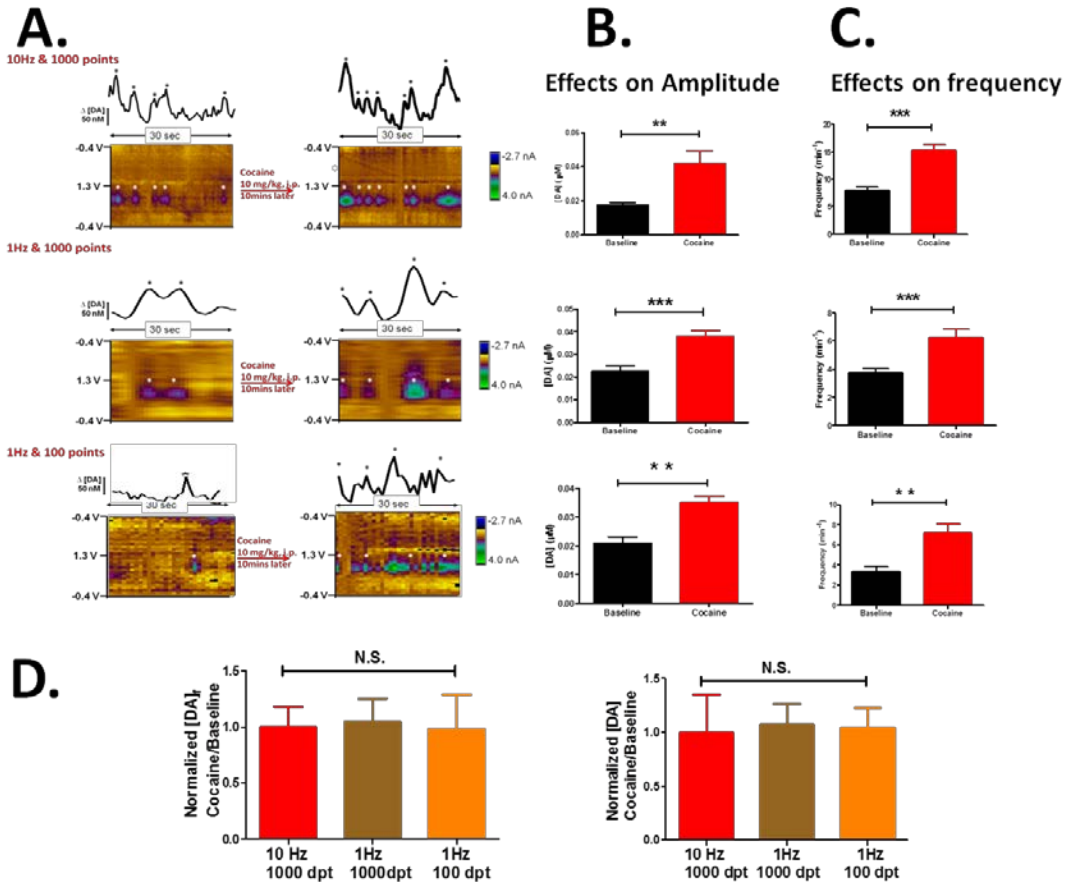

Figure 4.8 – Voltammetric change of dopamine transients after cocaine. (a) Representative data collected with varying data points in an intact animal before cocaine administration (left column) and 10 min after administration of cocaine (right column). (b) Cocaine significantly increased the amplitude of naturally occurring DA events measured with varying data points. (c) Cocaine significantly increased the frequency of spontaneous DA dynamics (n = 7 - 11 for each group, student t-test, * $p < 0.05$ **$p < 0.01$, *** $p < 0.001$). (d) There is no significant difference among the effects of cocaine measured with 3 different data points per cyclic voltammogram (n = 7 - 11, one-way ANOVA, $p > 0.05$).

4.4 CONCLUSIONS

In conclusion, our data provides the first experimental demonstration that real time *in vivo* DA fluctuations can be monitored by applying a combination of reduced sampling rate and data points to FSCV, with no negative impact on measurement performance. Utilizing the sampling rate of 1 Hz and collecting data at 100 data points per cyclic voltammogram reduces the quantity of data collected and transferred by two orders of magnitude compared to the traditional standard protocol. The reduction in overall volume of data generation and collection enables much longer experimental files to be taken without generating massive file sizes. We expect this reduction will also aid and facilitate the development of wireless FSCV systems for longitudinal biomedical measurements.

4.5 REFERENCES

[1] Y. Lu, et al., "Direct comparison of the response of voltammetry and microdialysis to electrically evoked release of striatal dopamine," J Neurochem, vol. 70, pp. 584-93, Feb 1998.

[2] A. S. Khan and A. C. Michael, "Invasive consequences of using micro-electrodes and microdialysis probes in the brain," Trac-Trends in Analytical Chemistry, vol. 22, pp. 503-508, Sep 2003.

[3] D. L. Robinson, et al., "Monitoring rapid chemical communication in the brain," Chem Rev, vol. 108, pp. 2554-84, Jul 2008.

[4] R. N. Adams, "*In vivo* electrochemical measurements in the CNS," Prog Neurobiol, vol. 35, pp. 297-311, 1990.

[5] P. Hashemi, et al., "Brain dopamine and serotonin differ in regulation and its consequences," Proc Natl Acad Sci U S A, vol. 109, pp. 11510-5, Jul 17 2012.

[6] J. Park, et al., "Catecholamines in the bed nucleus of the stria terminalis reciprocally respond to reward and aversion," Biol Psychiatry, vol. 71, pp. 327-34, Feb 15 2012.

[7] A. L. Sanford, et al., "Voltammetric detection of hydrogen peroxide at carbon fiber microelectrodes," Anal Chem, vol. 82, pp. 5205-10, Jun 15 2010.

[8] P. Takmakov, et al., "Characterization of local pH changes in brain using fast-scan cyclic voltammetry with carbon microelectrodes," Anal Chem, vol. 82, pp. 9892-900, Dec 1 2010.

[9] B. J. Venton, et al., "Correlation of local changes in extracellular oxygen and pH that accompany dopaminergic terminal activity in the rat caudate-putamen," J Neurochem, vol. 84, pp. 373-81, Jan 2003.

[10] J. J. Clark, et al., "Chronic microsensors for longitudinal, subsecond dopamine detection in behaving animals," Nat Methods, vol. 7, pp. 126-9, Feb 2010.

[11] J. J. Clark, et al., "Pavlovian valuation systems in learning and decision making," Curr Opin Neurobiol, vol. 22, pp. 1054-61, Dec 2012.

[12] J. M. Bledsoe, et al., "Development of the Wireless Instantaneous Neurotransmitter Concentration System for intraoperative neurochemical monitoring using fast-scan cyclic voltammetry," J Neurosurg, vol. 111, pp. 712-23, Oct 2009.

[13] F. Agnesi, et al., "Wireless Instantaneous Neurotransmitter Concentration System-based amperometric detection of dopamine, adenosine, and glutamate for intraoperative neurochemical monitoring," J Neurosurg, vol. 111, pp. 701-11, Oct 2009.

[14] C. J. Kimble, et al., "Wireless Instantaneous Neurotransmitter Concentration Sensing System (WINCS) for intraoperative neurochemical monitoring," Conf Proc IEEE Eng Med Biol Soc, vol. 2009, pp. 4856-9, 2009.

[15] C. J. Griessenauer, et al., "Wireless Instantaneous Neurotransmitter Concentration System: electrochemical monitoring of serotonin using fast-scan cyclic voltammetry--a proof-of-principle study," J Neurosurg, vol. 113, pp. 656-65, Sep 2010.

[16] P. A. Garris, et al., "Wireless transmission of fast-scan cyclic voltammetry at a carbon-fiber microelectrode: proof of principle," J Neurosci Methods, vol. 140, pp. 103-15, Dec 30 2004.

[17] A. N. Amos, et al., "Reducing the sampling rate of biochemical measurements using fast-scan cyclic voltammetry for *in vivo* applications," IEEE Sensors Journal, vol. 14, pp. 2975-2980, Sep 2014.

[18] J. G. Roberts, et al., "Real-time chemical measurements of dopamine release in the brain," Methods Mol Biol, vol. 964, pp. 275-94, 2013.

[19] G. W. Paxinos, C., The rat brain in stereotaxic coordinates, 2nd ed. ed. Orlando, FL,: Academic Press, 1986.

[20] D. Michael, et al., "Color images for fast-scan CV measurements in biological systems," Anal Chem, vol. 70, pp. 586A-592A, Sep 1 1998.

[21] L. A. Sombers, et al., "Synaptic overflow of dopamine in the nucleus accumbens arises from neuronal activity in the ventral tegmental area," J Neurosci, vol. 29, pp. 1735-42, Feb 11 2009.

[22] R. M. Wightman, et al., "Dopamine release is heterogeneous within microenvironments of the rat nucleus accumbens," Eur J Neurosci, vol. 26, pp. 2046-54, Oct 2007.

[23] G. D. Stuber, et al., "Extinction of cocaine self-administration reveals functionally and temporally distinct dopaminergic signals in the nucleus accumbens," Neuron, vol. 46, pp. 661-9, May 19 2005.

[24] M. L. Heien, et al., "Real-time measurement of dopamine fluctuations after cocaine in the brain of behaving rats," Proc Natl Acad Sci U S A, vol. 102, pp. 10023-8, Jul 19 2005.

[25] M. K. Zachek, et al., "Simultaneous monitoring of dopamine concentration at spatially different brain locations *in vivo*," Biosens Bioelectron, vol. 25, pp. 1179-85, Jan 15 2010.

[26] B. Giros, et al., "Hyperlocomotion and indifference to cocaine and amphetamine in mice lacking the dopamine transporter," Nature, vol. 379, pp. 606-12, Feb 15 1996.

[27] S. R. Jones, et al., "Different effects of cocaine and nomifensine on dopamine uptake in the caudate-putamen and nucleus accumbens," J Pharmacol Exp Ther, vol. 274, pp. 396-403, Jul 1995.

[28] Q. Wu, et al., "Preferential increases in nucleus accumbens dopamine after systemic cocaine administration are caused by unique characteristics of dopamine neurotransmission," J Neurosci, vol. 21, pp. 6338-47, Aug 15 2001.

[29] G. D. Stuber, et al., "Rapid dopamine signaling in the nucleus accumbens during contingent and noncontingent cocaine administration," Neuropsychopharmacology, vol. 30, pp. 853-63, May 2005.

CHAPTER 5

Tungsten-Based Carbon Microelectrodes Fabricated from Pyrolyzed Parylene-C for Biochemical Measurements using Fast-Scan Cyclic Voltammetry

This work was completed in collaboration with: James G. Roberts, Lingjiao Qi, Leslie A. Sombers and Gregory S. McCarty, and is in preparation for submission to *Analytical Chemistry.*

5.1 INTRODUCTION

There has been considerable interest recently in developing systems that report biochemical changes in functioning tissue or in behaving animals. These types of measurements are expected to provide insights into a wide variety of disease states and their treatments. Electroanalytical techniques have shown incredible promise for making these types of measurements. When coupled with microsensors, these techniques have demonstrated the ability to invasively probe changes in the biochemical environment with minimal damage. Due to the complexity of biological systems, microsensors that have versatility across a number of analytes and tissue types are of particular interest.

Because they resist biofouling and have a large potential window in aqueous solutions, carbon-based microelectrodes are becoming widely used microsensors for the electroanalytical characterization of biochemical signaling in functioning tissue [2], [4], [5], [7], [17], [18], [21], [22]. Carbon fiber microelectrodes (CFMs) are the most common microsensor for electroanalytical measurements due to their ease of fabrication and ability to

demonstrate consistent and accurate voltammetric measurements across a variety of analytes [7]. Fabrication of a CFM is done by hand. A carbon fiber is encapsulated in a glass capillary drawn to a sharp tip. The carbon fiber extending past the tip is manually cut to the desired length and the capillary glass is backfilled with electrolyte and fitted with wires for electrical contact. Despite their popularity as a microsensor, the design of CFMs is not well-suited for *in vivo* measurements in behaving animals. Specifically, the flimsy nature of the carbon fiber combined with the fragility of the glass seal is not ideal for long-term, sustainable microelectrodes. This limitation hampers the types of measurements that can be done with CFMs in behaving animals. Due to these limitations, efforts are being made to improve or replace CFMs as a sensor for electroanalytical measurements [4], [6], [7], [14], [21], [22].

Fast scan cyclic voltammetry (FSCV) is an electroanalytical technique frequently used with CFMs for measuring fluctuations in the concentration of electroactive analytes in tissue [19]. FSCV provides the required sensitivity and selectivity to monitor electroactive species *in vivo*.

Here, we present a tungsten-based carbon microelectrode (WCME) as an alternative to the conventional CFM. A tungsten wire treated to have a carbonous surface is used instead of a carbon fiber, and a flexible polymer is used for insulation instead of traditional capillary glass. This type of microelectrode is advantageous over the CFM in that the tungsten base is stronger and more rigid than the carbon fiber, and the polymeric insulation has increased flexibility compared to the capillary glass. This combination of properties makes the WCME less fragile than the CFM. These conditions are important for *in vivo* measurements and the

overall lifetime of the microelectrode. This work discusses the fabrication of WCMEs and the electrochemical performance of this sensor for monitoring dopamine (DA), a commonly studied electroactive neurotransmitter.

5.2 METHODS

5.2.1 Materials and Chemicals

Unless otherwise noted, all chemicals were analytical grade and purchased from Sigma Aldrich or Fisher Scientific. Sodium hydroxide was used to electrochemically etch the tungsten wire, and buffered oxide etch (Transene Company, Inc., Danvers, MA) was used to remove surface oxides from tungsten wires. Parylene-C dimer was used as received (Specialty Coating Systems, Indianapolis, IN). Paraffin wax was used to mask the tips of the electrodes. Phosphate buffered saline (PBS) (10mM Na_2HPO_4, 138 mM NaCl, 2.7 mM KCl) was used in all flow injection experiments. Stock solutions of analyte were prepared in PBS, and dilutions were prepared in PBS on the day of use. Artificial cerebral spinal fluid (aCSF) (124 mM NaCl, 3.7 mM KCl, 26mM $NaHCO_3$, 2.4 mM $CaCl_2$, 1.3 mM $MgCl_2$, 1.3 mM Na_2HPO_4, 10 mM Glucose) was used in all *ex vivo* experiments.

5.2.2 Scanning Electron Microscopy Imaging

Scanning electron microscopy (SEM) was carried out with a Hitachi S-3200N SEM (Analytical Instrumentation Facility, North Carolina State University) in variable pressure (VPSEM) mode to characterize the size and geometry of the electrodes after fabrication.

Energy-dispersive x-ray spectroscopy (EDS) was performed to chemically characterize the exposed carbon surface at the active area of the electrode and the electrode's insulation.

5.2.3 Raman Spectroscopy

Raman spectroscopy was used to verify the conversion of Parylene-C to a graphitic carbon during pyrolization. Samples of unpyrolyzed and pyrolyzed Parylene-C were excited using a 12 mW HeNe laser (Thorlabs Newton, NJ) coupled to an inverted microscope (Nikon, Melville, NY) with a 100 X dry objective (Nikon, Melville, NY). The Raman signal was analyzed through a spectrograph (Princeton Instruments, Acton, MA) and detected with a liquid nitrogen cooled CCD camera (Princeton Instruments, Acton, MA).

5.2.4 *In Vitro* Characterization of Microelectrodes using FSCV

In vitro FSCV experiments were performed using a procedure similar to previously reported studies [1]. Briefly, the working electrode for the FSCV experiments was either a WCME or a CFM for comparison. The working electrode and Ag/AgCl reference electrode (World Precision Instruments, Sarasota, FL) were placed in a custom-made electrochemical cell housed in a Faraday cage. PBS buffer was continuously supplied across the working and reference electrodes via a syringe pump at 1 mL/min. Single injections of analyte were delivered to the electrodes using an HPLC valve and air actuator controlled by a digital valve interface (Valco Instruments Co., Inc., Houston, TX). Cyclic voltammograms were acquired at a frequency of 10 Hz using a triangular waveform ranging from -0.4 V to +1.3 V and back

to -0.4 V at 400 V/s. The standard FSCV waveform was applied to the electrochemical cell within the flow injection apparatus using custom built instrumentation (University of North Carolina at Chapel Hill, Department of Chemistry, Electronics Facility).

5.2.5 *Ex Vivo* and *In Vivo* Methods

For *ex vivo* methods, male Sprague-Dawley rats (300 - 500 g, Charles River Laboratories, Raleigh, NC) were anesthetized with urethane (4 g/kg i.p.) before decapitation to rapidly remove the brain. Coronal slices (400 µm thick) containing the striatum were prepared using a vibratome (World Precision Instruments, Sarasota, FL). Slices were incubated in aCSF buffer with 20 mM HEPES, at pH 7.4, continually saturated with 95 % O_2, 5 % CO_2, and allowed to equilibrate in buffer for 45 minutes. Slices were then placed in a heated recording chamber (Warner Instruments, Hamden, CT) and superfused with aCSF at 34 °C to perform electrochemical measurements. DA was detected simultaneously at both a CFM and WCME placed in the caudate putamen (CPu) (1.2 mm anterior to bregma). Neurotransmitter release was electrically evoked using a biphasic constant current pulse (500 µA, 2 ms each pulse, 60 pulses, 60 Hz) delivered by a bipolar stimulating electrode (FHC Inc., Bowdoin, ME). The working electrode and stimulating electrode placements were made with the aid of a microscope (Nikon Instruments, Inc., Melville, NY), and the electrodes were positioned ~50 µm below the surface of the slice. The tips of the CFM and WCME were located 1 mm away from the stimulating electrode. All procedures were performed in

accordance with the North Carolina State University Institutional Animal Care and Use Committee (IACUC).

For *in vivo* methods, male Sprague-Dawley rats (300 - 500 g, Charles River Laboratories, Raleigh, NC) were deeply anesthetized with sodium urethane (1.5 g/kg i.p.) and placed in a stereotaxic frame (Kopf Instrumentation, Tujunga, CA). The skull was exposed to reveal reference points (bregma and lamda) that aided leveling and electrode placement. A WCME was positioned in the dorsal striatum (+1.2 mm AP, +1.5 mm ML, -4.5 mm DV) and a bipolar stimulating electrode was placed in the medial forebrain bundle (MFB) (-4.6 mm AP, +1.3 mm ML, -8.8 mm DV). A Ag/AgCl reference electrode was positioned in the contralateral hemisphere, relative to the WCME. The electrochemical waveform was applied to the WCME as described earlier to monitor electrically evoked DA fluctuations. The stimulating electrode was used to drive the electrically evoked release of DA in the dorsal striatum (60 Hz, 60 pulses, 150 μA). The animal's body temperature was maintained at 37 °C by a heating pad. Animal care and use was in accordance with North Carolina State University IACUC guidelines.

5.3 RESULTS AND DISCUSSION

5.3.1 Fabrication of Tungsten-based Carbon Microelectrodes

5.3.1.1 Creating a Conical Active Tip

Bare tungsten wires were cut to length and etched to a conical tip using an electrochemical etching procedure, schematically shown in **Figure 5.1 (a, b)**. The etching

parameters were tailored to acquire the desired conical geometry of the microelectrode, so as to minimize tissue damage. Previously fabricated microelectrodes have been etched in sodium hydroxide (NaOH) [7], [8], [15] and potassium hydroxide (KOH) [5], [8], [10], [11] at concentrations ranging from 1.0 M - 3.0 M. Both platinum and iridium loops have been reported as counter electrodes [5], [7], [8], [10]. For this work, a 2.0 M NaOH etching solution and a platinum coil as counter electrode were selected. Electrochemical etching potential and rate has also been studied relating to microelectrode fabrication [5], [7], [8], [10], [11], [15]. In this work, an etching potential of 5.0 V DC and a motion rate of 5.0 μm/sec was experimentally determined to yield the desired geometry for the WCMEs. Typically, the tungsten wire was lowered into the etching solution for 2 minutes at the desired motion rate and allowed to sit in the solution for 30 seconds before being removed from the solution at the same motion rate. This procedure resulted in a conical tip that was ~200 um long with an average cone angle of 8.11° ± 3.74° (n = 9).

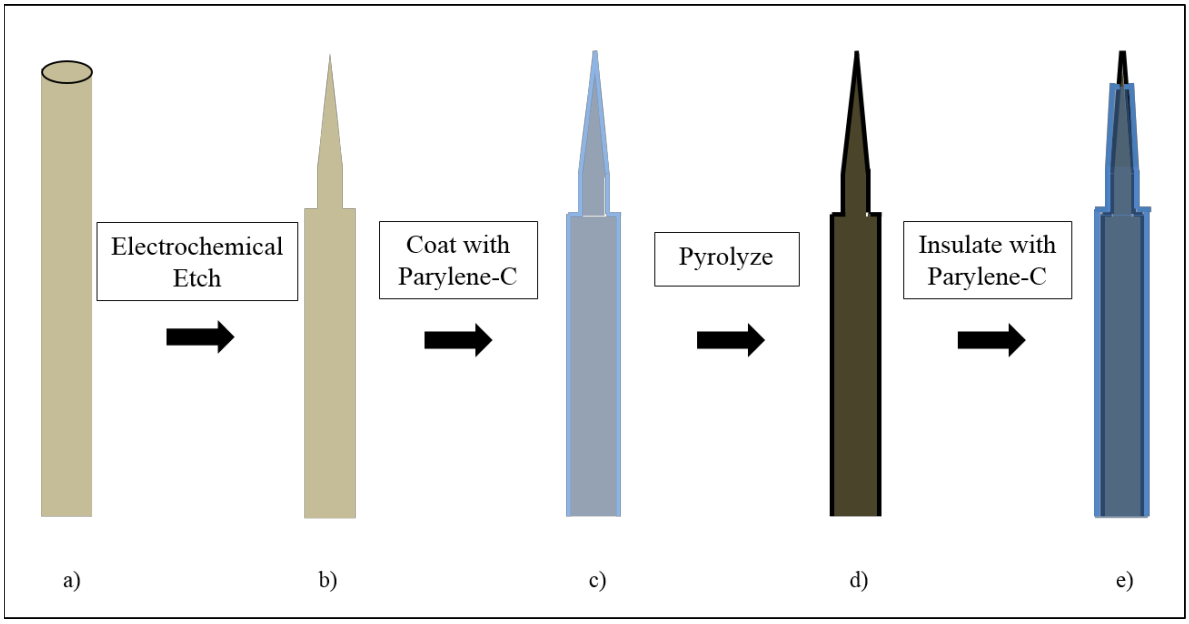

Figure 5.1 – Fabrication of tungsten-based carbon microelectrodes. (a) untreated tungsten wire, (b) tungsten wire wet etched in 2.0 M NaOH at 5.0 µm/sec, 5.0 V DC, (c) tungsten wire coated with 10 µm of Parylene-C, (d) graphitic carbon replacing Parylene-C on surface of tungsten wire after pyrolization, (e) carbonized tungsten wire insulated with 10 µm Parylene-C.

5.3.1.2 Generating a Carbonous Surface

The quality of the graphitic carbon surface of the microelectrode is central to its performance. The graphitic carbon surface must be free of defects and have good conductivity. For these reasons, it is important to choose a starting material that evenly coats the tungsten with no pin holes and that can be readily converted to graphitic carbon. Both photoresist and Parylene-C have been shown to pyrolyze into high conductivity graphitic carbon films in a reproducible and repeatable manner [8], [14], [16]. In this work, Parylene-C was selected as the precursor polymeric film for pyrolization because it evenly coats irregular surfaces without defects [13].

Prior to deposition of Parylene-C on the tungsten wires, a cleaning step was used to remove any surface oxides. Oxides reduce the adhesion of Parylene-C to the tungsten, resulting in the loss of the graphitic carbon from the surface of the tungsten during electrochemical testing. Detection of analyte species could not be carried out without the presence of carbon at the electrode surface. The formation of tungsten oxides has been characterized at approximately 1 nm/day when exposed to air [5] [12], [15]. Several different methods have been reported for removing tungsten's surface oxide [7], [8], [15]. Here, buffered oxide etch was used to remove any surface oxides present on the tungsten.

Immediately after surface oxides were removed from the etched tungsten wires, deposition of 10 μm Parylene-C was carried out using a commercially available chemical deposition system (Specialty Coating Systems, Indianapolis, IN), **Figure 5.1 (c)**. Pyrolysis of the Parylene-C layered tungsten wires was performed in a tube furnace (Sentro Tech Corporation, Strongsville, OH) under a forming gas environment, **Figure 5.1 (d)**, converting the Parylene-C to a conductive graphitic carbon. Verification of a graphitic carbon surface was done using Raman spectroscopy, **Figure 5.2 (a)**. The pyrolyzed Parylene-C showed peaks characteristic with previously reported Raman signals for glassy carbon [9], [21]. The Raman spectrum of graphitic carbon is dominated by two peaks. A peak at about 1600 cm^{-1}, called the graphite band (G), corresponds to the organized carbon rings in a graphite structure. Additionally, a defect band (D1) is present around 1380 cm^{-1} that originates from the disorder in the graphitic film. The presence of these two peaks indicates a successful pyrolization of Parylene-C to a graphitic carbon.

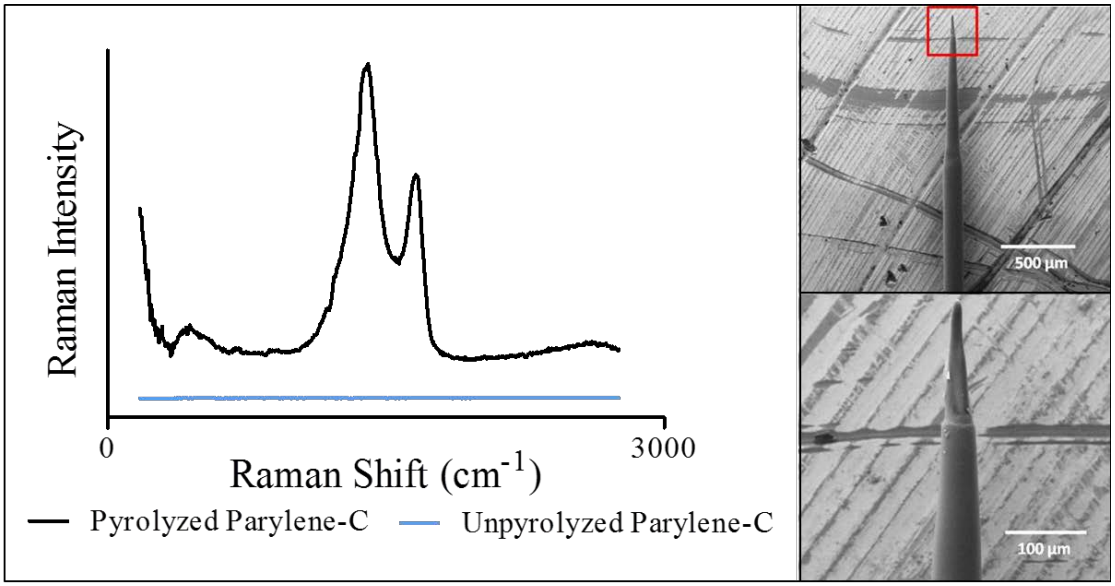

Figure 5.2 – Raman spectra for pyrolyzed and unpyrolyzed Parylene-C. (a) Raman spectrum of Parylene-C coated tungsten wire and tungsten wire treated to have a graphitic carbon surface after pyrolization. (b) SEM images of a representative tungsten-carbon electrode.

5.3.1.3 Insulation of Tungsten-based Carbon Microelectrodes

The graphitic carbonized tungsten wires were insulated with a second layer of 10 µm Parylene-C, **Figure 5.1 (e)** to isolate the conductive carbon, except for the tip that would serve as the active part of the microelectrode. A custom fixture was designed to lower and secure the tungsten wires in paraffin wax using a micromanipulator prior to the second deposition of Parylene-C. The paraffin wax was used to mask the tips of the electrodes and prevent them from being coated with Parylene-C. After Parylene-C deposition, the fabricated WCMEs were removed from the fixture, and excess paraffin wax was removed from the

electrode tips using turpentine. Scanning electron microscopy images characterized the size and geometry of the WCMEs, with representative images shown in **Figure 5.2 (b)**. Elemental analysis confirmed electrodes with a carbon surface on top of a tungsten base, insulated by Parylene-C (data not shown).

5.3.2 Comparison of Tungsten-based Carbon Microelectrodes to Carbon Fiber Microelectrodes

5.3.2.1 Mechanical Strength of Electrode Fabrication

In an effort to visualize the difference in fragility between the WCMEs compared to the traditional CFMs, electrodes of each type were inserted into 1.0 % agar [3], and displaced medially and laterally in 200 µm increments between 200 and 1000 µm. Displacement was simultaneously demonstrated visually with the aid of a microscope (Nikon Instruments, Melville, NY) and voltammetrically by looking at the background CV during the incremental movements. **Figure 5.3 (a)** shows a representative CFM inserted 500 µm in agar before displacement (left) and the corresponding voltammetric background CV (right). **Figure 5.3 (b)** displays a representative CFM inserted 500 µm in agar with a 600 µm displacement (left), and corresponding background CVs for 4 incremental displacements (right). The collected background current increases for the CFMs when it is incrementally displaced. Taking measurements *in vivo* in complex and heterogeneous brain tissue requires an electrode with strength and some flexibility while maintaining a stable background. 80 % of the CFMs tested failed at a displacements between 200 µm and 800 µm (n = 5 electrodes).

The WCMEs did not experience a bend like the CFMs. In fact, the strength of tungsten base kept the overall electrode straight, even when attempting to displace them in a similar fashion as the CFMs. The WCME displacement test was repeated in 2.0 % agar to verify their performance in a stiffer media, and the same results were observed. These data allude to the WCMEs offering a stronger base compared to the CFMs, suggesting they may be better suited for making measurements in behaving animals. Though some flexibility was observed with the CFMs, the displacement resulted in a substantial change in the background of the electrode, making it difficult to obtain stable measurements over time. Additionally, the glass insulation has the potential of breaking upon electrode failure, potentially leaving small pieces of glass behind and making it difficult to use another electrode in the vicinity.

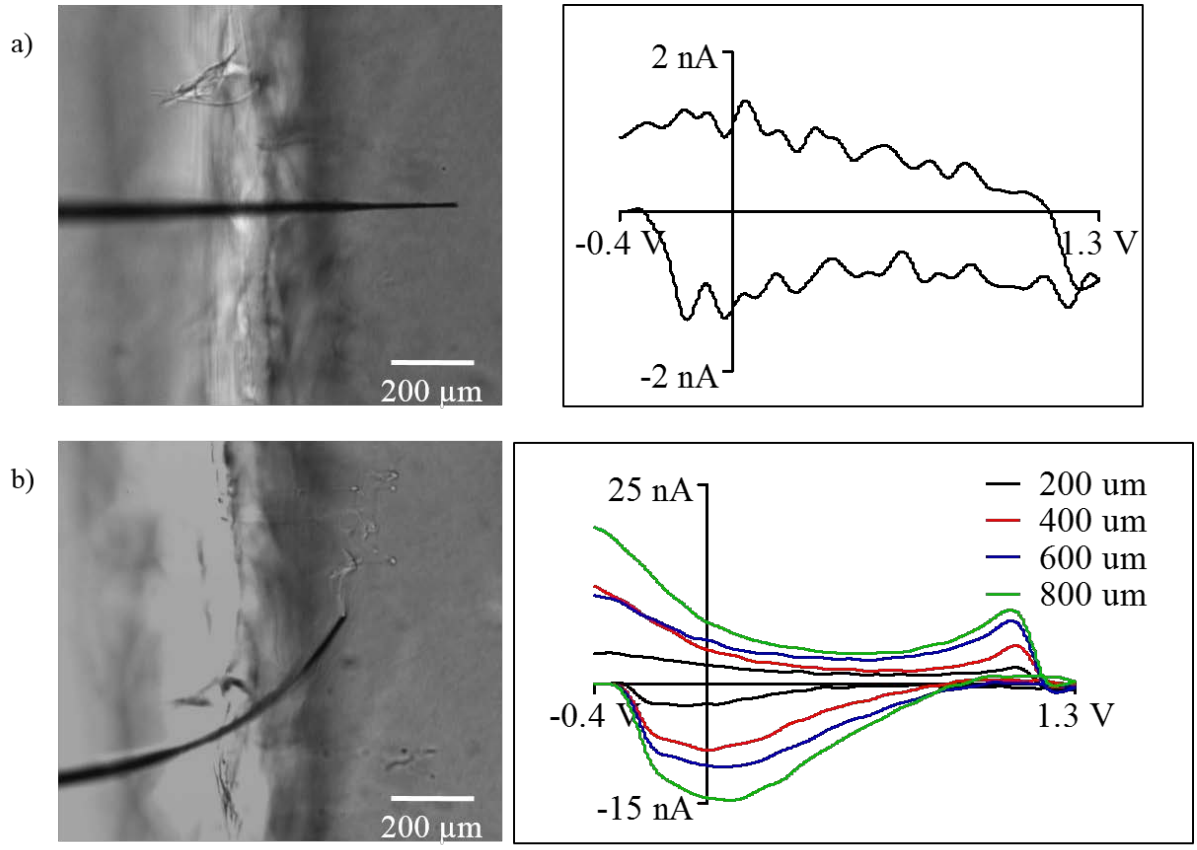

Figure 5.3 – Mechanical strength of microelectrodes. (a) Representative CFM inserted in 500 µm 1.0% agar (left) and resulting background CV (right). (b) Representative CFM inserted 500 µm in 1.0% agar, then displaced 600 µm using a micromanipulator (left); resulting background-subtracted CVs of incremental CFM displacement (right).

5.3.2.2 Responsivity and Limit of Detection for Dopamine

The real-time electroanalytical detection of catecholamines in tissue is becoming a more routine measurement in neuroscience research [16]. At this time, the standard protocol for making *in vivo* catecholamine measurements utilizes fast scan cyclic voltammetry (FSCV) at CFMs. For this reason, the electrochemical performance of the WCME is compared to the performance of the conventional CFM for DA detection using the

conventional FSCV protocol. Due to its biological importance and existing detection protocols, DA is a commonly studied catecholamine. **Figure 5.4** summarizes the electrochemical response of WCMEs to a 2 second injection of a 2 µM DA solution and compares it to a typical response with CFMs. An electrochemical color plot of the response of the sensor is shown in **Figure 5.4 (a)**. This color plot is comprised of 300 individual CVs taken in series over 30 seconds. Time is plotted on the x-axis, applied potential on the y-axis and current shown in false color. The color plot provides detailed information on the performance of the measurement. The DA injection is signified by the white arrow, and the response to DA is apparent from the features in the color plot. After the injection, the current signal returns to near baseline, indicating that no fouling occurred.

The electrochemical response can be visualized more traditionally by plotting the collected current versus time and the CV during the injection. The normalized current response at the peak oxidation potential of DA over time is shown in **Figure 5.4 (b)** for both the CFM and proposed WCME. The DA injection caused a large increase in current that rapidly cleared after the injection. The slight shift in baseline after the analyte injection is commonly observed during this measurement. A background-subtracted CV of both electrodes' response to a DA injection is given in **Figure 5.4 (c)**. This CV has peaks at the accepted oxidation and reduction potentials for DA at carbon using FSCV and has a similar magnitude of response to CFMs. These results suggest that the WCMEs are performing as well as CFMs electrochemically.

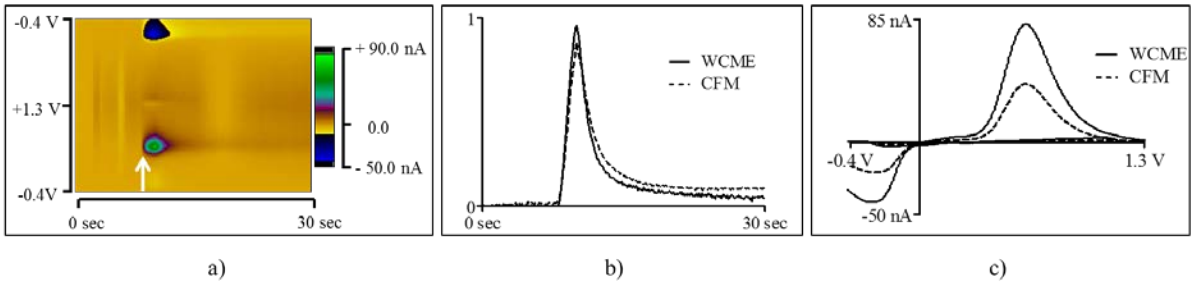

Figure 5.4 – Electrochemistry results of tungsten-based carbon microelectrodes using FSCV. (a) Color plot response of a representative tungsten electrode to a 2 µM DA solution in PBS using a potential of -0.4 V to +1.3 V and back to -0.4 V. Injection of DA is given by the white arrow. (b, c) Normalized current response over time and background subtracted CVs for injections of DA using a CFM (1uM) and a WCME (2uM).

To further explore the electrochemical performance of the WCMEs, the current response was collected at four biologically relevant concentrations of DA and compared to the response of CFMs. **Figure 5.5** depicts the current density of the peak oxidation potential versus concentration of DA for both electrode types. Average peak current density is reported with error bars representing standard deviation. To estimate the area of the microelectrodes, their backgrounds were compared. The WCME had a similar background to the CFM, suggesting their surface areas were also similar. From this information, the responsivity to DA and the theoretical limit of detection (LOD), defined as three times the RMS noise, were calculated. The responsivity of the WCMEs to DA was 38 ± 20 nA/µM with a LOD of 20 nM, similar to CFMs with a responsivity of 25 ± 10 nA/µM, and a LOD of 5 nM. Values are given as the average ± standard deviation, n = 5 electrodes. While the WCMEs exhibited a larger LOD compared to the CFM, it is still lower than physiological concentrations found in

the brain. The results indicate that using the proposed WCMEs had little impact ability to monitor DA when used with the standard FSCV protocol.

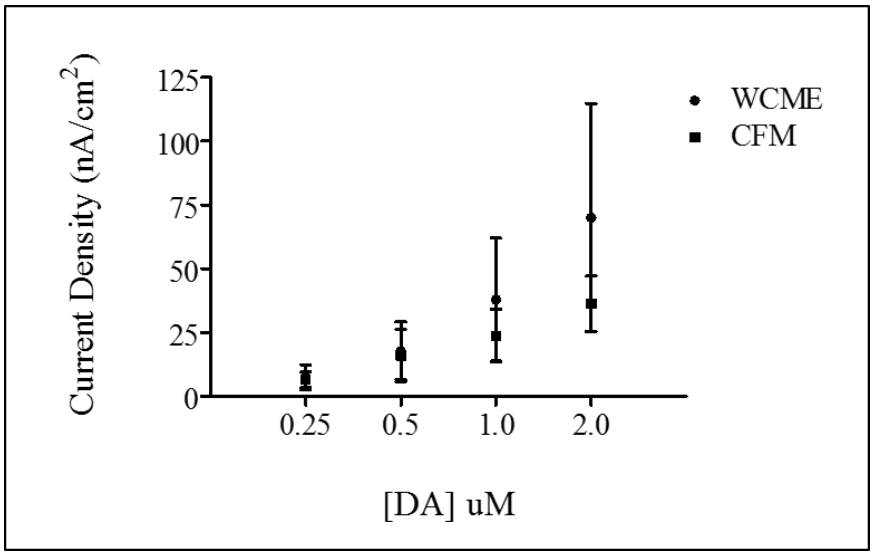

Figure 5.5 – Microelectrode responsivity to dopamine. Average response of tungsten-based carbon microelectrodes and conventional carbon fiber microelectrodes to various concentrations of dopamine (n = 5 electrodes). Values are average ± standard deviation.

5.3.2.3 Chemical Selectivity of WCMEs

After determining the responsivity and limit of detection for DA, the WCMEs were tested for chemical selectivity. The selectivity of the electrochemical response was assessed for several biologically relevant analytes by calculating correlation factors between the CVs of DA and those of hydrogen peroxide (H2O2), pH, adenosine, ascorbic acid, and 3, 4-dihydroxyphenylacetic acid (DOPAC). **Figure 5.6** reports the background subtracted CVs for these analytes at the WCMEs (solid line) and the CFMs (dotted line). Inspection of the CVs

in **Figure 5.6** suggests similar electrochemical selectivity between the CFMs and WCME. To further evaluate the selectivity, correlation factors were calculated for the two microelectrode types.

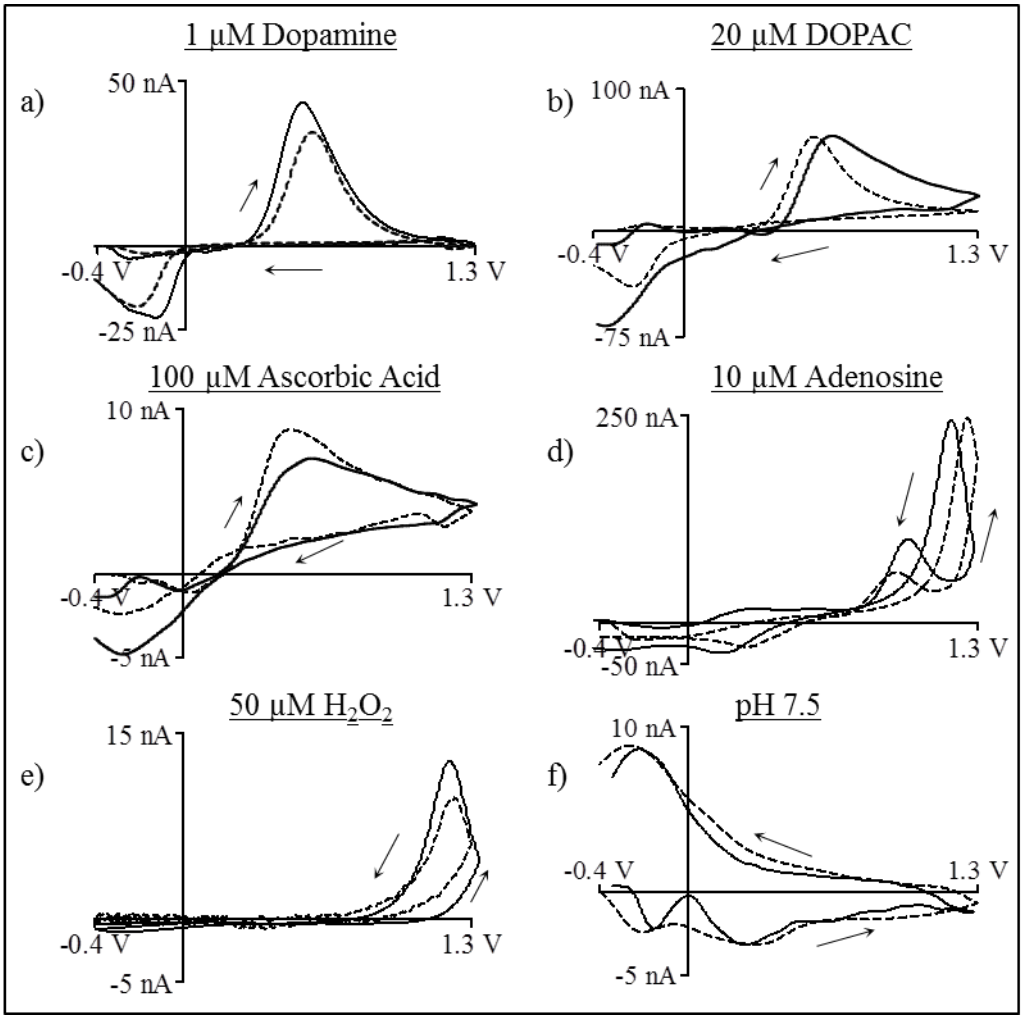

Figure 5.6 – Selectivity of tungsten-based carbon microelectrodes. Representative background-subtracted CVs of response to several biologically relevant analytes using conventional CFM (dashed line) and the proposed tungsten microelectrodes (solid line). Arrows indicate direction of the scan.

Table 5.1 reports correlation factors between the DA CV and the other analytes tested for both types of electrodes (n = 5 electrodes, values are given as the average ± standard deviation). To determine the correlation factor, CVs of DA and each analyte were compared, and the r^2 value reported. A correlation factor of 1 represents a true CV match. Molecules with CVs similar to DA exhibit higher correlation factors than those with significantly different CV shapes, or oxidation and reduction potentials, when compared to DA. Resulting correlation factors for the WCME were similar to those of the CFM, showing that the WCMEs exhibited similar selectivity for these species as the CFMs. Subtle differences in peak location and amplitude are expected between the two electrode types due to the difference in their conductivity and surface properties.

Table 5.1 – Correlation factors depicting voltammetric discrimination between analytes.

	DOPAC	AA	Adenosine	H_2O_2	pH
WCME	0.83 ± 0.05	0.70 ± 0.07	0.11 ± 0.04	0.03 ± 0.04	0.53 ± 0.05
CFM	0.89 ± 0.03	0.71 ± 0.03	0.01 ± 0.005	0.0 ± 0.0	0.41 ± 0.03

5.3.2.4 Electrode Performance in Tissue

After determining that the electrochemical performance of the WCMEs and the CFM were comparable *in vitro*, the electrodes were tested in tissue. Initial experiments were

performed in coronal slices of rat brain to see if the WCMEs could detect electrically elicited DA release in live tissue. A CFM and WCME were placed together in the dorsal striatum region of an excised rat brain slice and DA was elicited using external electrical stimulation. A stainless steel stimulating electrode provided 60 pulses of 500 µA amplitude at 60 Hz to the striatum and the CFM and WCME recorded the elicited DA response to the stimulation. **Figure 5.7** reports the results of the stimulated DA release for both the CFM and the WCME. In **Figure 5.7 (a)**, a color plot of the DA release is shown for each electrode, with the stimulation pulses occurring at the white arrows. **Figure 5.7 (b)** reports the same stimulated DA release in a background-subtracted CV for each electrode type. From these data, it was determined that the WCME could detect stimulated DA release similarly to that of a CFM in excised striatal tissue.

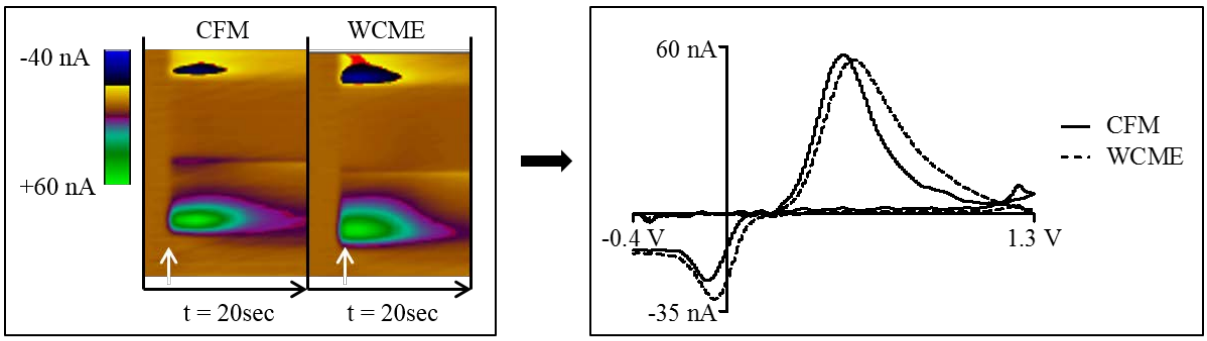

Figure 5.7 – *Ex vivo* response of microelectrodes to electrically stimulated dopamine in a rat brain slice. Color plot response (a) and background-subtracted CVs (b) of electrically elicited dopamine for a CFM and WCME, stimulated with 60 pulses, 500µA, at 60 Hz. Stimulation of DA release is indicated by the white arrows.

Lastly, the operation and stability of the WCME was verified for *in vivo* measurements. Many *in vivo* experiments can span several hours, and an electroanalytical sensor needs to be able to detect analytes reliably for at least this time period. The operation and stability of the WCME was tested *in vivo* by implanting one into the dorsal striatum of an anesthetized rat. Electrically evoked DA release was monitored over a period of six hours and compared to a control experiment with a CFM. **Figures 5.8 (a, b)** show the color plot response and background-subtracted CVs of evoked DA release, measured by both the CFM and WCME. White arrows mark the time of the electrical stimulation. **Figure 5.8 (c)** reports the average percent change in peak DA concentration evoked from the initial time point over a six hour period for both electrode types. The WCME reported a 78 % ± 12 % change in current over time, with the CFM showing a 71 % ± 18 % change in current over time. From these data, it was concluded that the WCME detected evoked DA release over time comparably to the traditional CFM.

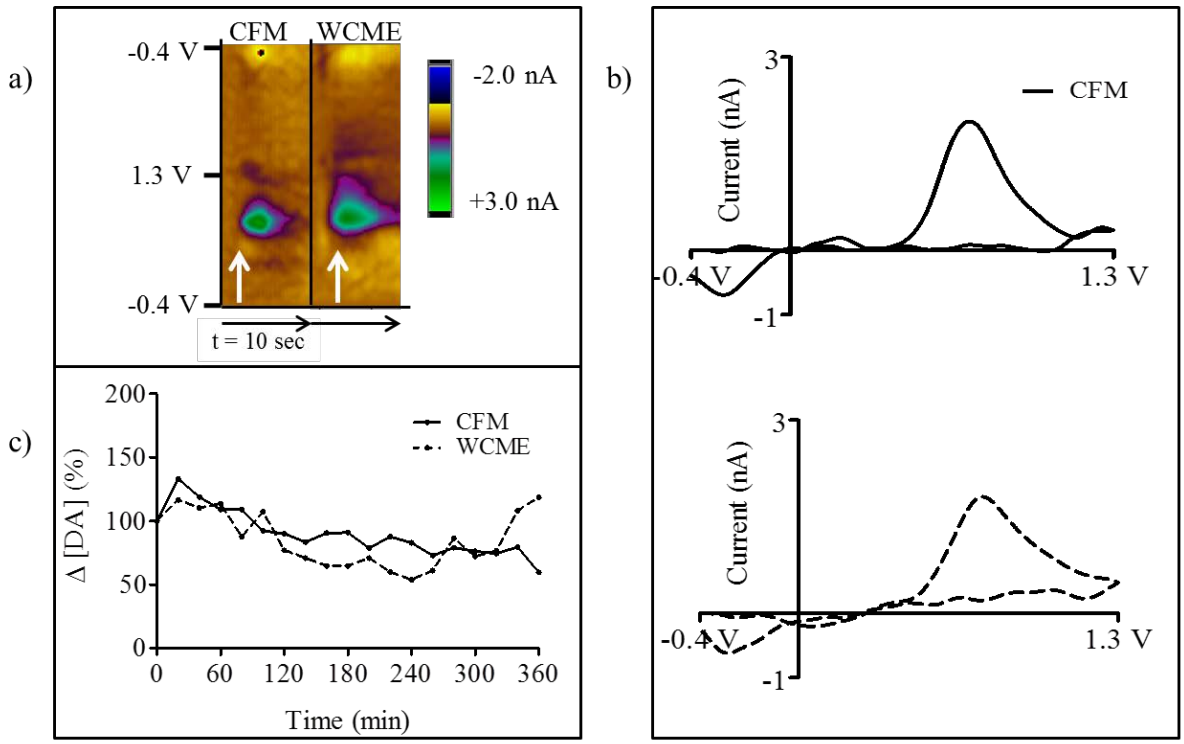

Figure 5.8 – *In vivo* response of microelectrodes to evoked dopamine release in the caudate putamen. (a, b) Color plots and background-subtracted CVs of evoked DA release for both electrode types. (c) Percent change in peak DA concentration compared to the initial concentration elicited at time 0 over a six hour period for both a standard CFM and WCME. Stimulation to evoke DA release occurs at the white arrows shown in (a).

5.4 CONCLUSIONS

Pyrolyzed Parylene-C was used in conjunction with a tungsten wire to create microelectrodes that enable FSCV measurements. These sensors are expected to be more practical for measurements in large animal models and for longer-term voltammetric measurements in tissue compared to traditional CFMs. In this work, a tungsten-based carbon microsensor is demonstrated for measuring fluctuations in DA and other biologically-relevant analytes. The tungsten-based carbon microsensor has comparable electrochemical

performance to CFMs both *in vitro* and *in vivo*, and over several hours of use. Using tungsten wire as the base of the microelectrode provides more strength and rigidity compared to a carbon fiber. Additionally, use of a polymer for insulation is advantageous over capillary glass in that it provides more flexibility, and reduces the size of electrode and the risk of breaking during use. Overall, the tungsten-based microsensor provides a more robust design than the conventional CFMs. Improving the ease of fabrication of these electrodes is being examined.

5.5 REFERENCES

[1] A. N. Amos, J. G. Roberts, L. Qi, L.A. Sombers, and G. S. McCarty. Reducing the sampling rate of biochemical measurements using fast-scan cyclic voltammetry for *in vivo* applications. *IEEE Sensors14,* 2975-2980 (2014).

[2] J. C. Conti, E. Strope, R. N. Adams, and C. A. Marsden. Voltammetry in brain-tissue - chronic recording of stimulated dopamine and 5-hydroxytryptamine release. *Life Sci. 23,* 2705-2715 (1978).

[3] R. Das, D. Gandhi, S. Krishnan, L. Saggere, and P. J. Rousche. A benchtop system to assess cortical neural interface micromechanics. *IEEE Trans. Biomed. Eng. 54,* 1089-1096 (2007).

[4] A. G. Ewing, and R. M. Wightman. Monitoring the stimulated release of dopamine *with in vivo* voltammetry. 2. Clearance of released dopamine from extracellular fluid. *J. Neurochem. 43,* 570-577 (1984).

[5] O. L. Guise, J. W. Ahner, M. C. Jung, P. C. Goughnour, and J. T. Yates. Reproducible electrochemical etching of tungsten probe tips. *Nano Letters 2,* 191-193 (2002).

[6] M. L. A. V. Heien, P. E. M. Phillips, G. D. Stuber, A. T. Seipel, and R. M. Wightman. Overoxidation of carbon-fiber microelectrodes enhances dopamine adsorption and increases sensitivity. *Analyst 128,* 1413-1419 (2003).

[7] A. Hermans, and R. M. Wightman. Conical tungsten tips as substrates for the preparation of ultramicroelectrodes. *Langmuir 22,* 10348-10353 (2006).

[8] R. Hobara, S. Yoshimoto, S. Hasegawa, and K. Sakamoto. Dynamic electrochemical etching technique for tungsten tips suitable for multi-tip scanning tunneling microscopes. *E-Journal of Surface Science andNanotechnology5,* 94-98 (2007).

[9] J. Jakabovic, et al. Preparation and properties of thin parylene layers as the gate dielectrics for organic field effect transistors. *Microelectron. J. 40,* 595-597 (2009).

[10] B. Ju, Y. Chen, M. Fu, Y. Chen, and Y. Yang. Systematic study of electropolishing technique for improving the quality and production reproducibility of tungsten STM probe. *Sensors and Actuators A-Physical 155,* 136-144 (2009).

[11] B. Ju, Y. Chen, and Y. Ge. The art of electrochemical etching for preparing tungsten probes with controllable tip profile and characteristic parameters. *Rev. Sci. Instrum.82,* 013707 (2011).

[12] R. S. Lillard, G. S. Kanner, and D. P. Butt. The nature of oxide films on tungsten in acidic and alkaline solutions. *J. Electrochem. Soc. 145,* 2718-2725 (1998).

[13] G. E. Loeb, M. J. Bak, M. Salcman, and E. M. Schmidt. Parylene as a chronically stable, reproducible microelectrode insulator. *IEEE Trans. on Biomed. Eng. 24*, 121-128 (1977).

[14] K. C. Morton, C. A. Morris, M. A. Derylo, R. Thakar, and L. A. Baker. Carbon electrode fabrication from pyrolyzed Parlyene-C. *Anal. Chem.83,* 5447-5452 (2011).

[15] A. D. Muller, et al. Characterization of electrochemically etched tungsten tips for scanning tunneling microscopy. Rev. Sci. Instrum. *70,* 3970-3972 (1999).

[16] M. Perry, Q. Li, and R. T. Kennedy. Review of recent advances in analytical techniques for the determination of neurotransmitters. *Anal. Chim. Acta653,* 1-22 (2009).

[17] S. Ranganathan, R. L. McCreery, S. M. Majji, and M. Madou. Photoresist-derived carbon for microelectromechanical systems and electrochemical applications. *J. Electrochem. Soc.147,* 277-282 (2000).

[18] S. Ranganathan, and R. L. McCreery. Electroanalytical performance of carbon films with near-atomic flatness. *Anal. Chem.73,* 893-900 (2001).

[19] J. G. Roberts, B. P. Moody, G. S. McCarty, and L. A. Sombers. Specific oxygen-containing functional groups on the carbon surface underlie an enhanced sensitivity to dopamine at electrochemically pretreated carbon fiber microelectrodes. *Langmuir26,* 9116-9122 (2010).

[20] D. L. Robinson, B. J. Venton, M. L. Heien, and R. M. Wightman. Detecting subsecond dopamine release with fast-scan cyclic voltammetry *in vivo*. *Clin. Chem.49,* 1763-1773 (2003).

[21] D. Takagi, Y. Suzuki, and N. Kasagi. Pyrolyzed Parylene structure as selective emitter for high-efficiency thermophotovoltaic power generation. *Proceedings of the IEEE Twentieth Annual International Conference on Micro Electro Mechanical Systems, Vols 1 and 2,* 710-713 (2007).

[22] M. K. Zachek, J. Park, P. Takmakov, R. M. Wightman, and G. S. McCarty. Microfabricated FSCV-compatible microelectrode array for real-time monitoring of heterogeneous dopamine release. *Analyst135,* 1556-1563 (2010).

[23] M. K. Zachek, P. Takmakov, B. Moody, R. M. Wightman, and G. S. McCarty. Simultaneous decoupled detection of dopamine and oxygen using pyrolyzed carbon microarrays and fast-scan cyclic voltammetry. *Anal. Chem. 81*, 6258-6265 (2009).

CHAPTER 6

Assessment of Tungsten-Based Carbon Microsensor for Biochemical Measurements in Behaving Animals using Fast-Scan Cyclic Voltammetry

This work is part of an ongoing study in collaboration with: Leslie R. Wilson, Lingjiao Qi, James G. Roberts, Xiaohu Xie, Leslie A. Sombers and Gregory S. McCarty.

6.1 INTRODUCTION

There has been significant interest in obtaining chronic biochemical measurements for the assessment of pharmacological effects and of more realistic behavioral paradigms. Electroanalytical techniques have the potential of being incredibly useful for these types of measurements. When coupled with microsensors, these techniques have been successfully used for real-time measurements of biochemical fluctuations *in vivo*.

Fast-scan cyclic voltammetry (FSCV) is a proven *in vivo* technology capable of monitoring rapid changes in the brain and associating them with behavior [1]. FSCV at carbon fiber microelectrodes (CFMs) provides the necessary sensitivity and selectivity to make biochemical measurements in tissue with excellent temporal and spatial resolution and has been used to monitor dopamine [2], [6], [12], [18], [19], [25], norepinephrine [10], [14], serotonin [5], [7], [11], hydrogen peroxide [17], [20], [21], oxygen [24], [26] and pH [23], [24]. Carbon-based microsensors have become very popular for characterizing biochemical signaling because of their resistance to biofouling and their large potential window [4], [8],

[9], [13], [16], [19], [26], [27]. Fabrication of a CFM is typically done by hand and features a carbon fiber encapsulated in a glass capillary, drawn to a sharp tip with a micropipette puller. The fiber extending past the glass seal is cut to the desired length and the capillary glass is fitted with a stainless steel wire and conductive silver epoxy for electrical contact. However, CFMs traditionally are difficult to use *in vivo* due to their fragility. The combination of a flimsy carbon fiber and glass seal make these sensors poorly-suited to long-term monitoring of biochemicals. Recently, a chronic microsensor has been developed in place of a CFM for monitoring rapidly fluctuating dopamine in intact animals [3]. This chronic microsensor utilizes a fused silica insulation, which has more flexibility compared to capillary glass, but still contains a carbon fiber. Often, the carbon fiber will break off at the interface with the fused silica, making this sensor tedious to fabricate and difficult to successfully implant in animals.

Here, we present an alternative microsensor with a more robust design for use in chronic experiments with implanted electrodes. We have shown in **Chapter 5** that this alternative microsensor performs similarly to a CFM *in vitro*, *ex vivo* and *in vivo*. This microsensor features a tungsten wire pretreated to have a carbon surface in place of the conventional carbon fiber and electrodeposited polymer insulation instead of the traditional glass capillary. The design is more advantageous than the current chronic microsensor as it improves on not one, but both of the major drawbacks to the CFM. This work is part of an ongoing study that evaluates the alternatively designed carbonized tungsten electrode in freely moving animals.

6.2 METHODS

6.2.1 Materials and Chemicals

Unless noted, all chemicals were purchased from Sigma Aldrich and used as received. Phosphate buffered saline (PBS) (10 mM Na_2HPO_4, 138 mM NaCl, 2.7 mM KCl) was used in flow injection experiments. Stock solutions of analyte were prepared in 0.1 N $HClO_4$, and dilutions were prepared in PBS buffer on the day of use.

6.2.2 Electrode Fabrication

The carbonized tungsten microsensors were fabricated as previously described in **Chapter 5** with a few modifications. All of the initial fabrication methods were used as previously, but an improved final insulation technique was employed. As part of the initial fabrication, bare tungsten wire (50 µm diameter) was cut and cleaned in buffered oxide etch to remove any surface oxides. The wires were then coated with 10 µm of Parylene-C using a commercially available chemical deposition system (Specialty Coating Systems, Indianapolis, IN). The Parylene-C was used to generate a graphitic carbon surface upon pyrolysis in a tube furnace (Sentro Tech Corporation, Strongsville, OH) under a forming gas environment. After pyrolysis, the carbonized tungsten wires were fed into 1 cm length fused silica tubing with polyamide coating (100 µm I. D.), leaving ~200 µm exposed on the active, or uninsulated, end. The silica was epoxied in place and the non-active end was soldered to a gold pin. Further insulation of the active end was necessary to obtain an active electrode length of 25 µm.

A new insulation technique was implemented to define the active area of the microsensor. In addition, this technique improved the sensor yield. Briefly, the carbonized tungsten electrodes were micropositioned above a conductive silicon sheet (Marian, Inc., Indianapolis, IN) and the measured impedance (Signal Recovery, Oak Ridge, TN) at the electrode/silicon interface signified surface contact. The conductive silicon sheet was raised the desired height (typically 25 µm), allowing the electrode to penetrate the silicon and mask the tip of the electrode from the insulation process. Additionally, there was a silicone ring (Ø1 cm) on top of the conductive silicon surrounding the masked electrode to retain ~0.5 mL of insulation solution around the exposed carbon surface. The phenolic insulation coating procedure was exactly followed from literature [22]. A phenolic mixture (phenol, 2-allylphenol, and 2-butoxyethanol in a 1:1 methanol: water solution, at pH 9.0) was electrodeposited on the carbon surface for 14 min at +4.0 V DC versus a platinum reference.

After coating, the electrode was removed from the silicon mask and oven dried for 30 min at 150 °C. Following the drying process, the electrodes were further coated in paraffin by dipping the electrode tip into liquid wax to form a thin coating. The wax coating on the uninsulated tip of the electrode was immediately removed by electrochemical cycling [24].

For comparison, a carbon-fiber-based chronic electrode was fabricated similar to previously described [3]. Briefly, these chronic electrodes utilize T-650/35 PAN based carbon fibers, insulated with a 1 cm long silica tubing with a polyimide coating (18 µm O.D.). After being placed in a bath of 70 % isopropyl alcohol, the carbon fiber was inserted though the silica tubing under a stereoscopic microscope. After insertion, the carbon fiber

and silica were allowed to dry for 24 hours. A seal was created using non-conductive epoxy at one end of the silica tubing (Devcon, Danvers, MA). An electrical connection to the carbon fiber was made using conductive silver epoxy (MG Chemical, Burlington, Ontario, Canada) and allowed to dry for 24 hours. The silver epoxy was covered with non-conductive epoxy and electrodes were subsequently placed in an oven at 100 ºC for 20 minutes to allow epoxy to completely cure. Carbon fibers were then cut at the sealed end under a stereoscopic microscope to a length of between 150 – 200 µm using a graduated microscope slide and microscissors (Westcott Corneal, Medline, Inc., Mundelein, IL).

6.2.3 Animals and Survival Surgery

Adult male Sprague-Dawley rats weighing between 250 - 300 g were purchased from Charles River Laboratories (Wilmington, MA). Animals were individually housed on a 12: 12 hr light: dark cycle with access to food and water. The surgical procedure was performed as described previously [18]. Briefly, rats were anesthetized with isoflurane (Vetqeuip; Pleasanton, CA), which was induced at 4 % and maintained at 1.5 - 2.0 % during surgery. Rats were positioned into a stereotaxic frame (Kopf Instrumentation; Tujunga, CA). A heating pad (Harvard Apparatus, Holliston, MA) was used to maintain body temperature at 37 °C. Holes for electrodes were drilled in the skull according to coordinates from the brain atlas of Paxinos and Watson [15]. The Ag/AgCl reference electrode was placed in the forebrain, and a carbonized tungsten electrode was placed above the contralateral nucleus accumbens (1.7 mm anterior, 0.8 mm lateral, 2.5 mm ventral relative to bregma). The bipolar

stimulating electrode (Plastics One, Roanoke, VA) was implanted unilaterally into the ventral tegmental area (VTA) (5.9 mm posterior, 1.0 mm lateral, 8.9 mm ventral relative to bregma). The components were permanently affixed with dental cement. The animals were allowed to recover for at least 14 days before experiments. All experimental procedures were approved by the Institutional Animal Care and Use Committees at North Carolina State University.

6.2.4 *In Vivo* Methods

On the experimental day, the electrodes were connected to a head-mounted amplifier attached to a commutator (Crist Instrument Company, Hagerstown, MD). After electrodes were electrochemically stable, a time course of evoked and non-evoked signals was collected with electrical stimulation applied every 5 min. A traditional FSCV waveform (10 Hz sampling rate, 850 data points/CV) was used to evaluate the electrodes performance. Electrically-evoked dopamine release was stimulated biphasically (2 ms/phase, 24 pulses, 150 μA).

6.2.5 Histology

At the completion of *in vivo* experiments, each animal was anesthetized with urethane (1.5 mg/kg i.p.). Brains were removed and stored in 10 % formalin for 24 hours, then removed from the fixative solution and sliced with a vibrotome (World Precision Instruments, Sarasota, FL) in 120 μm sections, which were mounted on glass microscope slides. After mounting, slides were stained with cresyl violet (Fisher Scientific, Waltham,

MA) for microscopic verification of electrode placement referencing the stereotaxic rat atlas [15].

6.3 RESULTS AND DISCUSSION

6.3.1 *In Vitro* Characterization of Microelectrodes using FSCV

To first explore the electrochemical performance of the carbonized tungsten microsensors, the current response was collected *in vitro* at four biologically relevant concentrations of DA before the sensor was implanted. **Figure 6.1** depicts the sensitivity to DA of each of the microsensors used for implantation. **Figure 6.1 (a)** shows background-subtracted CVs of peak current for 1 μM DA collected with both microsensors. Sensitivity of each electrode given as the peak current at the oxidation potential versus DA concentration is shown in **Figure 6.1 (b)** for each microsensor. From this information, the sensitivity to DA for the two electrodes implanted was 60 ± 3 nA/μM for Electrode 1 and 37 ± 3 nA/μM for Electrode 2.

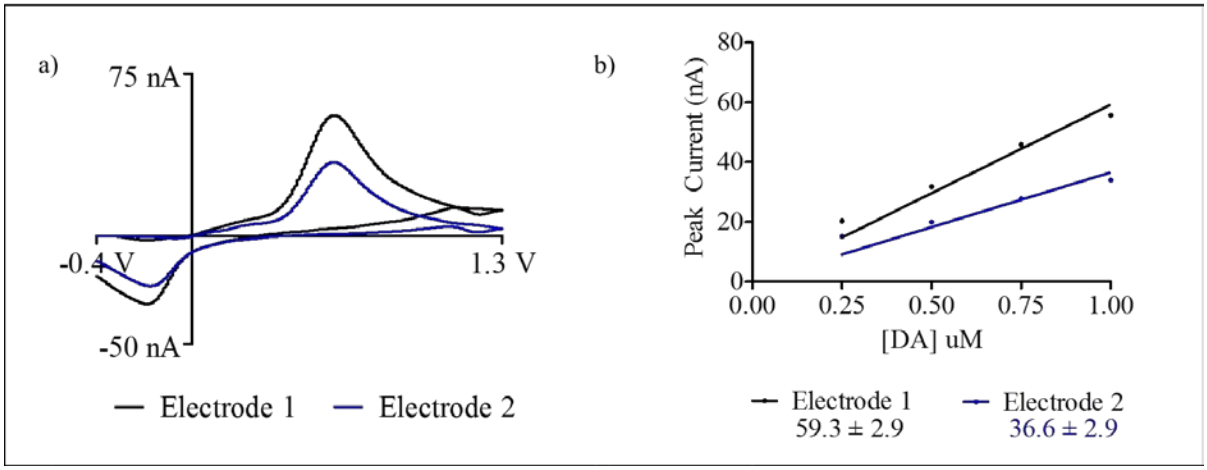

Figure 6.1 – Sensitivity to dopamine for carbonized tungsten microsensors. (a) *In vitro* background-subtracted CVs for both microelectrodes at 1 µM DA (b) Sensitivity to DA for the two microelectrodes, given by the slopes of the regression lines was determined to be 60 ± 3 nA/µM for Electrode 1 and 37 ± 3 nA/µM for Electrode 2.

Microsensors used in freely moving animal experiments are typically pre-calibrated in a flow cell setup for hydrogen peroxide (HPO) and pH to aid in data analysis after the experiment. With the potential waveform used here, HPO and pH are the most common interferents seen *in vivo*. Both electrodes tested for sensitivity to DA were used further for functionality *in vivo* by testing against 4 solutions of both HPO and pH in addition to DA. **Figure 6.2** depicts the calibration curves of these microsensors to four concentrations of HPO and four basic pH shifts for Electrodes 1 and 2. Sensitivity to HPO was determined to be 0.1 ± 0.0 nA/µM for Electrode 1 and 0.08 ± 0.00 nA/µM for Electrode 2, **Figure 6.2 (a)**, and 20 ± 1 nA/µM for Electrode 1 and 14 ± 1 nA/µM for Electrode 2 for sensitivity to pH, **Figure 6.2 (b)**.

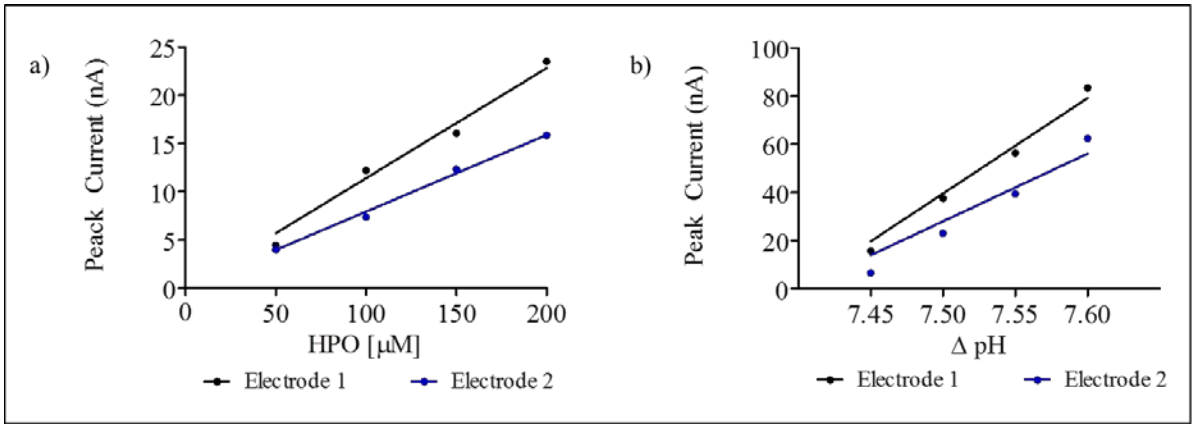

Figure 6.2 – Calibration curves for biologically-relevant analytes using carbonized tungsten microsensors. (a) Sensitivity to HPO was determined to be 0.1 ± 0.0 nA/µM for Electrode 1 and 0.08 ± 0.00 nA/µM for Electrode 2, with (b) sensitivity to pH given as 20 ± 1 nA/µM for Electrode 1 and 14 ± 1 nA/µM for Electrode 2.

6.3.2 Characterization of Implanted Tungsten-based Carbon Microelectrodes

Upon implantation of both Electrode 1 and 2 into regions of interest in the brain, the animals were allowed to recover for a period of weeks. The animal with Electrode 1 implanted was tested 3, 4 and 5 weeks after electrodes were implanted. Electrically-evoked dopamine release was stimulated via the stimulating electrode but a response was not detected at the carbonized tungsten electrodes on any of the three experimental days. The animal was euthanized and its brain was removed to verify electrode placement as a possible cause for lack of response. The histology results are shown in **Figure 6.3**, depicting the electrode placements for the working electrode (carbonized tungsten electrode), reference electrode (Ag/AgCl) and bipolar stimulating electrode. The carbonized tungsten electrode was placed in the nucleus accumbens shell, circled in red in **Figure 6.3 (a)**, but the histology indicates slightly dorsal placement, which could put it out of the signal pathway. **Figure 6.4**

(b) shows the reference electrode placement in the contralateral cortex. Infection and possible tissue damage was found around this electrode placement, shown circled in red. This could have also contributed to a disruption in the signal measurement. **Figure 6.3 (c)** verifies desired placement of the bipolar stimulating electrode in the ventral tegmental area, with the terminal region of the electrode circled in red.

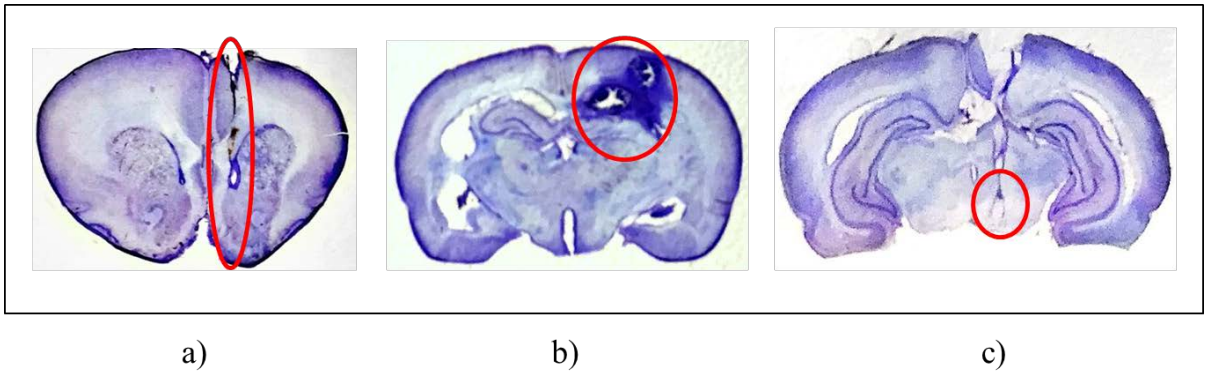

a) b) c)

Figure 6.3 – Evaluating electrode placement in freely moving animal experiments. (a) Placement of the carbonized tungsten electrode in the nucleus accumbens shell. (b) Reference electrode placement and infection in the contralateral cortex. (c) Stimulating electrode placement verified in the ventral tegmental area.

Initial testing with the second animal and Electrode 2 implanted did not result in electrically evoked dopamine release. However, recorded *in vivo* signals had characteristic background shapes that suggested the electrode was functioning as designed. As with the first animal, histology will be used to analyze electrode placement and assess possible issues at the conclusion of the experiment.

6.4 CONCLUSIONS

The carbonized tungsten microsensor presented in **Chapter 5** was optimized for initial use in freely moving animals. The tungsten wire substrate was miniaturized from 125 µm to 50 µm and a new insulation technique was implemented to improve batch yield. These sensors improve on the major weaknesses of the current gold standard sensors and are expected to be more practical for longer-term voltammetric measurements in tissue. This work details the beginning of an ongoing study for evaluating the use of a carbonized tungsten microsensor in freely moving animals. At the time of this writing, two microsensors were implanted in two freely moving animals and allowed to recover for a period of weeks. Neither animal showed response to electrically evoked dopamine release. The first animal was tested up to 5 weeks after surgery and the second animal was tested up to 3 weeks after surgery. Valuable information was obtained about electrode placements from histology results in the first animal. Further testing is needed in the future to establish chronic performance of these sensors.

6.5 REFERENCES

[1] R. N. Adams. *In vivo* electrochemical measurements in the CNS. *Prog. Neurobiol. 35(4),* pp. 297-311. 1990.

[2] B. D. Bath, D. J. Michael, B. J. Trafton, J. D. Joseph, P. L. Runnels and R. M. Wightman. Subsecond adsorption and desorption of dopamine at carbon-fiber microelectrodes. *Anal. Chem. 72(24),* pp. 5994-6002. 2000.

[3] J. J. Clark, S. G. Sandberg, M. J. Wanat, J. O. Gan, E. A. Horne, A. S. Hart, C. A. Akers, J. G. Parker, I. Willuhn, V. Martinez, S. B. Evans, N. Stella and P. E. Phillips. Chronic microsensors for longitudinal, subsecond dopamine detection in behaving animals. *Nat. Methods 7(2),* pp. 126-129. 2010.

[4] J. C. Conti, E. Strope, R. N. Adams and C. A. Marsden. Voltammetry in brain-tissue - chronic recording of stimulated dopamine and 5-hydroxytryptamine release. *Life Sci. 23(27-2),* pp. 2705-2715. 1978.

[5] E. C. Dankoski and R. M. Wightman. Monitoring serotonin signaling on a subsecond time scale. *Front. Integr. Neurosci. 7*pp. 44. 2013.

[6] A. G. Ewing and R. M. Wightman. Monitoring the stimulated release of dopamine with *in vivo* voltammetry .2.clearance of released dopamine from extracellular fluid. *J. Neurochem. 43(2),* pp. 570-577. 1984.

[7] P. Hashemi, E. C. Dankoski, R. Lama, K. M. Wood, P. Takmakov and R. M. Wightman. Brain dopamine and serotonin differ in regulation and its consequences. *Proc. Natl. Acad. Sci. U. S. A. 109(29),* pp. 11510-11515. 2012.

[8] M. L. A. V. Heien, P. E. M. Phillips, G. D. Stuber, A. T. Seipel and R. M. Wightman. Overoxidation of carbon-fiber microelectrodes enhances dopamine adsorption and increases sensitivity. *Analyst 128(12),* pp. 1413-1419. 2003.

[9] A. Hermans and R. M. Wightman. Conical tungsten tips as substrates for the preparation of ultramicroelectrodes. *Langmuir 22(25),* pp. 10348-10353. 2006.

[10] N. R. Herr, J. Park, Z. A. McElligott, A. M. Belle, R. M. Carelli and R. M. Wightman. *In vivo* voltammetry monitoring of electrically evoked extracellular norepinephrine in subregions of the bed nucleus of the stria terminalis. *J. Neurophysiol. 107(6),* pp. 1731-1737. 2012.

[11] C. E. John and S. R. Jones. "Fast scan cyclic voltammetry of dopamine and serotonin in mouse brain slices," in *Electrochemical Methods for Neuroscience*, A. C. Michael and L. M. Borland, Eds. 2007.

[12] R. B. Keithley, P. Takmakov, E. S. Bucher, A. M. Belle, C. A. Owesson-White, J. Park and R. M. Wightman. Higher sensitivity dopamine measurements with faster-scan cyclic voltammetry. *Anal. Chem. 83(9),* pp. 3563-3571. 2011.

[13] K. C. Morton, C. A. Morris, M. A. Derylo, R. Thakar and L. A. Baker. Carbon electrode fabrication from pyrolyzed parylene C. *Anal. Chem. 83(13),* pp. 5447-5452. 2011.

[14] J. Park, P. Takmakov and R. M. Wightman. *In vivo* comparison of norepinephrine and dopamine release in rat brain by simultaneous measurements with fast-scan cyclic voltammetry. *J. Neurochem. 119(5),* pp. 932-944. 2011.

[15] G. Paxinos and C. Watson. *The Rat Brain in Stereotaxic Coordinates* (2nd ed.) 1986.

[16] S. Ranganathan and R. L. McCreery. Electroanalytical performance of carbon films with near-atomic flatness. *Anal. Chem. 73(5),* pp. 893-900. 2001.

[17] J. G. Roberts, K. L. Hamilton and L. A. Sombers. Comparison of electrode materials for the detection of rapid hydrogen peroxide fluctuations using background-subtracted fast scan cyclic voltammetry. *Analyst 136 (17),* pp. 3550-3556. 2011.

[18] J. G. Roberts, L. Z. Lugo-Morales, P. L. Loziuk and L. A. Sombers. Real-time chemical measurements of dopamine release in the brain. *Methods Mol. Biol. 964,* pp. 275-294. 2013.

[19] J. G. Roberts, B. P. Moody, G. S. McCarty and L. A. Sombers. Specific oxygen-containing functional groups on the carbon surface underlie an enhanced sensitivity to dopamine at electrochemically pretreated carbon fiber microelectrodes. *Langmuir 26(11),* pp. 9116-9122. 2010.

[20] A. L. Sanford, S. W. Morton, K. L. Whitehouse, H. M. Oara, L. Z. Lugo-Morales, J. G. Roberts and L. A. Sombers. Voltammetric detection of hydrogen peroxide at carbon fiber microelectrodes. *Anal. Chem. 82(12),* pp. 5205-5210. 2010.

[21] M. Spanos, J. Gras-Najjar, J. M. Letchworth, A. L. Sanford, J. V. Toups and L. A. Sombers. Quantitation of hydrogen peroxide fluctuations and their modulation of dopamine dynamics in the rat dorsal striatum using fast-scan cyclic voltammetry. *ACS Chem. Neurosci. 4(5),* pp. 782-789. 2013.

[22] T. G. Strein and A. G. Ewing. Characterization of submicron-sized carbon electrodes insulated with a phenol-allylphenol copolymer. *Anal. Chem. 64 (13),* pp. 1368-1373. 1992.

[23] P. Takmakov, M. K. Zachek, R. B. Keithley, E. S. Bucher, G. S. McCarty and R. M. Wightman. Characterization of local pH changes in brain using fast-scan cyclic voltammetry with carbon microelectrodes. *Anal. Chem. 82(23),* pp. 9892-9900. 2010.

[24] B. J. Venton, D. J. Michael and R. M. Wightman. Correlation of local changes in extracellular oxygen and pH that accompany dopaminergic terminal activity in the rat caudate-putamen. *J. Neurochem. 84(2),*pp. 373-381. 2003.

[25] R. M. Wightman, M. L. Heien, K. M. Wassum, L. A. Sombers, B. J. Aragona, A. S. Khan, J. L. Ariansen, J. F. Cheer, P. E. Phillips and R. M. Carelli. Dopamine release is heterogeneous within microenvironments of the rat nucleus accumbens. *Eur. J. Neurosci. 26(7),* pp. 2046-2054. 2007.

[26] M. K. Zachek, P. Takmakov, B. Moody, R. M. Wightman and G. S. McCarty. Simultaneous decoupled detection of dopamine and oxygen using pyrolyzed carbon microarrays and fast-scan cyclic voltammetry. *Anal. Chem. 81(15),* pp. 6258-6265. 2009.

[27] M. K. Zachek, P. Takmakov, J. Park, R. M. Wightman and G. S. McCarty. Simultaneous monitoring of dopamine concentration at spatially different brain locations *in vivo*. *Biosens. Bioelectron. 25(5),* pp. 1179-1185. 2010.

CHAPTER 7

Summary of Findings and Recommendations for Future Research

This work chronicles the steps taken to transition a proven *in vivo* technology, FSCV, towards chronic biochemical measurements with *in vivo* applications. The development of practical chronic systems for taking biochemical measurements is largely affected by overall power consumption and data transfer limitations. FSCV was developed initially for use in acute studies, thus emphasis was not placed on robustness of the sensor or software parameters that conserved data generation. Despite these limitations, FSCV has several advantages that make it practical for long-term measurements. The results reported in this dissertation focus on studying the FSCV protocol with an emphasis on data conservation as well as the development of an alternative microsensor with comparable electrochemical performance to the conventional microsensors that also can be used for chronic implantation.

The work in **Chapters 2, 3** and **4** presents manipulations in the current FSCV measurement protocol most commonly used for observing biochemical signaling *in vivo* to address these limitations. **Chapter 2** details the effects of reducing the sampling rate from the standard 10 Hz to 1 Hz on the electrode performance. The results demonstrate that *in vitro* and *in vivo* dopamine fluctuations can be monitored using a reduced sampling rate, with minimal impact on measurement performance. The quantity of data collected and transferred per second can be reduced by an order of magnitude compared to the standard protocol by using this reduced sampling rate.

Chapter 3 evaluates the reduction of a second FSCV measurement parameter, data density, on performance. Additionally, several combined parameter protocols are assessed for efficacy in living tissue featuring a reduced sampling rate and reduced data density. These studies examined the performance of data collection parameters on the performance of FSCV measurements of dopamine. Emphasis was placed on understanding changes in performance for experimental protocols to monitor dopamine and other analyte fluctuations that have reduced data densities compared to conventional experiments. Results are also presented for *in vitro* and *ex vivo* protocols that combine reduced sampling rates and data density for monitoring DA without significantly impacting measurement performance. The overall data collected and transferred from the reduced data density protocols is decreased by two orders of magnitude compared to the standard protocol.

Chapter 4 reports the findings of adapting reduced parameter protocols to make electrochemical measurements in freely moving animals. This work provides the first experimental demonstration that real-time *in vivo* dopamine fluctuations can be monitored using an FSCV protocol with a reduced sampling rate and reduced data density, with no negative impact on measurement performance.

The work in **Chapters 5** and **6** looks at another aspect of the FSCV technology that is currently limited in its ability to be used in long-term measurements with freely moving or behaving animals. **Chapter 5** presents an alternatively fabricated microsensor for use with FSCV that provides more strength and rigidity compared to the traditional sensor. These sensors are expected to be more practical for measurements in large animal models and for

longer-term voltammetric measurements in tissue compared to the traditional carbon fiber microelectrode used with FSCV. In this work, a tungsten-based carbon microsensor was demonstrated for measuring fluctuations in dopamine and other biologically-relevant analytes. The tungsten-based carbon microsensors showed comparable electrochemical performance to the conventional carbon-fiber sensor both *in vitro* and *in vivo*, and over several hours of use.

Chapter 6 is an ongoing study that further explores the use of tungsten-based carbon microelectrode for chronic applications in freely moving animals. The aim of this study is a proof of concept for implantation of an alternative sensor that is more robust than the current chronic sensor used, thus being more suited for use in behaving or freely moving animals.

Opportunity for future research exists in minimizing the diameter of the tungsten base wires for further miniaturization of the sensor. Additionally, research in batch insulation would be beneficial to reduce the time needed to fabricate the sensors. We expect that the reduction in data generation from the studies presented in this work will facilitate chronic and wireless biochemical measurement systems without compromising the quantitative and qualitative performance of this approach to *in vivo* molecular monitoring. These results will help to guide future longer-term *in vivo* electrochemical experiments without the need for modifying existing software or hardware. This work also lays a foundation for future studies of power consumption during experimentation, including the development and integration of hardware to monitor real-time power usage with the use of a low-power potentiostat better suited to a wireless system than the current hardware.

The adaptations to FSCV presented in this work provide insight critical to moving measurements of biochemical signaling to chronic behavioral paradigms. Furthering this research will facilitate a better understanding of the transport of neurotransmitters and signaling molecules, relating them to healthy and diseased individuals to better evaluate the long term neuroplasticity during behavioral and pharmacological challenges associated with neurological disorders.